Stony Brook University

Francisella tularensis: Interactions with Hepatocytes and Pathways for the Acquisition of Iron

A Dissertation Presented

by

Cindy A. Thomas-Charles

to

The Graduate School

in Partial Fulfillment of the

Requirements

for the Degree of

Doctor of Philosophy

in

Genetics

Stony Brook University

December 2013

Stony Brook University

The Graduate School

Cindy A. Thomas-Charles

We, the dissertation committee for the above candidate for the

Doctor of Philosophy degree,

hereby recommend acceptance of this dissertation.

Martha B. Furie, Ph.D., – Dissertation Advisor
Professor, Department of Pathology

David G. Thanassi, Ph.D., - Chairperson of Defense
Professor, Department of Molecular Genetics and Microbiology

James B. Bliska, Ph.D.
Professor, Department of Molecular Genetics and Microbiology

Richard Kew, Ph.D.
Associate Professor, Department of Pathology

Satdarshan P. Singh Monga, M.D.
Professor of Pathology, Professor of Medicine,
University of Pittsburgh School of Medicine

This dissertation is accepted by the Graduate School

Charles Taber
Dean of the Graduate School

ABSTRACT OF THE DISSERTATION

***Francisella tularensis:* Interactions with Hepatocytes and Pathways for the Acquisition of Iron**

by

Cindy A. Thomas-Charles

Doctor of Philosophy

in

Genetics

Stony Brook University

2013

Francisella tularensis is a Gram-negative, facultative intracellular bacterium and the causative agent of tularemia. Due to its high virulence, this organism has been classified as a Tier 1 select agent of bioterrorism. Regardless of the route of inoculation, the lungs, spleen, and liver are major targets of infection. Furthermore, this organism replicates to high numbers in hepatocytes, the predominant cells in the liver. Factors that mediate the uptake by and replication of *F. tularensis* in hepatocytic cell lines or primary mouse hepatocytes were investigated. *F. tularensis* was observed to be taken up by hepatocytes in a process that required polymerization of the hepatocyte actin cytoskeleton, but not the bacterial type I secretion system or type IV surface pili. Killed bacteria and bacteria rendered incapable of synthesizing protein were still ingested efficiently, suggesting involvement of a pre-formed bacterial surface structure in uptake. *F. tularensis* transposon mutants were subsequently screened for their ability to be taken

up by or replicate in hepatocytes. Two mutants with decreased replicative capacity were identified. Additionally, primary mouse hepatocytes were used to determine the response of these host cells to infection with *F. tularensis*. Following infection, hepatocytes increased the expression of several genes encoding cytokines involved in inflammation. Furthermore, two potent chemotactic cytokines, CXCL1 and CXCL5, were secreted in increased amounts by infected hepatocytes. The ability to acquire extracellular iron is a key requirement for the replication of *F. tularensis* in hepatocytes. In some bacterial species, FeoB forms the core of the ferrous iron acquisition system. A mutant strain of *F. tularensis* lacking FeoB was used to investigate this protein's role in growth and virulence. Loss of FeoB diminished the growth of *F. tularensis* in medium with restrictive levels of iron and in hepatocytes and epithelial cells. The FeoB-deficient mutant was still capable of causing lethal disease in mice. However, its ability to colonize the liver, spleen, and lungs of mice was markedly impaired. These studies suggest that the interactions between *F. tularensis* and hepatocytes are important in the pathogenesis of tularemia.

TABLE OF CONTENTS

LIST OF TABLES

LIST OF FIGURES

LIST OF ABBREVIATIONS

ATCC	American Type Culture Collection
BHI	Brain heart infusion
BMP	Bone morphogenic protein
CCL	CC ligand
CDM	Chamberlain's defined medium
CFU	Colony-forming unit
Che-CDM	Chelex-100-treated Chamberlain's defined medium
CXCL	CXC ligand
DAMP	Danger-associated molecular pattern
DAPI	4', 6-diamidino-2-phenylindole
DCYTB	Duodenal cytochrome-B
DMEM	Dulbecco's modified Eagle medium
DMSO	Dimethyl sulfoxide
EEA1	Early endosome antigen 1
EMEM	Eagle minimum essential medium
FBS	Fetal bovine serum
Feo	Ferrous iron transport system
FITC	Fluorescein isothiocyanate
FPI	*Francisella* pathogenicity island
Fsl	*Francisella* siderophore locus
Fur	Ferric uptake regulator
HBSS	Hank's buffered saline solution

HI	Heat-inactivated
HIF	Hypoxia-inducible factor
ICAM-1	Intercellular adhesion molecule-1
IL	Interleukin
IRE	Iron responsive element
IRP	Iron regulatory protein
LAMP	Lysosome-associated membrane protein
LPS	Lipopolysaccharide
LVS	Live vaccine strain
MH	Mueller-Hinton
MOI	Multiplicity of infection
NF-κB	Nuclear factor κB
NOD	Nucleotide-oligomerization domain
Nramp2	Natural-resistance-associated macrophage protein 2
OD	Optical density
PAMP	Pathogen-associated molecular pattern
PBS	Phosphate-buffered saline
PYHIN	Pyrin and HIN domain
Ssp.	Subspecies
TGF	Transforming growth factor
TLR	Toll-like receptor
TNF	Tumor necrosis factor
TRF-1	Transferrin receptor 1

TRITC	Tetramethylrhodamine isothiocyanate
VCAM-1	Vascular cell adhesion molecule-1
VEGF-A	Vascular endothelial growth factor A

ACKNOWLEDGEMENTS

I would like to thank Dr. Huaixin Zheng for his invaluable contributions to the iron acquisition studies. Thanks to Dr. Kari Nejak-Bowen and William C. Bowen for providing indispensible instruction in techniques for the isolation of primary mouse hepatocytes. I would also like to thank Varya Kirillov for her work in the construction of the LVS transposon collection used in this dissertation, Jason Tam for sharing his knowledge of the isolation of leukocytes, and members of the Thanassi laboratory for sharing reagents and knowledge of molecular cloning. I am grateful for the assistance with *in vivo* studies provided by Dr. Patricio Mena, and technical support provided by Dr. Indra Jayatilaka. I would like to express gratitude to the members of my dissertation committee, Dr. David G. Thanassi, Dr. James B. Bliska, Dr. Richard Kew, and Dr. Satdarshan P. Singh Monga, for the expert guidance they afforded me throughout these studies. Special thanks to my dissertation advisor, Dr. Martha B. Furie, for the excellent supervision and guidance she provided me throughout my dissertation research. Thanks to the NSF Bridges to the Doctorate Program, the Dr. W. Burghardt Turner Fellowship, and the Molecular and Cell Biology of Infectious Disease (MCBID) Training Program (NIAID T32 AI07539), for financial support. Finally, thank you to my family and friends for their unwavering support of my scientific endeavors.

INTRODUCTION

I. Overview of *Francisella tularensis*

i. *Francisella tularensis* and tularemia

Francisella tularensis is a facultative intracellular, Gram-negative coccobacillus. This bacterium was named for Edward Francis, who in 1922 identified it as the causative agent of tularemia (1). The recognized subspecies (ssp.) of *F. tularensis* are *tularensis*, *holarctica*, *novicida*, *mediasiatica*, and *philomiragia* (2). Ssp. *tularensis* and *holarctica,* also known respectively as Type A and Type B, are human pathogens (3). Ssp. *tularensis* is prevalent throughout North America, while ssp. *holarctica* is widespread throughout the Northern Hemisphere. The live vaccine strain (LVS) of *F. tularensis* is derived from ssp. *holarctica,* and it is commonly used as a laboratory model of tularemia. This strain is attenuated in healthy humans but retains its virulence in mice. The LVS was developed in the former Soviet Union from a virulent bacterial strain. Although the LVS has been used to vaccinate at-risk individuals, it is not used for the general public, because the exact mechanism of attenuation and protection remains unknown (2). Like the LVS, ssp. *novicida* is used in the laboratory as a model for tularemia, since it is also lethal for mice but is avirulent in healthy humans (4). Ssp. *tularensis*, which is typified by the Schu S4 strain, is highly virulent, with as few as 10 particles being sufficient to cause disease when administered via the respiratory or intracutaneous routes (5,6). This highly virulent organism has been considered for use as a biological weapon by China, the former Soviet Union, and Japan. Furthermore, the United States has also developed weapons for the dissemination of aerosolized *F. tularensis* (7). Due to its high infectivity and virulence,

F. tularensis ssp. *tularensis* is classified a Tier 1 select agent by the Centers for Disease Control and Prevention (1,8).

Tularemia was first described in 1911 by McCoy and Chapin as a plague-like illness affecting squirrels in Tulare County, California (9). It is now known that tularemia is a zoonotic disease that affects a large variety of wildlife including rodents, lagomorphs, and insectivores. The natural vectors and potential long-term reservoirs of *F. tularensis* include ticks, tabanid flies, and mosquitoes (1). The manifestations, severity, and specific symptoms of tularemia vary depending on the route of infection, as well as the infecting subspecies of *F. tularensis*. Following infection, there is usually a 3 to 5 day incubation period before symptoms of tularemia are observed. Early non-specific symptoms include general malaise, fever, chills, sore throat, and headache (7,10). The most common clinical presentations are ulceroglandular and glandular tularemia. Ulceroglandular tularemia occurs from direct contact with contaminated animal material or vector-borne transmission through the skin or mucus membranes. This form of tularemia is characterized by swollen lymph nodes and the formation of an ulcer at the infection site. Glandular tularemia, which results from the ingestion of contaminated food or water, is characterized by enlarged lymph nodes. There is a <5% mortality rate associated with ulceroglandular and glandular tularemia (1,10). Pneumonic tularemia caused by ssp. *tularensis* is the most severe form and occurs following direct inhalation of aerosolized bacteria. This form of the disease is associated with a mortality rate as high as 30 to 60% if left untreated, and it often results in systemic illness (7). Less common clinical presentations of tularemia are oculoglandular, which is caused by infection of the conjunctiva; oropharyngeal, which is caused by ingestion of contaminated food or water;

and typhoidal, which is characterized by gastrointestinal symptoms and systemic illness (7). Tularemia is effectively treated with antibiotic therapy using streptomycin, gentamicin, doxycyclin, or fluoroquinolones such as ciprofloxacin. The treatment period can last from 7 to 28 days depending on the therapeutic agent (11).

ii. Environmental adaptation of *F. tularensis*

F. tularensis has evolved numerous mechanisms to facilitate its survival in a variety of hosts. Transmission of the organism from a non-mammalian to mammalian host results in an increase in environmental temperature. This temperature change causes the organism to shift its gene expression profile, so that mammal-specific genes are expressed, and those genes required for survival in non-mammalian hosts are repressed. Many of the host-specific genes expressed by *F. tularensis* following an increase in environmental temperature have been implicated in virulence and pathogenesis of the organism (12). The difference between an animal host and the *in vitro* environment also affects the *F. tularensis* gene expression profile. More than 400 proteins are differentially regulated when mammalian-grown *F. tularensis* is compared with bacteria grown in Mueller-Hinton (MH) broth; however, the protein expression profile of *F. tularensis* grown in brain heart infusion (BHI) broth closely resembles that of bacteria recovered from macrophages (13,14).

iii. The *F. tularensis* lipopolysaccharide

Gram-negative bacteria, such as *F. tularensis*, express lipopolysaccharide (LPS) in the outer leaflet of the outer bacterial membrane. The LPS has three components: O-antigen, core, and lipid A, which is the biologically active component (15). Some bacteria have the ability to express modified LPS in response to environmental temperature

changes. In *Yersinia pestis*, when the environmental temperature is increased from 25^{o}C to 37^{o}C, the structure of the lipid A is modified from the hexa-acylated form, which is capable of triggering an inflammatory response, to the immunologically inert tetra-acylated form (16). Similarly, in *F. tularensis* ssp. *novicida,* the amide-linked fatty acid of the reducing glucosamine in the lipid A shifts to a 3-hydroxyhexadecanoic acid substituent at 25^{o}C, compared to a 3-hydroxyoctadecanoic acid substituent at 37^{o}C (17). An additional structural change that distinguishes the LPS of *F. tularensis* subspecies from that of Gram-negative enteric bacteria is the absence of a phosphate residue at the 4' position of the lipid A glucosamine backbone, a lack that prevents signaling through toll-like receptors (TLR) 2 and 4. Together, the structural modifications of the *F. tularensis* LPS enable the organism to circumvent host immune responses and thus are a form of adaptation for survival within the mammalian host (15).

iv. *F. tularensis* type I secretion system and type IV pili

Gram-negative bacteria produce a number of proteins that are involved in virulence, efflux of drugs and toxins, acquisition of nutrients, and biogenesis of bacterial structures such as pili and flagella (18). *F. tularensis* possesses a type I secretion system. The type I secretion system is a three-component structure that is used to export high-molecular weight proteins directly from the bacterial cytoplasm to the extracellular environment. In *E. coli*, the innermost component is usually a member of the ATP-binding cassette superfamily, e.g., HlyB, while the outermost component is an integral protein that forms a β-barrel that spans the periplasm and outer membrane. The outermost and innermost proteins are connected by a fusion protein, e.g., HlyD. TolC is the integral membrane protein that forms a hydrophilic pore across the bacterial membrane (19). *F.*

tularensis has two genes, *tolC* and *ftlC*, whose protein products have high homology to the *E. coli* TolC (20,21). In *F. tularensis*, both *tolC* and *ftlC* are involved in drug efflux. Deletion of either of the two genes results in sensitivity to drugs, including aminoglycosides, quinolones, and detergents. Furthermore, *tolC*, but not *ftlC,* is important for virulence of *F. tularensis* in mice, and its deletion renders *F. tularensis* hypercytotoxic to host cells (20,21).

A wide range of Gram-negative bacteria express type IV pili. The structure and function of the type IV pilus expressed by *Neisseria meningitidis* is well understood and often used as a model for the structure. The Type IV pilus is typically composed of multiple copies of major pilins, plus several minor pilins. PilE is the major pilin and is capped by PilC, which is an adhesin. PilC may also associate with the bacterial outer membrane, where it regulates pilus retraction. PilF and PilT are ATPases responsible for powering pilus assembly and retraction, respectively. PilQ is a secretin that forms a channel in the bacterial outer membrane through which the pilus fiber passes (18,22). PilD is a prepilin peptidase that is located near the inner membrane, where it is involved in methylation of the mature pilin. The functions of PilO and PilN are not known (22,23). *F. tularensis* subspecies also possess genes that are involved in the biosynthesis of type IV pili, and they express these structures on their surface (23). Furthermore, this structure plays a role in adherence of this organism to host cells (24). The genes for the *Francisella* type IV pili exist in separate clusters including *pilNOPQ,* which are similarly grouped in *N. meningitidis* and *Pseudomonas aeruginosa* (22). *F. tularensis* also has *pilT*, *pilD*, and five *pilE* genes (*pilE1-5*), as well as a second gene cluster containing *pilFG* (23). In ssp. *novicida*, *pilE4* encodes a major pilin subunit, and its deletion eliminates pilus expression

(25). The *F. tularensis* PilF and PilT ATPases are also required for surface expression of the type IV pilus (24,26). Deletion of *pilT* and *pilF* renders the LVS defective for adherence to macrophages, pneumocytes, and hepatocytes (24). However, another study found that deletion of the *pilE4*, *pilE5,* or *pilE6* genes in the LVS results in bacteria that are more adherent to host cells, while the absence of *pilE5*, *pilE6*, or *pilT* results in decreased virulence of the LVS in mice (26).

II. Intracellular lifestyle of *Francisella tularensis*

i. Macrophages

Macrophages and monocytes are important for the pathogenicity of *F. tularensis.* As a result, the lifestyle of the organism within these phagocytic host cells has been well studied (FIGURE 1). Phagocytosis of *F. tularensis* by macrophages is mediated in part by a number of host cell receptors, including the macrophage mannose receptor, class A scavenger receptors, macrophage Fcγ receptors, and complement receptor 3; also involved are surfactant proteins A and D, which aid in the association of *F. tularensis* with lung alveolar macrophages (27-30). Additionally, nucleolin, which is expressed on the surface of monocytes and associates with the actin cytoskeleton, binds to elongation factor-Tu, an *F. tularensis* GTP-binding protein that is involved in protein translation. The *F. tularensis*-nucleolin complex is subsequently internalized by monocytes. Interestingly, nucleolin continues to associate with the bacteria in the phagosomal compartment of the macrophage (31,32). In addition to uptake mediated by surface receptors, *F. tularensis* targets cholesterol-rich lipid domains on the surface of macrophages to trigger its ingestion. As is the case with nucleolin, the lipid domain remains associated with the bacteria during the early stages following internalization

(33). *F. tularensis* is taken up by macrophages through the process of looping phagocytosis (34). During this process, the bacteria are engulfed by asymmetric pseudopod loops extended by the macrophage. The pseudopod loops subsequently fuse, enclosing the bacteria in a spacious intracellular vacuole that rapidly shrinks. Structurally, the looping phagocytosis that occurs with *F. tularensis* is distinct from other forms, such as conventional phagocytosis, coiling phagocytosis, and triggered macropinocytosis, which are observed when other bacteria are taken up by macrophages. Mutation of the *F. tularensis* LPS O-antigen results in uptake via pseudopod loops that are more tightly associated with the bacteria. Furthermore, while neither heat killing nor formalin fixation of *F. tularensis* is capable of altering the uptake process, oxidation of bacterial surface carbohydrates results in a shift to conventional phagocytosis (8). The phagocytosis of *F. tularensis* is also dependent on rearrangement of the macrophage actin microfilaments and signaling through phosphotidylinositol 3-phosphokinase (8,30).

Once *F. tularensis* has been internalized by a macrophage, it initially resides within a phagosome that has a clearly discernible lipid bilayer. A phagosome containing live or killed *F. tularensis* transiently acquires markers for early endosomes, as indicated by acquisition of early endosome antigen 1 (EEA1), that reach a maximum association within the first 15 minutes after infection. As it matures, the *F. tularensis*-containing phagosome acquires limited amounts of markers that are associated with late endosomes and lysosomes, including CD63 and lysosome-associated membrane proteins (LAMP) 1 and 2. Maximum co-localization (about 70%) with markers for late endosomes and lysosomes occurs by 2 to 4 hours after infection, and it steadily declines to about 15% by 16 hours after infection. Interestingly, only phagosomes containing live, not killed, *F.*

tularensis are able to resist acidification (35). The pH within phagosomes containing live bacteria remains at about 6.7, while vacuoles containing killed bacteria are acidified to a pH of about 5.5. At later times, the previously distinct bilayer, which forms the membrane of phagosomes containing live *F. tularensis,* acquires a dense fibrillar coat on the outer leaflet. The phagosomal membrane subsequently fragments, releasing the bacterial cargo into the cytoplasm of the macrophage. By 14 hours post-infection, only about 20% of bacteria still reside in the phagosomes of macrophages. The escape of bacteria from the phagosome is not reliant on phagosomal acidification, since the pH of phagosomes containing live *F. tularensis* is not significantly reduced, even at early time points (35,36). Additionally, intracellular replication and phagosomal escape are regulated in part by the receptor that is engaged for phagocytosis. Serum-opsonized bacteria, which engage scavenger receptor A or complement receptor 3, have a reduced ability to replicate intracellularly. Phagosomes containing opsonized bacteria co-localize with markers for early endosomes and lysosomes for significantly longer periods than do phagosomes containing unopsonized bacteria. Additionally, bacteria that are taken up via complement receptor 3 or Fcγ receptor have a diminished ability to escape the phagosome (37).

The macrophage growth locus of *F. tularensis* is a master regulator that is expressed within 1.5 hours after the bacterium infects macrophages. The macrophage growth locus is also essential for phagosomal escape and virulence, as it positively regulates the transcription of genes found in the *Francisella* pathogenicity island (FPI), as well as other non-FPI virulence genes (22). *PmrA* also positively regulates the genes of the FPI. *PmrA* is an orphaned response regulator that may be part of a two-component

signal transduction system. Typically, one component of the signal transduction system detects environmental signals and subsequently phosphorylates a cytoplasmic response regulator that initiates intracellular signaling cascades. These cascades usually conclude with the modulation of gene expression (22). The FPI is 30 kilobases in length and encodes a number of genes that are required for phagosomal escape, intracellular replication, and virulence. *F. tularensis* ssp. *tularensis* and ssp. *holarctica* each have two identical copies of the FPI, while ssp. *novicida* has a single copy. The FPI consists of two large operons, the *pdpDiglABCD* operon and the *pdpA* operon, which contains eleven genes. Interestingly, while both ssp. *tularensis* and ssp. *novicida* have a copy of *pdpD*, this gene is not present in ssp. *holarctica*. The copy number of the FPI and the genes that are present may be related to the virulence of the different *F. tularensis* subspecies. Every gene within the FPI, with the exception of *pdpD*, is required for intramacrophage survival and virulence of *F. tularensis* (22). For example, while strains of *F. tularensis* lacking *iglC* or the macrophage growth locus are readily taken up, they are incapable of escaping the phagosome, replicating intracellularly, or inducing apoptosis of the host cell. Furthermore, phagosomes containing mutants lacking *iglC* or the macrophage growth locus continue to co-localize with lysosomal markers at late time points (38-40). A similar pattern of prolonged co-localization with markers for lysosomes has been noted for phagosomes containing a *pdpA* mutant in ssp. *novicida*. Moreover, this mutant has diminished ability to replicate intracellularly (41). Replication of *F. tularensis* in the cytoplasm of macrophages results in the induction of the intrinsic apoptosis pathway between 6 and 12 hours post-infection. The intrinsic apoptosis pathway involves the

release of mitochondrial cytochrome C into the host cytosol, the subsequent activation of caspase 9 and caspase 3, and eventual cell death (42).

ii. Epithelial cells and hepatocytes

In addition to macrophages, *F. tularensis* is also taken up by non-phagocytic host cells, such as epithelial cells and hepatocytes (which have an epithelial lineage). There are a number of similarities between the phagocytosis of *F. tularensis* by macrophages and the internalization of this organism, as well as other Gram-negative bacteria, by epithelial cells and hepatocytes. Internalization of *F. tularensis* by epithelial cells is mediated by the binding of a cell surface receptor to a bacterial ligand. One such bacterial ligand is the *Francisella* surface protein FsaP (43). *F. tularensis* targets cholesterol domains on the hepatocyte membrane to gain entry into these cells (44).

Like macrophages, epithelial cells take up live and killed *F. tularensis* with similar efficiency (45). Internalization of *F. tularensis* by lung epithelial cells is dependent on polymerization of the host cytoskeleton and to some extent on polymerization of microtubules. Both phosphotidylinositol 3-phosphokinase and tyrosine kinase signaling play an important role in the internalization of *F. tularensis* by epithelial cells (45). Upon initial interaction of epithelial cells with *F. tularensis*, genes involved in the macropinocytosis pathway are upregulated, suggesting that this is the mechanism by which the bacterium is taken up by this host cell (46). Once it is internalized by epithelial cells, *F. tularensis* traffics along the endocytic pathway, as evident by the co-localization of *F. tularensis*-containing vacuoles with EEA1 or LAMP-1. The maximum association of the bacterium-containing vacuole with EEA1 occurs by 30 minutes post-infection, while association of the vacuoles with late endosomes or lysosomes peaks at about 2

hours post-infection and steadily decreases thereafter. By 2 hours after the initial infection, degradation of the vacuolar membrane occurs, releasing the bacteria into the host cytoplasm where they are free to replicate (45). The uptake of *F. tularensis* by BNL CL.2 hepatocytic cells is also dependent on polymerization of the hepatocyte actin cytoskeleton. Internalization of the bacterium by these hepatocytes occurs via classical clathrin-mediated endocytosis and requires the adaptor proteins Eps15 and AP2 (44).

III. Innate immune response to infection

i. Overview of inflammation

Inflammation is a natural response of living, vacularized tissue to injury. The goal of the inflammatory response is to remove the offending agent so that healing may occur. This response can be either acute or chronic depending on the time it takes for the offending agent to be eliminated. The inflammatory response can be triggered by a wide variety of molecules that are separated into two broad categories: pathogen-associated molecular patterns (PAMPs) and damage-associated molecular patterns (DAMPs). The former are usually microbe-specific molecules, such as LPS, that are not present in higher organisms. On the other hand, DAMPs are endogenous molecules, such as DNA and RNA, which are normally contained within intact cells but are released following chemical or mechanical injury. Germ-line encoded pattern-recognition receptors are responsible for the detection of PAMPs and DAMPs. These receptors include TLRs and C-type lectin receptors, which detect extracellular PAMPs, as well as nucleotide-oligomerization domain (NOD)-like receptors, retinoic-acid inducible gene-I-like helicase, and pyrin and HIN domain (PYHIN) -containing protein families, which detect cytoplasmic PAMPs.

TLRs are expressed by most mammalian species and are the best characterized class of PRRs. These receptors detect a variety of PAMPs, e.g., TLR4 senses LPS, while unmethylated CpG motifs in DNA are detected by TLR 9. In addition to ligand specificity, these receptors also exhibit functional diversity. The function of TLRs is determined by their pattern of expression and the signal transduction pathways that they activate (47). In general, dimerization of TLRs occurs following interaction of the receptors with their specific ligands. PAMPs in the extracellular compartment and endosomes activate TLRs, and result in the production of proinflammatory cytokines via the nuclear factor κB (NF-κB) signaling pathway (48). Extracellular PAMPs are also detected by the C-type lectin receptor class of PRRs. These molecules are expressed on the surface of myeloid and natural killer cells and initiate inflammation in response to PAMPs such as mannan and β-glucan (48,49).

The detection of microbial pathogens in the cytoplasm is also an important function of PRRs. One of the major players in this process is NOD-like receptors. These receptors are expressed by a variety of cell types, including leukocytes and epithelial cells. Interaction of cytoplasmic PRRs with their respective ligands stimulates signaling through NF- κB or formation of inflammasome complexes. In mammalian systems, assembly of the inflammasome is a high-molecular weight platform that is required for the activation of caspase-1, a mediator of the innate inflammatory response (48).

The inflammatory response is mediated by a variety of cellular and chemical components and is characterized by swelling, heat, redness, and pain in the affected area. These characteristics are the result of physiological changes that occur at the site of injury. Specifically, the heat and swelling occur as a result of increases in blood flow and

vascular permeability. The increased blood flow to the affected area is facilitated by dilation of blood vessels and allows an influx of cellular and chemical mediators to the injured tissue. In terms of cellular responders, neutrophils are the first cells to exit the vasculature and accumulate in injured tissues. However, by 24 to 48 h after injury, the neutrophils are replaced by mononuclear leukocytes (50).

ii. Leukocyte recruitment

A hallmark of the inflammatory response is the recruitment of leukocytes from the vasculature to injured tissue. Extravasation of leukocytes occurs primarily in postcapillary venules. This process also occurs under normal circumstances, in that small numbers of monocytes constitutively exit the blood and enter tissues where they differentiate into resident macrophages. During inflammation, the process of extravasation is initiated by the transient adhesion of circulating leukocytes to endothelial cells lining the blood vessels. This loose interaction is subsequently replaced by tight adhesion, and then the leukocytes cross the endothelium and basement membrane. Leukocytes are capable of crossing the endothelium paracellularly (between adjacent cells) or transcellularly (through the endothelial cell), as occurs in the brain. Extravasation occurs via a series of coordinated events involving adhesion molecules and chemoattractants (51).

The vast majority of endothelial-leukocyte adhesion molecules belong to one of three families: selectins, integrins, or the immunoglobulin superfamily. Selectins are single-chain, transmembrane glycoproteins that bind to carbohydrate ligands (52). This family has three members that are expressed by specific cell types. L-selectin is expressed by leukocytes, including neutrophils and monocytes; E-selectin is expressed

only by endothelial cells; and P-selectin is expressed by platelets and endothelial cells. In inflammation, the major players from this family of adhesion molecules are E-selectin and P-selectin, which bind the carbohydrate moiety of ligands expressed by leukocytes (51,53). Integrins are composed of an α chain and a β chain that are non-covalently linked to form a heterodimer. Humans have 18 α chains and eight β chains that are capable of forming 24 unique heterodimers. Integrins expressed by leukocytes bind to members of the immunoglobulin superfamily, expressed by endothelial cells. This interaction facilitates tight adhesion, a key step in the extravasation of leukocytes. Integrins involved in this process include αLβ2 and αMβ2, which bind to intercellular adhesion molecule 1 (ICAM-1), and α4β1, which binds to vascular cell adhesion molecule 1 (VCAM-1) (51,53). The members of the immunoglobulin superfamily of adhesion molecules have a domain structure that is similar to that of antibodies. Apart from the adhesion molecules, members of this family have a wide variety of functions including roles as cytokine receptors, antigen receptors, and antigen-presenting molecules. VCAM-1 and ICAM-1 are members of the immunoglobulin superfamily that are expressed by endothelial cells. As previously mentioned, these adhesion molecules interact with integrins expressed by leukocytes (51,53).

Adhesion molecules work in concert with chemoattractants, including host-derived chemokines. Chemokines are a specialized group of cytokines that act as molecular messengers and induce the movement of leukocytes along a concentration gradient (54). Chemokines can have either homeostatic or inflammatory functions. Those in the homeostatic group are constitutively secreted, while the inflammatory chemokines

are secreted in response to infection or injury. It should be noted that some homeostatic chemokines can also have a proinflammatory effect.

The structure of chemokines is determined by the arrangement of conserved cysteine residues. These residues form intramolecular disulfide bonds that dictate the tertiary structure of the molecules. Chemokines fall into four structural categories based on the location of the two cysteine molecules nearest the amino terminus of the protein. In CC chemokines, such as CCL2, the two N-terminal cysteines are located adjacent to each other. For CXC chemokines, such as CXCL5, the two cysteines are separated by one amino acid (denoted as "X"). The two less common categories are XC chemokines, such as XCL1, where only one cysteine is present at the N-terminus, and the CX3C chemokine CX3CL1, where the two N-terminal cysteines are separated by three intervening amino acids. There are 24 members of the CCL family of cytokines and 16 members of the CXCL family. The XC and CX3C families have two and one members, respectively (55).

Chemokines are a subset of chemoattractants, and they promote the chemotaxis of specific types of leukocytes along a concentration gradient. Neutrophils are primarily recruited by CXC chemokines, while CC chemokines recruit monocytes and macrophages (e.g., CCL2), T cells (e.g., CCL17), mast cells (e.g., CCL5), and eosinophils (e.g., CCL11). Chemokines bind to G protein-coupled receptors located on the surface of the target cells. The receptors are separated into four categories that correspond to the structural nomenclature of the ligands. The receptors are therefore classified as CCR, CXCR, CX3CR or XCR. Once a chemokine binds to its receptor, an intracellular signaling cascade is initiated. The key signaling molecules include

phosphotidylinositide 3-kinase and protein kinase C. The intracellular signaling ultimately results in rearrangement of the actin cytoskeleton and activation of integrins, which allow chemotaxis and stimulation of antimicrobial capabilities that enable the leukocyte to eliminate invading pathogens (55).

There are other classes of molecules apart from chemokines that have the ability to attract leukocytes. These molecules include lipid-derived chemoattractants, such as leukotriene B_4, and complement-derived peptides, such as fragments of complement components 3 and 5 (termed C3a and C5a). Peptides containing formylated methionine, which are a distinguishing feature of prokaryotic proteins, also function as chemoattractants (56).

As mentioned, adhesion molecules and chemoattractants recruit leukocytes through a series of carefully orchestrated events. Following tissue injury, resident leukocytes release cytokines that cause endothelial cells located near the site of infection to express selectins. By binding to carbohydrate ligands on leukocytes, the selectins facilitate loose tethering of leukocytes to the endothelium. During the next step, chemokines bind chemokine receptors located on leukocytes, leading to their activation and increased expression of integrins. The integrins on leukocytes bind to members of the immunoglobulin superfamily on endothelial cells. The interaction between the two sets of adhesion molecules facilitates tight adhesion of the leukocytes to the endothelium (52). Transmigration occurs as the leukocytes extend pseudopodia between the junctions of endothelial cells in response to a chemoattractant gradient. The leukocytes are essentially pulled through the endothelium via interactions between a series of juctional molecules, including platelet-endothelial cell adhesion molecule (also called CD31), which is largely

concentrated at endothelial junctions. Alternatively, in certain circumstances leukocytes can exit the vasculature by migrating through a single endothelial cell (53,57). Once they have left the vessel, the leukocytes are guided to their final destination by chemoattractants.

iii. *Francisella tularensis* and innate immunity

The host inflammatory response to *F. tularensis* is complex. Some *in vitro* studies indicate that host cells produce proinflammatory mediators when challenged with *F. tularensis*. Human macrophages infected with the LVS secrete a number of potent chemoattractants including CCL2, which attracts monocytes and macrophages, and CXCL8, which attracts neutrophils (58). The *Francisella* LPS does not by itself induce a strong immune response from macrophages or endothelial cells. However, in the presence of *F. tularensis* GroEL, a bacterial heat shock protein, LPS is proinflammatory (59). Additionally, an LVS lipoprotein, designated LpnA, is capable of stimulating the secretion of proinflammatory chemokines by human macrophages and endothelial cells in a TLR-2 dependent manner (60).

However, *F. tularensis* is also known to suppress the immune response of many cells. *F. tularensis* LVS recovered from human or murine macrophages stimulates only limited secretion of proinflammatory cytokines, including tumor necrosis factor (TNF)-α, interleukin (IL)-1, IL-6 and CCL2, from subsequently infected macrophages (61). Following infection of the lungs, *F. tularensis* interacts with alveolar macrophages and dendritic cells. The organism is able to evade early detection by suppressing the response of dendritic cells to the infection (62,63). Moreover, intranasal infection of mice with the virulent Schu S4 strain leads to the transient production of transforming growth factor β

(TGF-β) at early times (16). TGF-β is a potent immunosuppressive cytokine. This molecule dampens the immune response of dendritic cells infected with the Schu S4 strain by restricting the production of IL-12p40 (64). Similarly, dendritic cells do not increase the expression of molecules critical for antigen presentation in response to this organism (62). *F. tularensis* weakly stimulates the secretion of CXCL8 by endothelial cells, but only the killed bacteria stimulate secretion of CCL2 (65). Furthermore, live *F. tularensis* suppresses the inflammatory response of endothelial cells to the killed organism. This suppression is dependent on the endothelial protein C receptor (66). LPS derived from Gram-negative bacteria such as *E. coli* typically activates and induces the secretion of proinflammatory cytokines by mononuclear phagocytes via signaling through TLR-4. However, live *F. tularensis* has the ability to suppress the TLR-4-mediated activation of macrophages by *E.coli* LPS. The ability of this organism to inhibit cytokine release by macrophages involves targeting of both the NF-κB and MAPK pathways (67). Thus, suppression of innate immunity by *F. tularensis* appears to be an important component of its pathogenicity.

IV. Response of the liver to infection

i. The liver

The liver is the largest internal organ and receives its blood supply via the hepatic artery and the hepatic portal vein, which brings material including bacterial, environmental, and food toxins from the gastrointestinal tract. Hepatocytes are the most dominant cell type of the liver, accounting for 80% of the total volume of the organ, and are responsible for carrying out its detoxifying, synthetic, and metabolic roles. In addition to hepatocytes, the liver is composed of nonparenchymal cells including endothelial cells,

hepatic stellate cells, Kupffer cells (which are liver-resident macrophages), and other immune cells such as natural killer cells (FIGURE 2). Passage of blood through the sinusoids of this organ facilitates communication between intrahepatic cells and cells of the innate and adaptive immune systems (68).

ii. Pathology of the liver during infection

The liver is often a major target for infection by facultative intracellular bacterial pathogens. Bacteria, including *Listeria monocytogenes, Salmonella typhimurium,* and *Francisella tularensis,* are capable of extensive replication in hepatocytes, a feature that allows them to evade the immune system. Early defense against infection of the liver is the role of cells of the innate immune system, specifically, neutrophils and Kupffer cells (69,70). Within the first 24 hours, neutrophils are recruited to the sites of infection, where they cause lysis of the infected hepatocytes. Destruction of infected hepatocytes results in the release of intracellular bacteria, thereby preventing their unrestricted growth (69-72). The lytic activity of neutrophils is facilitated in part by the enzymatic action of NADPH oxidase, which leads to the generation of superoxide. Superoxide spontaneously dismutates to hydrogen peroxide and oxygen. The hydrogen peroxide is then used by myeloperoxidase for the generation of hypochlorous acid, a potent chlorinating and oxidizing agent. In addition to generating reactive oxygen species, neutrophils contain granules that enclose a variety of proteolytic enzymes and bactericidal proteins such as elastase and matrix metalloproteinases (70,73,74).

iii. Leukocyte recruitment to infected livers

The exit of immune cells from the vasculature to areas of infection in the liver is dependent on a series of well-orchestrated events. Mediators, including TNF-α, activated

complement factors (such as C5a), and CXC chemokines, cause the accumulation of neutrophils in the vasculature of the liver. The expression and interaction of the β_2 integrin/ICAM-1 and β_1 integrin/VCAM-1 adhesion molecules facilitate tight adhesion of neutrophils to the endothelial lining of post-sinusoidal or portal venules. Unlike in other tissues, the expression of selectins is not essential for the adhesion and recruitment of leukocytes to infected livers (75). The process of tight adhesion to, and transmigration through, the endothelial lining triggers the release of gelatinase from neutrophils. This enzyme degrades the extracellular matrix, facilitating passage of the neutrophils into the liver parenchyma (74). In addition to neutrophils, monocytes are also recruited to infected livers. In the case of infection with *L. monocytogenes*, the exit of monocytes from the bone marrow is dependent on chemokine receptor CCR2. However, recruitment to the hepatic foci of infection occurs independently of this chemokine receptor (76).

Liver pathology following infection with *F. tularensis* includes the formation of microabscesses and granulomas that eventually spread throughout the organ. These granulomatous lesions are present by day 4 post-infection and are composed of large numbers of immune cells (77). The formation of granulomas is generally considered a host mechanism that provides a physical barrier to contain the invading pathogen (78). The development of granulomas in the liver is not unique to *F. tularensis* and occurs following infection by other bacteria, including *Brucella abortus*. *B. abortus* replicates to high numbers in hepatocytes, and it subsequently induces apoptotic death of these host cells. Additionally, *B. abortus* promotes the secretion of CXCL8 and increases the expression of ICAM-1 by hepatocytes (79). Furthermore, stimulation of hepatocytes with IL-1β increases the production of CXCL8 and CCL2 (80). Hepatocytes are also capable

of secreting cytokines in response to drug-induced injury. By 24 h following acetaminophen-induced injury, hepatocytes secrete mediators that are capable of inducing macrophages to express proinflammatory cytokines, including CXCL2, CCL2, and CCL3 (81). These observations indicate that hepatocytes can play a role in innate immunity.

V. Bacterial iron acquisition

i. The host as a source of iron

Iron is easily oxidized to the ferric (Fe^{3+}) form or reduced to the ferrous (Fe^{2+}) form. This property of iron makes it important for a myriad of prokaryotic and eukaryotic processes. The most commonly known iron-containing compounds involved in biological processes include cytochromes, which are involved in electron transfer during respiration; oxygen-binding hemeproteins (hemoglobin and myoglobin); metalloproteins in which iron is a cofactor; and numerous enzymes such as catalase. In the case of humans, about 80% of the iron demand is used for the synthesis of hemoglobin, the functional component of the approximately 200 billion new erythrocytes produced daily (82). The remaining pool of functional iron is utilized by muscle and other parenchymal cells for survival and proliferation, while macrophages and hepatocytes are the major sites of iron storage (83).

ii. Iron uptake by mammalian cells

In mammals, duodenal enterocytes are responsible for taking up the daily requirement of 1-2 mg of dietary iron by intestinal absorption (84). Duodenal enterocytes are polarized so that the apical side, characterized by the brush border, is exposed to the contents of the gut lumen while the basal side is in contact with the blood supply (85). The structure of these specialized cells allows the absorption of nutrients from the

intestines and their subsequent transfer to the blood. A key first step in the uptake of dietary iron is its reduction from the ferric to the ferrous form. This reduction is facilitated by a combination of the low pH of the stomach and membrane-associated ferrireductases located on the brush border of duodenal enterocytes. The conversion of ferric to ferrous iron is so critical that if ferrous iron is made unavailable by chelation, uptake of any iron by duodenal enterocytes is inhibited (86). The ferrireductases that perform this essential step include Steap2 and duodenal cytochrome B (DCYTB) (87). Following reduction, ferrous iron is carried across the cell membrane by a protein transporter. The natural-resistance-associated macrophage protein 2 (Nramp2) has been identified as a duodenal iron transporter. The highly conserved Nramp family of proteins transports divalent metallic cations along an electrochemical gradient (88). Nramp2 (also known as DMT1, SLC11A2, and DCT1) is expressed in all tissues; however, based on studies of mice with microcytic anemia, this protein appears to be critical for intestinal absorption of iron and the synthesis of hemoglobin (89). The mechanism of iron transport by Nramp2 is believed to be linked to the movement of H^+ along its electrochemical gradient. Cotransport of iron and H^+ is particularly interesting, because the presence of H^+ within the cell could sustain a low intracellular pH. Furthermore, low intracellular pH levels are likely responsible for allowing iron to remain soluble prior to being bound by specialized proteins such as ferritin (90).

Iron within enterocytes is eventually exported into the blood bound to transferrin. To date, only the ferroportin receptor (also known as SLC40A1, IREG1, and MTP1) has been identified as responsible for the export of iron from cells, including enterocytes. In the case of enterocytes, ferroportin is located on the basal side and exports iron into the

intestinal capillaries (91-93). Inactivation of ferroportin in the intestines of postnatal mice causes severe iron deficiency that can be resolved by parenteral introduction of iron. The resultant iron deficit indicates that the functional ferroportin is required for the absorption of dietary iron in mice (92). Ferroportin is believed to transport ferrous iron. Once iron enters the blood, it is quickly bound by transferrin; however, transferrin only binds ferric iron (85). The conversion of ferrous iron to the ferric form is the role of ferroxidases. Hephaestin is one such ferroxidase necessary for iron egress from duodenal enterocytes to the circulation (FIGURE 3). Hephaestin was discovered in mice suffering from sex-linked anemia, where the hephaestin gene is mutated. In these animals, absorption of iron is normal, but the iron accumulates in the intestinal enterocytes and is eventually lost as these cells are shed (94). Haphaestin is a transmembrane protein and has sequence similarity to ceruloplasmin, a known ferroxidase, suggesting that the two proteins share a similar function (95). There is no evidence to support an interaction between hephaestin and transferrin. However, ferroportin requires the action of a ferroxidase, either ceruloplasmin or hephaestin, to avoid degradation and remain functional (96). Another ferroxidase, amyloid precursor protein, is also expressed in intestinal enterocytes and may have a role in regulating iron absorption (85).

iii. Intracellular distribution of iron

Access of iron to cells is mediated by the surface-bound transferrin receptor 1 (TFR-1). Diferric iron-bound transferrin binds to TFR-1. The cell, via receptor-mediated endocytosis, internalizes the entire complex in a process that involves the formation of clathrin-coated pits and vesicles. Iron is released in the endosome due to a combination of decreased pH, reduction by a Steap family reductase, and association of transferrin with

its receptor. The transferrin-TFR-1 complex is then recycled to the cell membrane where the two components subsequently dissociate. Ferrous iron is transported from the endosome via Nramp2, the same metal transporter that allows entry of ferrous iron into duodenal enterocytes. The iron is then free to be transported, via mechanisms that are not well understood, to areas where it becomes bioactive (97).

iv. Iron homeostasis: storage and turnover

Iron is an essential element, but it is toxic in large quantities due to its ability to catalyze reactions that result in the formation of reactive oxygen species. To prevent iron-related toxicity, iron homeostasis is carefully regulated to equal the body's requirements via a combination of systemic and local cues. These cues control storage and release of iron, as well as recycling of previously used iron. There are no known mechanisms by which iron is systematically removed from the body. However, iron loss occurs most commonly when epithelial cells are shed and through blood loss. At the systemic level, the 25-amino acid peptide hepcidin is the principal regulator of iron absorption and export. This hormone is primarily produced by hepatocytes and is released into the blood. Hepcidin regulates iron export by binding its receptor, ferroportin. The binding of hepcidin to ferroportin causes the internalization and subsequent degradation of the receptor-ligand complex. Degradation of the ferroportin-hepcidin complex occurs in lysosomes and results in the reduction of cellular iron export (85,98,99).

Central to the regulation of hepcidin expression is the bone morphogenic protein (BMP)/SMAD pathway. Several members of the BMP family, but particularly BMP6, are secreted by hepatocytes in proportion to their iron content. BMP6, a member of the TGF-β family of cytokines, binds to the BMP receptor complex, leading to the phosphorylation

and subsequent activation of receptor-regulated cytoplasmic SMAD1, 5, and 8. The activated SMADs then form a complex with SMAD4. The entire SMAD complex translocates to the nucleus, where it leads to the transcription of *HAMP*, the hepcidin encoding gene. Coreceptors, including hemojuvelin, are involved in regulating BMP signaling. Expression of hepcidin is also regulated by a number of other factors including iron transferrin. In this case, the major players are transferrin receptor 2 and hemochromatosis protein. Interaction of the two molecules is required for the induction of hepcidin in response to the levels of transferrin-bound iron. Furthermore, infection, the induction of inflammatory cytokines, activation of the JAK-STAT signaling pathway, erythropoietic activity, and hypoxia are all known to regulate expression of hepcidin (85,98).

At the local level, the uptake and export of iron are regulated by cellular iron content and hypoxia. In intestinal enterocytes, the iron responsive element (IRE) and iron regulatory protein (IRP) system is responsible for regulating iron absorption. This system influences the post-transcriptional regulation of proteins that affect iron metabolism. Under iron-deficient conditions, IRP1 or IRP2 binds to the IRE in the 3' UTR of TFR-1 or Nramp2 mRNA. This binding stabilizes the mRNA and leads to increases in the levels of protein translation. IRP can also bind the IREs located at the 5' end of the mRNA for ferritin, amyloid precursor protein, and a minor splice variant of ferroportin. Under low-iron conditions, this binding inhibits translation of the respective proteins. The major splice variant of ferroportin lacks this IRE, and thus the levels of this protein are maintained during low-iron conditions. Hypoxia-inducible factor (HIF) 2α is part of a larger transcription factor complex that binds to the HIF-responsive elements in the

promoter regions of iron metabolism genes including Nramp2, DCYTB, and ferroportin. This binding leads to increased transcription of the HIF target genes and subsequent increased absorption of iron. Although HIF2α is constitutively expressed by the cells, under normal conditions it is rapidly degraded in the proteosome following hydroxylation by prolyl hydroxylase proteins. However, the levels of HIF2α increase when oxygen levels decrease, causing the activity of the prolyl hydroxylases to also decrease (82,85,98).

Dietary iron is important for maintaining iron homeostasis; however, this source only accounts for a small percentage of the iron in circulation. Macrophages contribute the majority of the iron by recycling iron from damaged and senescent erythrocytes. Another major cell type involved in iron homeostasis is hepatocytes. Hepatocytes function as a major site of storage for iron under normal conditions and in conditions of iron overload. These liver cells have access to iron when it enters the gut, via the portal circulation. Hepatocytes are believed to be capable of taking up transferrin-bound iron via receptor-mediated endocytosis and non-transferrin-bound iron via mechanisms that are not yet clear. Although Nramp2 is present on hepatocytes, the level of expression is low. Furthermore, Nramp2 is known to transport iron along a proton gradient. However, the pH of the hepatocyte extracellular environment is close to neutral, making this an unlikely mechanism of iron absorption (100).

v. Iron and bacterial pathogens

The ability to acquire iron is a fundamental characteristic of intracellular bacterial pathogens. As for mammalian cells, iron is an essential element for bacteria and is required for a number of processes including respiration, DNA synthesis, and scavenging

of free radicals. Bacterial pathogens maintain the homeostasis of iron using a variety of mechanisms. Specialized iron transporters allow the acquisition of iron from the surroundings, and intracellular stores are used to provide iron when external sources are limited. There are also systems that manage redox stress, regulate iron consumption based on iron availability, and employ iron regulatory systems for control of uptake, storage, and consumption of iron (101). In response to infections that result in inflammation, the host restricts availability of iron to the invading organisms. Consequently, bacterial pathogens have developed several mechanisms for acquiring iron from their host. Bacteria can make extracellular iron more accessible by lowering the extracellular pH to increase the solubility of ferric iron, reducing ferric iron to the more soluble ferrous iron, or by using high-affinity iron chelators. Of these mechanisms, reduction to ferrous iron and the use of chelators are the primary ones (102,103).

vi. Mechanism of iron uptake

Many bacteria produce and secrete high-affinity iron chelators called siderophores. The high binding affinity of siderophores for iron allows these molecules to remove iron that is bound to iron-binding proteins such as transferrin and ferritin. It is generally accepted that siderophore synthesis is dependent on the availability of iron in the extra-bacterial environment (103). The siderophore iron acquisition system of *E. coli* has been well studied. In these Gram-negative bacteria, the siderophore-iron complex must cross the outer and inner bacterial membranes and the periplasm in order to enter the cytoplasm. The size of the siderophore-iron complex does not permit passive diffusion into the bacterium. Passage of the siderophore-iron complex across the *E. coli* outer membrane requires the formation of an energy transduction complex comprising

the proteins TonB, ExbB, and ExbD. This TonB protein complex then binds to its receptor in the periplasm and is actively transported across the inner bacterial membrane by an ATP-transporter (103).

Francisella tularensis produces and secretes a siderophore for the acquisition of ferric iron. This siderophore is similar in structure to rhizoferrin and promotes the growth of the LVS and Schu S4 strain in iron-limiting medium (104). When *F. tularensis* is grown in iron-restrictive conditions, the ferric uptake regulator (Fur) and genes of what is now known as the *Francisella* siderophore locus (*fsl*) operon are upregulated (105). It is important to note that the *fur-fsl* locus is highly conserved between the LVS and Schu S4 strain (106). A *fur* homolog and a *fur* box are located upstream of the *fslA* gene, which is followed by *fslB*, *fslC, fslD*, and *fslE*. The arrangement of the *fsl* genes suggests that they are regulated by a *fur*-mediated response to iron and are therefore co-transcribed when iron is limited (104,106). Production of the *F. tularensis* siderophore is dependent on the expression of *fslA* (104). Both *fslB* and *fslD* bear similarities to the major facilitator superfamily of transporters. Based on sequence homology to the *L. pneumophila* transporter, *fslD* is predicted to be the inner membrane siderophore transporter. Utilization of the siderophore is dependent on *fslE,* which functions as the siderophore receptor (106,107). FTT0918, an *fslE* homolog in the Schu S4 strain, is required for the acquisition of siderophore-bound iron. Both *fslE* and FTT0918 contain a signal peptide that indicates that they localize to the bacterial outer membrane. Based on structural prediction, *fslE* forms a β-barrel in the bacterial membrane in a conformation similar to TonB-dependent receptors. However, unlike *fslE*, FTT0918 is not affected by iron availability (106,108,109). There are *fslE* paralogous genes in both the LVS (*fupA*/*B)* and

Schu S4 strain (*fupA* and *fupB)*. Both sets of genes are also predicted to form β-barrels. The LVS *fupA/B* hybrid gene is involved in siderophore acquisition and utilization and is capable of compensating for the loss of *fslE*. Similarly, the Schu S4 paralog *fupA*, but not *fupB*, is involved in iron acquisition and virulence (108).

In addition to ferric iron, bacteria are capable of taking up free ferrous iron from the environment. Uptake of ferrous iron is accomplished via transporters, such as the metal-ABC permeases, that have specificity for divalent ions. In many bacteria, the uptake of ferrous iron is facilitated by the ferrous iron transport system (Feo). The *feo* operon was first discovered in *E. coli* and encodes three proteins, FeoA, FeoB, and FeoC. FeoA and FeoC of *E. coli* are small hydrophilic proteins. The absence of an N-terminal signal sequence suggests that FeoA is a cytosolic protein. FeoC, on the other hand, has structural properties that suggest it acts as a transcriptional regulator for the expression of the *feoABC* operon. The three genes, *feoA*, *feoB* and *feoC*, are Fur-repressed with iron as a co-repressor. FeoB is a large integral cytoplasmic membrane protein that acts as a ferrous permease (110). The N-terminus of FeoB shows similarities to G proteins, and the GTPase activity is required for ferrous iron uptake (111). FeoB homologs are found in all bacterial species, and the general structure is conserved. Mutation of *feoB* in many bacteria, including *Campylobacter jejuni*, *Helicobacter pylori,* and *E. coli*, results in reduced uptake of iron and defects in their ability to colonize the intestines and establish infection (112-114). Mutation of the *Y. pestis* homolog of *feoB* alone does not affect its growth in macrophage-like cells. However, mutation of *feoB,* along with the *yfeAB* genes that are also implicated in ferrous iron uptake, inhibits the growth of this organism in macrophages (115). In *H. pylori*, the *feoB* mutant is unable to acquire iron supplied as

either Fe^{2+} or Fe^{3+}, suggesting that FeoB plays a role in both pathways (112). Homologs of *feoA* and *feoB* have also been identified in *F. tularensis* (116). Transposon mutagenesis of the *F. tularensis feoB* gene diminishes the growth of this pathogen in a murine model of respiratory tularemia (117).

FIGURE 1. Life cycle of *Francisella tularensis* in macrophages. *F. tularensis* is taken up by macrophages via phagocytosis. Following ingestion, the bacteria are contained in a membrane-bound phagosome. The organism inhibits maturation and acidification of the phagosome, which then develops a dense fibrillar coat. The phagosomal membrane subsequently ruptures, releasing the bacteria into the cytoplasm of the macrophage. Once in the cytoplasm of the host cell, *F. tularensis* is free to replicate. Replication of the bacteria leads to the induction of apoptosis of the host cell, and the subsequent release of the organism into the extracellular environment. Reprinted by permission from Macmillan Publishers Ltd: Nature Publishing Group. (Oyston *et al.* Tularemia: Bioterrorism defense renews interest in *Francisella tularensis*. *Nat. Rev. Microbiol*. 2: 967-978), copyright 2004 (118).

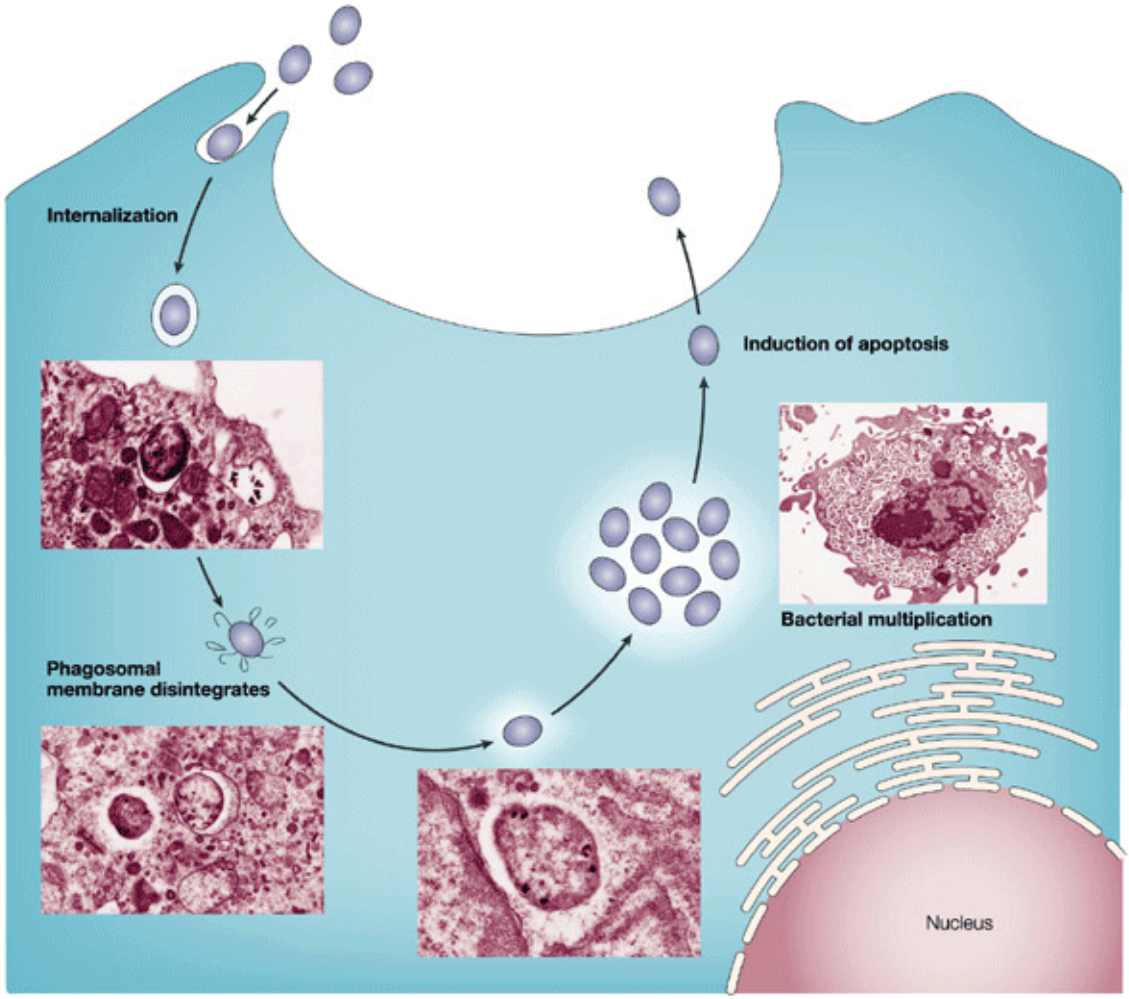
Internalization
Induction of apoptosis
Bacterial multiplication
Phagosomal
membrane disintegrates
Nucleus
Nature Reviews | Microbiology

FIGURE 2. Architecture of the liver. The liver is composed of different types of cells. These cells include endothelial cells that line the vasculature and leukocytes such as natural killer cells, also known as pit cells, and resident macrophages, which are called Kupffer cells when in the liver. The dominant cell type of this organ is hepatocytes, which make up about 80% of the liver. The liver also contains hepatic stellate cells, which provide factors that contribute to the maintenance of hepatocytes.

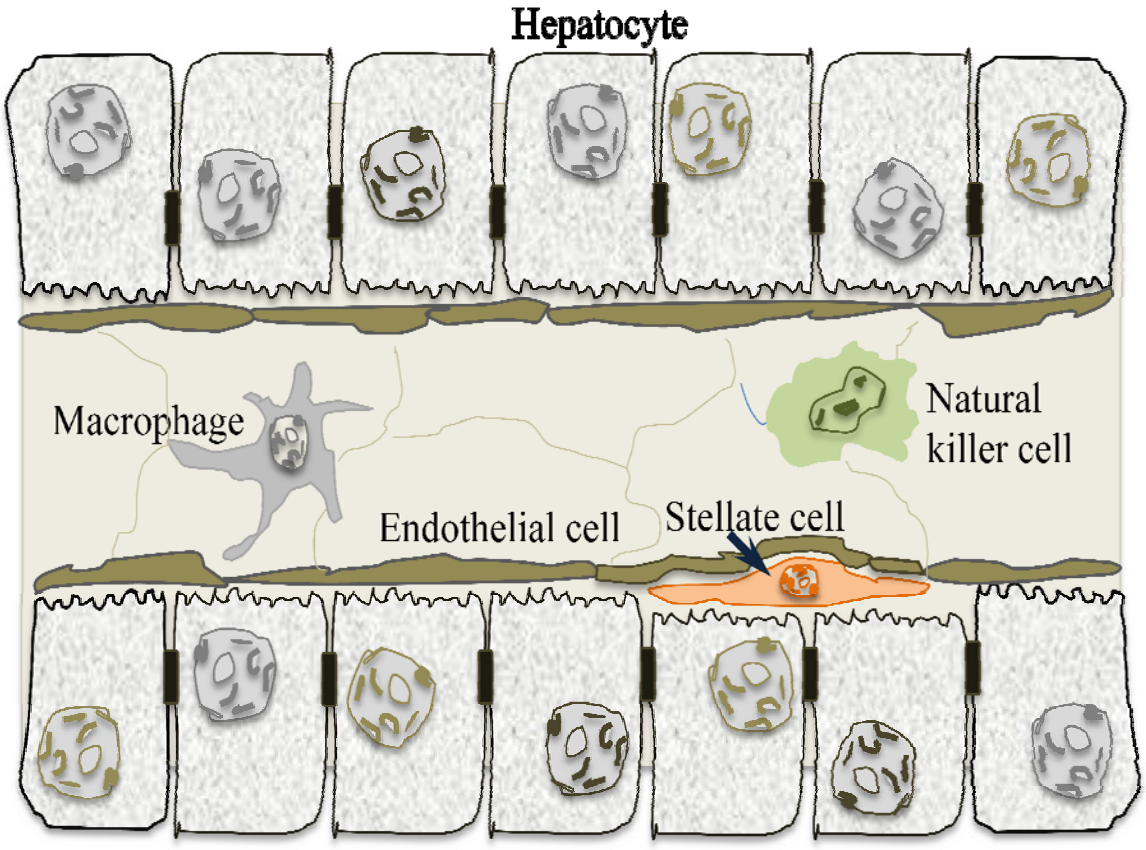
Hepatocyte
Macrophage
Natural
killer cell
Endothelial cell
Stellate cell

FIGURE 3. Transport of iron across duodenal enterocytes. Iron is present in the intestine in a variety of forms, including ferric iron (Fe^{3+}) and bound to ferritin and heme. At the brush border, ferric iron is reduced to ferrous iron by duodenal cytochrome B (Dcytb). Ferrous iron is then transported across the cell membrane via Nramp2 (also called DMT1). The mechanism by which heme and ferritin enter the cell is unknown. Export of intracellular iron into the blood occurs via ferroportin (Fpn1). Once outside of the cell, ferrous iron is oxidized to ferric iron by hephaestin (Hp). At the systemic level, export of iron is inhibited by binding of hepcidin to ferroportin. A complex of ferric iron bound to transferrin (Tf) is transported by the blood. Reprinted from *Journal of Trace Elements in Medicine and Biology*, Vol 26, Fuqua *et al*., Intestinal iron absorption, Pages 115-119., Copyright 2004, with permission from Elsevier (85).

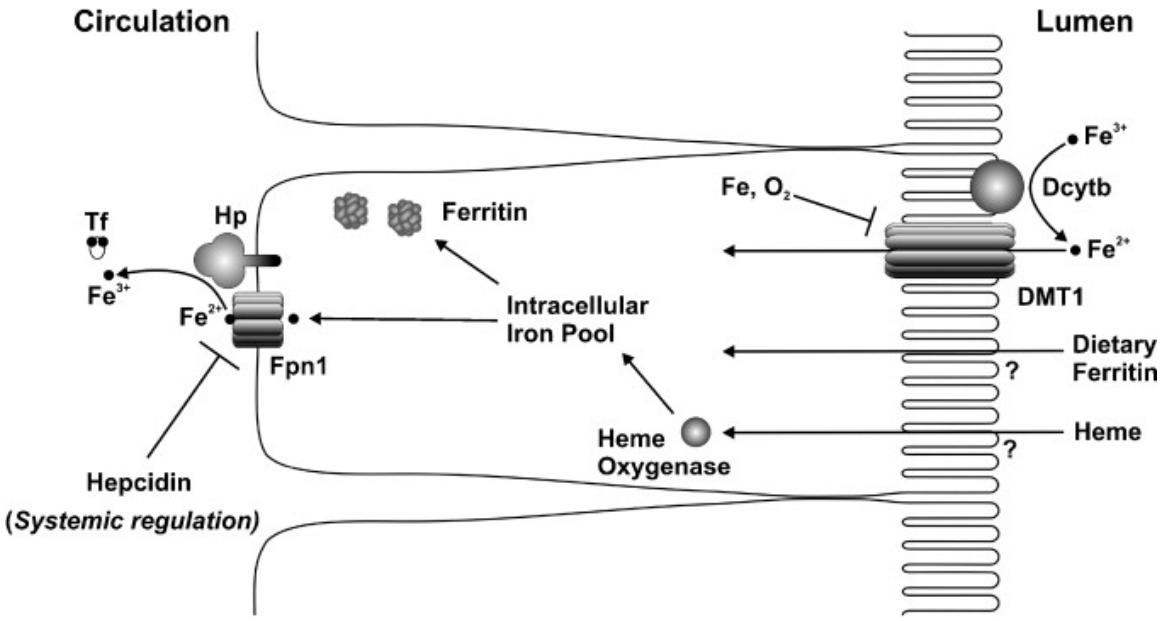
Circulation
Lumen
Fe3+
Dcytb
Fe, O2
Tf
Hp
Ferritin
Fe2+
Fe3+
DMT1
Fe2+
Intracellular
Iron Pool
Dietary
Ferritin
?
Fpn1
Heme
Oxygenase
Heme
?
Hepcidin
(Systemic regulation)

SPECIFIC AIMS

Tularemia is a naturally occurring disease caused by *Francisella tularensis*, a facultative intracellular organism of high virulence and infectivity. The most severe form of *F. tularensis* infection occurs from the inhalation of aerosolized infectious particles, as few as 10 to 50 of which are sufficient to cause disease (6). These properties cause concerns for the potential use of this pathogen as a biological weapon and, as such, it is classified as a Tier 1 select agent. It is likely that *F. tularensis* utilizes its ability to invade and replicate within host cells to evade the host immune system. It is well known that *F. tularensis* grows in macrophages, but it also replicates in non-phagocytic hepatocytes, the main cells of the liver (69,77,119,120). Furthermore, regardless of the route of infection, the liver is a major target of this pathogen. During infection of the liver, leukocytes are recruited to the foci of bacterial replication, and their action results in lysis of infected hepatocytes and subsequent widespread liver damage (69). At the onset of this dissertation project, almost nothing was known of how hepatocytes become infected with *F. tularensis* or of the response of hepatocytes to that infection. I therefore decided to explore the hypothesis that interactions between hepatocytes and *F. tularensis* contribute to the exceptional infectivity and pathogenicity of the organism.

The goal of Aim 1 was to investigate the mechanisms that control interactions between *F. tularensis* and hepatocytes. Despite the fact that this organism invades and replicates to large numbers within hepatocytes, the process by which this pathogen is taken up and its intracellular trafficking pattern once ingested were unknown. For these studies, I examined the role of the hepatocyte cytoskeleton in uptake using an inhibitor of actin polymerization. The contribution of the bacterium was also studied using non-viable

bacteria. *F. tularensis* strains with mutations in genes involved in the type I secretion system and the type IV pilus system were used to investigate the participation of those structures in the uptake process. Collections of *F. tularensis* transposon mutants were screened for genes that are important for *F. tularensis* to be taken up by or replicate in hepatocytes. Lastly, the inflammatory response of primary mouse hepatocytes to infection with *F. tularensis* was studied. Hepatocytes are known to secrete an array of cytokines in response to infection or injury and for the maintenance of liver function. In these experiments, I assessed changes in gene expression and secretion of proinflammatory cytokines by hepatocytes infected with *F. tularensis*.

The goal of Aim 2 was to investigate the role of the FeoB protein in the growth and virulence of *F. tularensis* LVS. Previous studies in our laboratory showed that the *F. tularensis fslC* gene is the most highly upregulated when the bacterium is grown in hepatocytes and is required for production of a siderophore. However, deletion of this gene in the LVS did not affect growth of the organism in liquid culture, leading to a search for a potential compensatory mechanism for iron acquisition. In many bacteria, the ferrous iron transport (Feo) system serves as an alternative pathway for acquisition of ferrous iron, with FeoB being an essential component. In this dissertation, the growth of LVS organisms lacking FeoB was investigated in iron-replete and iron-restrictive media. Intracellular growth of the Δ*feoB* and Δ*fslC* mutants was then investigated in hepatocytes, epithelial cells, and macrophages. The contribution of FeoB and FslC to virulence and colonization of target organs was also evaluated, using the mouse model of tularemia.

MATERIALS AND METHODS

I. Bacterial strains and culture media

Frozen stocks of *F. tularensis* LVS (American Type Culture Collection [ATCC] 28684 provided by Karen L. Elkins, Center for Biologics Evaluation and Research, Food and Drug Administration, Rockville, MD) and *F. tularensis* Schu S4 (Biodefense and Emerging Infections Research Resources Repository, Manassas, VA) were prepared as previously described (65). For each experiment, frozen bacteria were thawed and grown on Chocolate II agar (BD Biosciences) at 37^{o}C in 5% CO_2 for 2 to 3 days. A single colony was used to inoculate MH II broth (BD Biosciences) supplemented with 2% IsoVitaleX Enrichment (BD Biosciences), 5.6 mM D-glucose, 625 µM $CaCl_2$, 530 µM $MgCl_2$, and 335 µM ferric pyrophosphate or BHI broth (BD Biosciences). *F. tularensis* ssp. *novicida* U112 (EBI) was grown on tryptic soy agar (BD Biosciences) at 37^{o}C in 5% CO_2 for 2 days. A single colony was used to inoculate tryptic soy broth. All bacterial cultures were grown to mid-log phase at 37^{o}C with shaking at 100 rpm. The approximate number of colony-forming units (CFU) was estimated by measuring the optical density (OD) at 600 nm.

The *F. tularensis* type I secretion system and type IV pilus mutants were gifts from David Thanassi (Stony Brook University, Stony Brook, NY). The Δ*tolC* and Δ*ftlC* strains were constructed by Horacio Gil (20). The Δ*pilT* mutant, Δ*pilF* mutant, and the Δ*pilE4* mutant that was used to infect AML-12 cells were generated by Subhra Chakraborty (24). The Δ*pilE4* mutant used to infect primary mouse hepatocytes was constructed by Vinaya Sampath. The Δ*fslC*, complemented Δ*fslC*, Δ*feoB,* and complemented Δ*feoB* strains were generated by Huaixin Zheng (Stony Brook University,

Stony Brook, NY) (121). All bacterial deletion mutants were produced by allelic exchange (122). The complemented strains were constructed by chromosomal insertion of the gene of interest (123).

II. Mammalian cells and culture media

The AML12 cell line (CRL-2254; ATCC) was derived from hepatocytes of a mouse transgenic for human transforming growth factor α (124). The AML-12 cells were grown in Dulbecco's modified Eagle medium (DMEM)-F-12 (ATCC) supplemented with 5 μg/ml of insulin, 5 μg/ml of transferrin, 5 ng/ml of sodium selenite, 40 ng/ml of dexamethasone, and 10% heat-inactivated (HI) (56°C for 30 min) fetal bovine serum (FBS; HyClone). The human HH4 hepatocytic cell line was provided by the late Nelson Fausto (University of Washington School of Medicine, Seattle, WA). These cells were cultured in Williams' Medium E (Invitrogen) supplemented with 6.25 μg/ml ITS premix (BD Biosciences), 0.2 mM L-ascorbic acid, 14 mM glucose (Life Technologies), 1 mM sodium pyruvate (BD Biosciences), 2 mM L-glutamine, 10 mM nicotinamide, 100 nM dexamethasone, 20 mM HEPES (pH 7.2-7.5), 20 ng/ml mouse epidermal growth factor (BD Biosciences) and 10% HI FBS (HyClone). FL83B (CRL-2390; ATCC) is a hepatocytic cell line derived from the normal liver of a fetal mouse (125). FL83B cells were cultured in F-12K medium (ATCC) supplemented with 10% HI FBS. A549 (CCL-185; ATCC) is a human lung epithelial cell line derived from carcinomatous pulmonary tissue. A549 cells were cultured in DMEM (Life Technologies) containing 10% HI FBS.

Human macrophages were derived from monocytes isolated from peripheral blood of healthy adult donors as described by Bolger *et al*. (58). Sixty ml of blood was collected and immediately mixed with 1 ml of 7% EDTA, to prevent clotting. The

mixture was then combined with an equal volume of Accuprep Lymphocyte gradient medium (Axis-Shield). The blood was centrifuged at 300 x *g* for 20 min, followed by the collection of the band of peripheral blood mononuclear cells. The monocytes were purified using a MACs Human Monocyte Isolation Kit II, according to the manufacturer's protocol. Purified monocytes were cultured for 5 days in RPMI 1640 medium (Invitrogen) supplemented with 10% HI FBS and 50 ng/ml of macrophage colony-stimulating factor (R&D Systems). Collection of human blood was approved by the Stony Brook University Committee on Research Involving Human Subjects.

Primary mouse hepatocytes were isolated from the livers of 6-12 week old, female C3H/HeN mice (Taconic) via a modification of a multi-step collagenase perfusion method (126,127). Mice were anesthetized via the intraperitoneal route with 100-200 µl of a cocktail of 10% ketamine (100 mg/ml, Butler Laboratories) and 5% xylaxine (100 mg/ml, Akorn, Inc) in saline. The mouse liver circulation was isolated by placing a surgical clamp on the anterior vena cava just above the liver and securing a 24 gauge catheter into the posterior vena cava. The hepatic portal vein was severed to allow drainage of the liver vasculature. The liver was perfused for 10 min with 40 ml of Hank's buffered saline solution (HBSS) without calcium and magnesium (Life Technologies) containing 1 mM EDTA. This was followed by a 5-min perfusion with 20 ml of only HBSS. The organ was then digested by perfusion for 10 min with 40 ml of Eagle's minimum essential medium (EMEM) containing 0.5 mg/ml of collagenase A (Roche) and 0.5 mg/ml of calcium chloride (Fisher). The cells were dispersed and washed three times using EMEM. Cell viability was determined by trypan blue exclusion. In a few cases where the cell viability was lower than 70%, the cells were resuspended in 30% Percoll

(GE Healthcare) and centrifuged for 10 min at 100 x *g* to separate the viable and non-viable cells. To facilitate attachment, primary mouse hepatocytes were cultured in EMEM with 10% HI FBS for 2-4 h in a 37^{o}C, 5% CO_2 environment on 6-well plates (BD Biosciences) that were previously coated with 0.6 mg/ml of type I rat tail collagen (BD Bioscience). Following attachment of the cells to the culture dish, the attachment medium was replaced with hepatocyte growth medium. The formula for the hepatocyte growth medium was provided by Kari Nejak-Bowen (University of Pittsburgh, Pittsburgh, PA). The exact components of this medium have not yet been published, and it has been requested that we not include the full formulation. However, a similar medium has been used previously to culture primary rat hepatocytes (126). These studies were approved by Stony Brook University's Institutional Animal Care and Use Committee.

All supplements for the various media were from Sigma-Aldrich unless otherwise indicated.

III. Analysis of the purity of hepatocyte cultures

Cardiac puncture was used to collect 500 µl of blood from an anesthetized C3H/HeN mouse (Taconic). The sample was immediately centrifuged at 209 x *g* for 5 min. The pellet was resuspended in 0.15 M ammonium chloride, 10 mM potassium bicarbonate, and 0.1 mM EDTA, pH 7.2, to lyse red blood cells. As soon as the sample became clear, phosphate buffered saline (PBS) (Life Technologies) was added, and the mixture was centrifuged as above. The pellet was resuspended in PBS and smeared onto glass slides. The slides were dried and used as a positive control for the visualization of leukocytes. Additionally, sections were prepared from the liver of a C3H/HeN mouse. The liver was excised, placed on ice in a 50-ml tube, and submitted to the Research

Histology Core Laboratory (Department of Pathology, Stony Brook University, Stony Brook, NY) for cryo-sectioning. The liver sections were mounted on slides and used as positive controls for the visualization of endothelial cells.

To assess the purity of primary mouse hepatocytes, freshly isolated cells were plated in 6-well plates on glass coverslips that were coated with collagen as previously described. The leukocyte smears, liver sections and hepatocyte cultures were fixed for 20 min with 2.5% paraformaldehyde (Electron Microscopy Sciences) in PBS. The samples were blocked with 3% bovine serum albumin (Sigma-Aldrich) in PBS for 5 min at room temperature. The presence of leukocytes was determined by incubating the smears or hepatocyte cultures with a rat anti-mouse CD45 monoclonal antibody or a rat IgG2b isotype-matched control antibody (both from eBioscience). The presence of endothelial cells was examined in hepatocyte cultures and liver sections using a rat anti-mouse CD31 primary monoclonal antibody or a rat IgG2a isotype-matched control antibody (both from eBioscience). In all the studies, primary antibodies were diluted 1:25 in PBS, and 25 µl were applied to specimens for 30 min. The specimens then were incubated for 30 min with a 1:100 dilution of tetramethylrhodamine isothiocyanate (TRITC)-conjugated goat anti-rat IgG secondary antibody (eBioscience). Samples were mounted with VectaShield mounting medium containing 4',6-diamidino-2-phenylindole (DAPI) (Vector Laboratories, Inc) for analysis with a Zeiss Axioplan 2 fluorescence microscope (Carl Zeiss MicroImaging, Inc).

IV. Construction of LVS gene-deletion mutants

To produce an in-frame deletion of the genes FTL_0009, FTL_0687 and FTL-1371/1372, total bacterial DNA was isolated using the GenElute Bacterial Genomic

Miniprep kit (Sigma). An upstream and downstream fragment of each gene was amplified using the Platinum PCR SuperMix High Fidelity kit (Invitrogen). The primers used for the upstream and downstream fragments of these genes are shown in TABLE 1. The fragments for each gene and the pMP812 plasmid vector (a gift from Martin S. Pavelka, Jr., University of Rochester Medical Center, Rochester, NY) were digested with Sal I (Roche) and BamHI (Roche), then separated by agarose gel electrophoresis and purified using the Qiaquick Gel Extraction Kit (Qiagen) (122,128). The fragments then were ligated and inserted into the pMP812 plasmid (128). Correct insertion of the fragments was verified by using the PCR primers pMP812F and pMP812R (TABLE 1). The plasmid vector then was transformed into competent *E. coli* DH5α for amplification. The amplified plasmids were purified using agarose gel electrophoresis and used to transform the LVS by electroporation. Deletion of the specific genes was achieved by allelic exchange as previously described (122). Colonies that were successfully transformed were identified by their resistance to sucrose and those that underwent allelic exchange by their sensitivity to kanamycin. The deletion of each gene was verified by PCR and by DNA sequencing using gene-specific primers 1 and 2 (TABLE 1).

V. Preparation of bacterial DNA for sequencing

Bacterial genomic DNA was isolated using the GenElute Bacterial DNA Isolation Kit (Sigma) according to the recommendations of the manufacturer. Samples of bacterial DNA were prepared for sequencing by combining 1 ng of DNA with 3.2 pM of primer in RNAase/DNAse free water (Life Technologies) to bring the final volume of the sample to 8 µl. The TnSeqF1 and TnSeqR1 primers were used to sequence the LVS transposon mutants (TABLE 1). These primers are positioned within the Tn5 transposon and read in

either direction. For sequencing of the ssp. *novicida* mutant FTN::1276, Kan2 transposon specific primers were used (TABLE 1). The samples were submitted to the DNA Sequencing Facility (Stony Brook University) for further processing.

VI. Intracellular growth of bacteria

To quantify the numbers of intracellular bacteria, a target number of 2.5 x 10^5 hepatocytes were cultured in 24-well dishes (Corning). Prior to infection, the actual number of hepatocytes was determined. Bacteria were grown in supplemented broth, then centrifuged at 4,000-5,000 x *g* for 10 min. The pellet was resuspended in the appropriate cell culture medium to the desired multiplicity of infection (MOI). The number of bacteria was estimated by measuring the OD_{600}, and the precise number was determined by retrospective plating on Chocolate II agar. Infection protocols were carried out for each type of host cell as follows: primary mouse hepatocytes, MOI of 150 for 3 h; hepatocyte cell lines, MOI of 150-5000 for 2-3 h; epithelial cells, MOI of 250 for 3 h; and macrophages, MOI of 50 for 2 h. After addition of the bacteria, plates were centrifuged at 240 x *g* for 5 min for FL83B cells or 252 x *g* for 5 min for all other cells. The cells were then incubated at 37°C for the times indicated above to allow uptake of the bacteria. After incubation, the cultures were washed and treated with 5 to 25 µg/ml of gentamicin (Invitrogen) for 1 h to kill extracellular organisms. At this point, some cultures were washed and lysed with 1 ml of saponin (Sigma-Aldrich) (10 mg/ml in PBS) for 15 min at 37°C to measure uptake. To measure replication, infected hepatocytes or epithelial cells were incubated until 24, 48, or 72 h post-infection in the presence of gentamicin, and macrophages were cultured for an additional 13 h in antibiotic-free medium. Lysis was then performed as for the 4-h time point. The bacterial lysates were

serially diluted in PBS. Ten µl of each dilution was plated on Chocolate II agar. The plates were incubated at for 48 h 37°C, and CFU were enumerated.

A 96-well assay was used to screen an LVS transposon collection for mutants with altered uptake by and replication in hepatocytes. This collection was generated by Varya Kirillov (Stony Brook University, Stony Brook, NY). The library consists of 5542 mutants carrying random insertions of the EZ Tn5 transposon (Epicentre Biotechnologies). Each mutant and the wild-type LVS were grown for 48 h in 96-well plates (Corning). The OD_{600} was measured on a plate reader (VERSAmax, Molecular Devices) to confirm bacterial growth. Mutants that did not grow were not used in the subsequent infection assay. Hepatocytes were also plated in 96-well dishes (5×10^4 cells in 100 µl of growth medium) and infected with 5 µl of each bacterial strain. The plates were centrifuged at 252 x *g* for 5 min, then incubated for 3 h at 37°C to allow uptake of the bacteria. After incubation, the cultures were washed and cultured with 5 to 25 µg/ml of gentamicin for 1 h to measure uptake or 21 h to measure replication. Following incubation, cultures were washed and lysed with 50 µl of saponin (10 mg/ml in PBS) for 15 min at 37°C. The hepatocyte lysates (2 to 5 µl) were spotted on Chocolate II agar. After 48 h of incubation at 37°C, growth of the bacterial strains was compared to that of the wild-type LVS.

VII. Visualization of *F. tularensis* by immunofluorescence

To view *F. tularensis* microscopically, infected cells on coverslips were washed and fixed for 20 min with 2.5% paraformaldehyde (Electron Microscopy Sciences) in PBS. In some experiments, the cells were differentially stained to distinguish between intracellular and extracellular bacteria. In those studies, the hepatocytes were blocked

with 3% bovine serum albumin in PBS for 5 min at 37°C. Samples were then incubated with mouse anti-*Francisella tularensis* LPS 12.4 monoclonal antibody (10 μg/ml) (a gift from Anne Savitt, Stony Brook University) followed by Cy3-conjugated donkey anti-mouse Ig secondary antibody (1:300) (Jackson Immuno Research). The cells were then permeabilized with 0.5% Triton X-100 (Sigma-Aldrich) in PBS for 5 min at 37°C, blocked with 3% bovine serum albumin, and incubated sequentially with rabbit antiserum to *F. tularensis* LVS (1:100) (also a gift from Anne Savitt) and fluorescein isothiocyanate (FITC)-conjugated goat anti-rabbit Ig secondary antibody (BD Biosciences). Hepatocytes were incubated at room temperature for 30 min with 25 μl of each antibody. For experiments where distinction between intracellular and extracellular bacteria was not necessary, only the second staining protocol was used. Coverslips were mounted with either VectaShield mounting medium containing DAPI or SlowFade Light Antifade medium (Molecular Probes) for analysis with a Zeiss Axioplan 2 fluorescence microscope.

VIII. Mechanism of uptake of *F. tularensis* by hepatocytes

Stocks of cytochalasin D (Sigma-Aldrich) were prepared at 1 mg/ml in dimethyl sulfoxide (DMSO) (Research Organics). Two hours before infection, hepatocytes were incubated in medium alone, medium containing 0.2% DMSO, or medium containing 3.9 μM cytochalasin D. The hepatocytes were infected at the previously described MOIs for 3 h with the LVS in medium alone or with the LVS in the presence of 3.9 μM cytochalasin D or 0.2% DMSO. Following the infection, hepatocytes were incubated with medium containing 5 μg/ml of gentamicin until the end of the experiment. CFU assays were conducted at 24 h post-infection. Chloramphenicol (Sigma-Aldrich) stocks

(2 mg/ml) were prepared in ethanol. Fifteen minutes before infection of the hepatocytes, the bacteria were pelleted and resuspended in the appropriate hepatocyte culture medium containing 2 μg/ml of chloramphenicol. Hepatocytes then were infected with the LVS for 4 h in the presence of chloramphenicol, and uptake was analyzed by immunofluorescence. For the preparation of fixed LVS organisms, the appropriate number of bacteria in MH II broth was centrifuged for 10 min at 300 x *g*. The bacterial pellet was resuspended in 4% paraformaldehyde fixation buffer (BioLegend) and incubated in the dark at room temperature for 10 min. Following the incubation, the bacteria were again centrifuged for 10 min at 300 x *g*, and the fixation buffer was removed. The bacteria were then washed three times with cell culture medium. To verify complete killing of the organisms, 10 μl of the bacterial preparation was plated on Chocolate II agar. The plate was incubated at 37^{o}C with 5% CO_2 for 48 h and then inspected for bacterial growth. For killing with heat, the appropriate number of bacteria in MH II broth was centrifuged for 10 min at 300 x *g*. The bacterial pellet was then resuspended in the relevant hepatocyte growth medium and incubated in a 56^{o}C water bath for 1 h. The bacterial sample was gently swirled every 15 min to ensure even heat distribution. Following incubation, complete killing of the organism was verified as described above for the fixed bacteria.

IX. Measurement of hepatocyte gene expression following LVS infection

Mouse Proinflammatory Cytokines & Receptors RT^2 Profiler PCR Arrays (Qiagen) were used to analyze the expression of genes by hepatocytes infected with *F. tularensis.* The RT^2 Profiler Array includes the probes for 84 genes encoding proinflammatory cytokines and receptors, five housekeeping genes, a genomic DNA

control, and three PCR efficiency controls. Primary mouse hepatocytes were left uninfected, sham-infected, or infected with the LVS at an MOI of 150 for 8 h. The cultures then were washed, and five volumes of RNA Cell Protect reagent (Qiagen) were added to each culture. The cells were subsequently collected and pelleted by centrifugation at 5000 x *g* for 5 min. Total hepatocyte RNA was isolated using the RNeasy Mini kit (Qiagen, Valencia, CA). The RNA was converted to cDNA by reverse transcription PCR using the RT^2 First Strand Kit (Qiagen). The cDNA was combined with the RT^2 SYBR Green Mastermix (Qiagen) and then used as a template for real-time PCR. Twenty-five µl of the cDNA and master mix was dispensed into each well of a RT^2 Profiler Array. These experiments were completed with LVS grown in MH II broth or BHI broth, or with LVS that was grown in MH II broth then heat-killed.

The preparation of material from heat-killed bacteria was produced as described by Bublitz *et al*. (66). LVS organisms grown in MH II broth were killed by heating at 56^{o}C for 1 h as described above. The killed bacteria were then further incubated at 37^{o}C for 24 h to permit lysis of the bacteria. Following the incubation, the lysed bacteria were centrifuged at 2560 x *g* for 10 min to remove bacterial debris. A portion of the supernatant was removed to verify complete killing by plating on agar. The remaining supernatant was stored at -80^{o}C until use. A 1:10 dilution of the material from heat-killed LVS was added to hepatocytes to evaluate their transcriptional response.

X. Measurement of cytokine secretion by hepatocytes infected with the LVS

Primary mouse hepatocytes were left uninfected, sham-infected or infected for 24 h or 48 h with the LVS at an MOI of 150. Following the infection, the conditioned media were collected, and LVS organisms were removed by centrifugation for 10 min at 2560 x

g. The conditioned media were assayed using individual ELISA kits (R&D) for the presence of CXCL5, CXCL1, CCL2, and CCL20 according to the manufacturer's protocol.

XI. Growth of bacteria in iron-replete and iron-restricted media

Growth of the LVS, the Δ*fslC* and Δ*feoB* mutants, and their complemented strains was evaluated using Chamberlain's defined medium (CDM). To prepare Chelex-100-treated CDM (Che-CDM) with known levels of iron, CDM lacking $FeSO_4$ and $MgSO_4$ was treated twice with 1% (wt/vol) Chelex-100 (sodium form; Bio-Rad Laboratories) overnight with stirring, and the beads were removed by filtration (109). The medium then was supplemented with essential divalent cations (550 μM $MgSO_4$, 1.5 μM $ZnSO_4$, 0.2 μM $CuCl_2$, 1 μM $MnCl_2$, and 5 μM $CaCl_2$). Che-CDM was prepared with highly purified water and stored in plastic bottles to avoid any contamination with iron. Che-CDM supplemented with 7.2 μM $FeSO_4$ is considered to be replete with iron; that with 720 nM or less is considered to have restricted iron (104). Bacteria of each strain were scraped from Chocolate II agar plates and resuspended in Che-CDM with 7.2 μM $FeSO_4$ to the same OD_{600}. Equal volumes were inoculated into Che-CDM with 7.2 μM $FeSO_4$, grown overnight to approximately the same OD_{600}, and washed three times with PBS. The OD_{600} of suspensions of each strain were adjusted to the same level, and 500 μl was inoculated into Che-CDM supplemented with various amounts of a freshly prepared solution of $FeSO_4$. Bacterial growth then was assessed by determining the OD_{600} of the cultures at different times.

XII. Infection of mice with *F. tularensis*

To measure the ability of *F. tularensis* to disseminate to and/or grow in organs of inoculated mice, the wild-type LVS or mutant strains were grown overnight in MH broth to exponential phase. Groups of 3 to 5 C3H/HeN mice (Taconic, Hudson, NY) from 6 to 8 weeks old were infected intradermally with sublethal inocula (3×10^5 CFU in 100 µl of PBS). We chose to use intradermal infections for these studies, since they yield more consistent results than intranasal inoculation. The mice were euthanized on day 3 postinfection, and their lungs, livers, and spleens were harvested and weighed. Organs were homogenized in PBS in sterile Whirl-Pak bags (Nasco), and serial dilutions of the homogenates were plated on Chocolate II agar to determine the CFU per g of tissue. To test the ability of the LVS mutant strains to cause fatal disease, groups of 5 mice were infected intradermally with 2×10^7 CFU. In our experience, this is the smallest inoculum of the LVS that reproducibly causes death of wild-type animals. The mice then were monitored, and the time of death was recorded. The infectious doses for all experiments were confirmed by retrospective plating. These studies were approved by Stony Brook University's Institutional Animal Care and Use Committee.

XIII. Statistics

The results from organ burden assays were analyzed using the Kruskal-Wallis test for nonparametric data, followed by the Dunn's multiple-comparison post-test. The log-rank test was used to analyze survival of infected mice. Statistical significance of all other data was determined using an unpaired analysis of variance and the Tukey-Kramer multiple-comparison posttest (Prism version 5.0; GraphPad Software, San Diego, CA). With Bonferroni's correction, a difference between survival curves was considered

significant if the *P* value was less than 0.008. For all other studies, the criterion for significance was a *P* value of less than 0.05.

TABLE 1: List of primers. Primers 1 to 16 were used for generation and verification of the *F. tularensis* LVS mutants LVSΔ0009, LVSΔ0687, and LVSΔ1371/1372. Primers 17 and 18 are specific to the Tn5 transposon and were used to determine the location of the insertion mutation in the LVS::9a1E and LVS::9a5B mutants.

No.	PRIMER	SEQUENCE
1	0009 #1	TAAATGGATCCGGATAAATTAGGTATTGAGCGT
2	0009 #2	GAAATATTATTGCATCTTAGCTATTTTTTCTTCCTTGCTTGTTGAGC
3	0009 #3	GCTCAACAAGCAAGGAAGAAAAAATAGCTAAGATGCAATAATATTTC
4	0009 #4	ACGTGTCGACGTACAAAAACCTGCTCAAAACCTT
5	0687 #1	TAAATGGATCCGCAAGCAAACTTTTCTCCTACCGC
6	0687 #2	ACGTGTCGACCTCACCTAATTTAAACTGCCTAGCG
7	0687 #3	TTTCGTATCATTGTTGTGACCTATTCTGACATTTTTAATTATCCTATAATAATTT
8	0687 #4	AAATTATTATAGGATAATTAAAAATGTCAGAATAGGTCACAACAATGATACGAAA
9	1371 #1	TAAATGGATCCCTGGAATTACAAGTAATAGTGTACTAAAACCAA
10	1371 #2	GGACCACATCCACCAGAGAACTTCCAAACTCCATCTTATCTTCCCTAC
11	1372 #3	GTAGGGAAGATAAGATGGAGTTTGGAAGTTCTCTGGTGGATGTGGTCC
12	1372 #4	TAATGTCGACGAAACTAGTTCAGGATAATGAAATCTACTACTTT
13	pMP812F	TGTGGATAACCGTATTACCGCCTTTGAG
14	pMP812R	ATCCATCTGACTACTTACTAGATGG
15	Kan2F	AACAAAGCTCTCATCAACCGTGGC
16	Kan2R	CCCGTTGAATATGGCTCATAACACCC
17	Tn5SeqF1	ACGACTACGCACTAGCCAACAAGA
18	Tn5SeqR1	CCAATATGCGAGAACACCCGAGAA

Chapter 1: Interactions between hepatocytes and *Francisella tularensis*

RESULTS

I. Replication of *Francisella tularensis* in hepatocyte cell lines

It has been reported that *F. tularensis* replicates in murine hepatocytes *in vivo* (69,77,78,120) and in hepatocytic cell lines (44,119,121,129,130). To confirm that *F. tularensis* grows in the hepatocytic cell lines that we intended to study, the LVS or the ssp. *novicida* U112 strain was incubated with human HH4 or murine AML-12 hepatocytic cell lines for 3 h to permit uptake of the bacteria. Incubation was continued in medium containing gentamicin for an additional 1 h or 21 h to kill all extracellular bacteria. The intracellular bacteria were quantified after 4 h and 24 h of infection. The numbers of U112 bacteria increased by more than two logs in both the HH4 and AML-12 hepatocytes (FIGURE 4). Similarly, after 24 h the LVS increased by about two logs in the AML-12 hepatocytes (FIGURE 4B), although the number of CFU recovered in the HH4 line at the later time point was less extensive (FIGURE 4A). These results clearly demonstrate that human and murine hepatocytic cell lines support the replication of *F. tularensis*.

Initial infection assays with the AML-12 and HH4 hepatocytes were performed using MOIs that ranged from 2000 to 5000. However, due to concern that the high numbers of bacteria did not reflect physiological conditions, the relationship between MOI and uptake was explored. For these studies, HH4 hepatocytes were infected for 3 h at MOIs ranging from 150 to 3500. The infected cells then were treated with gentamicin for 1 h to kill the extracellular bacteria. The number of ingested bacteria was subsequently enumerated by CFU assay. Interestingly, the amount of bacteria taken up by

the hepatocytes was similar throughout the range of MOIs (FIGURE 5). This observation suggests that hepatocytes have a finite capacity to take up *F. tularensis*. As a result, a target MOI of 150 was used for all subsequent experiments.

II. Isolation and culture of primary mouse hepatocytes

Initial studies exploring interactions between *F. tularensis* and hepatocytes employed hepatocytic cell lines. However, in order to obtain results more relevant to the *in vivo* situation, it was necessary to use primary cells. Primary mouse hepatocytes were isolated as described in Materials and Methods using a three-step protocol. The cells were grown on collagen-coated plates and remained viable for up to 7 days after plating (FIGURE 6A).

The liver contains other cells, such as leukocytes and endothelial cells, which are capable of interacting with *F. tularensis*. Therefore, prior to investigating the response of hepatocytes in primary cultures, it was necessary to confirm the absence of contaminating cells of these lineages. The purity of the primary hepatocyte cultures was investigated by immunofluorescence assays using antibodies against CD45 to identify leukocytes and CD31 to identify endothelial cells. Cultures from three independent isolations were examined, and in all cases no contaminating cells of these types were detected. The efficacy of the antibodies was confirmed by staining mouse leukocytes for CD45 (FIGURE 6B) or a section of mouse liver for CD31 (FIGURE 6C).

III. Uptake and replication of the LVS and Schu S4 strain in primary mouse hepatocytes

As described above, *F. tularensis* LVS is taken up by murine AML-12 hepatocytes and human HH4 hepatocytes. Furthermore, this organism replicates

extensively within the AML-12 cells. Experiments were conducted to measure the extent to which primary mouse hepatocytes ingest and support the replication of *F. tularensis* LVS and Schu S4. Primary mouse hepatocytes were incubated with the LVS or highly virulent Schu S4 strain at an MOI of 150 for 3 h. Extracellular bacteria then were killed by incubation in medium containing gentamicin until 4, 24, or 48 h post-infection. Intracellular bacteria were quantified by CFU assay at the various time points. A total of seven experiments was performed with the LVS, and in all cases more than 10^4 organisms were recovered from the primary hepatocytes at the 4 h time point. In four experiments (Experiments 1-4 in TABLE 2), similar numbers of the LVS were recovered from the hepatocytes at the 24 h time point, compared with 4 h. Two of those four experiments were extended to 48 h. In one instance, the CFU recovered at the 48 h time point were lower than at the 24 h point. In the second experiment, there was no difference in the CFU recovered at 24 h and 48 h. In another three independent studies (Experiments 5-7 in TABLE 2), lower numbers of organisms were recovered after 24 h than after 4 h. These data indicate that the LVS is taken up by primary mouse hepatocytes. Although viable bacteria persisted in the cells, there was no net increase in the number of organisms with time.

In a single experiment conducted with the Schu S4 strain (Experiment 8 in TABLE 2), an average of 10^3 bacteria was recovered after 4 h. By 24 h, there was no significant change in the number of CFU recovered. By 48 h, however, the numbers of bacteria within those cells increased significantly. This study suggests that *F. tularensis* Schu S4 is not only taken up by but also replicates in primary mouse hepatocytes.

IV. Role of the actin cytoskeleton in the uptake of *F. tularensis* by hepatocytes

Polymerization of globular actin to the filamentous form is a critical process required for rearrangement of cell membranes. Many bacteria are capable of triggering this process to facilitate their uptake by host cells (131-134). While the specific process and mediators of invasion vary among species, the end result is the induction of uptake of the bacteria by the host cell. Cytochalasin D, an inhibitor of filamentous actin formation, was used to determine the role of actin polymerization in the uptake of *F. tularensis* by hepatocytes. The ability of AML-12 hepatocytes treated with the inhibitor to internalize the LVS was determined using immunofluorescence microscopy (FIGURE 7A-C) and CFU assays (FIGURE 7D). CFU assays were also carried out in primary mouse hepatocytes (FIGURE 7E). The immunofluorescence study showed that uptake and subsequent replication of *F. tularensis* in AML-12 hepatocytes treated with cytochalasin D (FIGURE 7C) were greatly diminished compared with untreated cells (FIGURE 7A) or cells treated with DMSO, the vehicle for cytochalasin D (FIGURE 7B). Similarly, CFU assays confirmed that 98% fewer bacteria were taken up by and replicated in AML-12 hepatocytes treated with cytochalasin D (FIGURE 7D), and 95% fewer bacteria were ingested by and replicated in treated primary mouse hepatocytes (FIGURE 7E). These studies determined that polymerization of the hepatocytes' actin cytoskeleton is required for efficient infection by *F. tularensis*.

V. Uptake by hepatocytes of killed LVS or LVS incapable of synthesizing new proteins

Following the observation that ingestion of *F. tularensis* by hepatocytes requires polymerization of the host actin cytoskeleton, the question of the bacterial state needed

for uptake arose. Specifically, it was examined whether the bacteria would still be taken up if they were dead or unable to synthesize new proteins. To address this question, AML-12 hepatocytes (FIGURE 8A-E) or primary mouse hepatocytes (FIGURE 8F-J) were incubated for 4 h with live, chloramphenicol-treated, heat-killed, or formalin-fixed LVS organisms. Chloramphenicol prevents the bacteria from synthesizing new proteins. Uptake of the bacteria was analyzed by differential immunofluorescence labeling, where bacteria internalized by the hepatocytes appear green and external bacteria appear orange (FIGURE 8A-D and F-I). In all cases, the bacteria were readily taken up by hepatocytes, as indicated by the numbers of green bacteria within the hepatocytes. Quantitation of the number of internalized bacteria per field at 40X magnification confirmed that AML-12 cells (FIGURE 8E) and primary mouse hepatocytes (FIGURE 8J) take up live and killed *F. tularensis* with similar efficiency. These studies raise the possibility that *F. tularensis* utilizes a pre-formed surface structure to mediate its uptake by hepatocytes.

VI. Involvement of the *F. tularensis* type IV pilus and type I secretion systems in uptake by hepatocytes

All *F. tularensis* subspecies contain homologs of genes responsible for the biogenesis of type IV pili. Furthermore, these structures are present on the surface of both the LVS and the Schu S4 strain and have been implicated in adherence of *F. tularensis* to host cells (23,24). The type IV pilus system is composed of several different proteins, and absence of PilT, PilF, or PilE results in loss of pilus expression (24). To determine whether these pili participate in interactions of *F. tularensis* with hepatocytes, CFU assays were conducted using LVS mutants in which *pilT*, *pilF*, or *pilE4* was deleted. Uptake of the mutants by AML-12 cells and primary mouse hepatocytes was measured

following 4 h of infection. The three mutants were observed to be taken up at a level similar to the wild-type LVS by both AML-12 hepatocytes (FIGURE 9A) and primary mouse hepatocytes (FIGURE 9B). Therefore, type IV pili are not required for internalization of *F. tularensis* by hepatocytes.

Gram-negative bacteria often contain secretion systems that allow them to inject virulence factors into host cells (19). These secretion systems facilitate the transport of a wide range of protein effectors to the bacterial surface by providing a channel across the inner membrane, periplasm, and outer membrane of the organism. Some of these effectors can provide an uptake "signal" for the internalization of the organism (135). The requirement for the *F. tularensis* type I secretion system for the uptake of the bacterium by hepatocytes was investigated using LVS mutants lacking *tolC* or *ftlC.* These two genes are orthologs of *E. coli tolC,* a main component of its type I secretion system. AML-12 hepatocytes or primary mouse hepatocytes were infected with the LVS mutants for 4 h to permit uptake of the bacteria. CFU assays then were used to enumerate the intracellular organisms. Similar numbers of the Δ*tolC* and Δ*ftlC* mutants compared to the wild-type LVS were internalized by both AML-12 hepatocytes (FIGURE 10A) and primary mouse hepatocytes (FIGURE 10B). As for type IV pili, then, the *F. tularensis* type I secretion system is not required for uptake of the bacterium by hepatocytes.

VII. Screen of a ssp. *novicida* transposon library and an LVS transposon collection for mutants deficient in the ability to be taken up by or replicate in hepatocytes

A comprehensive ssp. *novicida* transposon library (4) was used to look for mutants with altered uptake by or replicative ability in hepatocytes, compared to the

U112 parental strain. Thirty-nine strains with transposon insertions in genes encoding known or putative outer-membrane proteins were used to infect AML-12 hepatocytes. This screen revealed two mutants, FTN::0119 and FTN::1276, that exhibited altered uptake compared with the wild-type strain, as confirmed by immunofluorescence microscopy (FIGURE 11A) and CFU assays (FIGURE 11B and C). FTN_0119 encodes a hypothetical protein. Based on sequence homology FTN_1276 is believed to encode a membrane fusion protein (http://www.ncbi.nlm.nih.gov). Unexpectedly, both strains showed an enhanced, rather than diminished, ability to be taken up by AML-12 hepatocytes after 4 h of infection. The CFU experiment was repeated two more times, and in both cases the mutants exhibited a modestly, but significantly, enhanced uptake. In these experiments, replication was calculated as a fold change by dividing the CFU recovered at 24 h by the CFU recovered at 4 h. This calculation compensates for differences in uptake of strains. In all three experiments, the FTN::0119 strain replicated less than the wild-type strain (FIGURE 11C). The FTN::1276 mutant, on the other hand, replicated comparably to the wild-type in two cases (FIGURE 11C) and nearly twice as well as the wild-type strain in a third experiment.

Ssp. *novicida* is different enough from ssp. *holarctica* that it is often classified as a separate species; thus it was necessary to replicate these mutations in the LVS. FTN_0119 corresponds to FTL_0009. A targeted deletion of FTL_0009 was constructed in the LVS strain, producing a strain denoted LVSΔ0009. Uptake and replication of the LVSΔ0009 mutant was quantified in three independent CFU assays using AML-12 cells. In one of the three cases, this mutant displayed enhanced uptake compared to the wild-type LVS, a phenotype that was shared with the corresponding ssp. *novicida* mutant. In

the other two studies, however, uptake of LVSΔ0009 organisms was lower than or comparable to that of the wild-type bacteria (FIGURE 12A). Replication was measured as the fold change in CFU between 4 and 24 h. In only one instance was growth of LVSΔ0009 comparable to that of the wild-type strain. In the other two experiments, replication of the mutant was either enhanced (FIGURE 12B) or diminished compared to the wild-type strain.

FTN_1276 is homologous to FTL_0687, and a successful deletion of the corresponding LVS gene was made. A total of six CFU assays was completed with the LVSΔ0687 mutant. In one experiment, the mutant displayed enhanced uptake compared to the wild-type LVS, similar to its ssp. *novicida* counterpart. However, in three other studies, its uptake was comparable to the parental LVS (FIGURE 12A), while two additional experiments showed uptake that was diminished compared to the wild-type strain. Replication, as determined by fold change, was modestly but consistently higher than that of the parental LVS (FIGURE 12B). These observations prompted a verification of the site of transposon insertion in the U112 strain. It was discovered that the transposon was incorrectly reported as being in locus FTN_1276 and actually resided in FTN_0714. FTN_0714 corresponds to two sequential loci in the LVS, FTL_1371 and FTL_1372. A targeted deletion of FTL_1371/1372 was made. Four experiments examining uptake by AML-12 cells were completed using this strain, and in all but one case, ingestion was comparable to that of the wild-type LVS (FIGURE 12A). Replication, as determined by the fold change between 4 and 24 h, was calculated in three independent experiments. In two cases, replication was similar to that of the wild-type strain (FIGURE 12B). However, in a third study, this mutant displayed decreased

replication compared with the LVS. In summary, the FTN::0119 and FTN::0714 ssp. *novicida* transposon mutants were consistently taken up at higher levels compared with the parental U112 strain. However, the corresponding LVS mutants, LVSΔ0009 and LVSΔ1371/1372, respectively, were generally ingested at levels comparable to or less than the wild-type LVS. From these studies, it was concluded that ssp. *novicida* genes whose interruption results in altered uptake by hepatocytes do not necessarily produce the same phenotype when deleted in the LVS.

Therefore, it was decided to screen an LVS transposon collection composed of 5542 mutants that was constructed by Varya Kirillov, a member of our group. Again, the goal was to identify mutants with an altered ability to be taken up by or replicate in hepatocytes. A total of 1248 LVS transposon mutants was screened in AML-12 hepatocytes. The screen was carried out in a 96-well semi-quantitative format that distinguished between mutants with normal or greatly reduced uptake and/or replication. Of the 1248 mutants screened semi-quantitatively, nine were identified as potentially defective and further analyzed by quantitative CFU assays as described earlier in this chapter. These studies identified two mutants, LVS::9a1E and LVS::9a5B, which were completely unable to replicate in AML-12 cells (FIGURE 13). These mutants were subsequently sequenced to identify the location of the mutation. In the mutant LVS::9a5B, the gene *fumA*, which catalyzes the conversion of fumarate to malate in the tricarboxylic acid cycle, contained the transposon insertion. The sequencing data for the second mutant, LVS::9a1E, showed multiple peaks, which correspond to nucleotides, in the same positions. This mutant was sequenced twice, and both attempts yielded similar results. The inability to detect single nucleotides in each position suggests the presence of

multiple transposon insertions. These data indicate that *F. tularensis* possesses genes that contribute to its replication in hepatocytes.

VIII. Change in expression of genes encoding inflammatory cytokines and receptors by primary mouse hepatocytes infected with *F. tularensis*

In addition to mechanisms that influence the uptake by and replication of *F. tularensis* in hepatocytes, the subsequent response of hepatocytes to the bacteria was also of interest to me. Hepatocytes are known to secrete cytokines for maintenance and in response to infection and injury (79,81). However, prior to these dissertation studies it was unknown whether hepatocytes are capable of responding to infection with *F. tularensis*. To address this question, total RNA was isolated from primary mouse hepatocytes that were incubated with medium alone, a sham preparation of bacteria, or the LVS for 8 h. The RNA was converted to cDNA and used as a template for RT-PCR. A 96-well RT^2 Profiler Array was used to examine the expression of 84 genes encoding proinflammatory cytokines and receptors. In these experiments, there was no difference between the response of hepatocytes incubated with medium alone and hepatocytes incubated with a sham preparation of bacteria. In response to *F. tularensis*, the expression of genes for four chemoattractants, CXCL5, CCL20, CXCL1, and CCL2, was increased by more than 4-fold compared to control cells incubated with medium alone. Also increased was the expression of the gene encoding a colony-stimulating factor, CSF3. Down-regulation was observed for a single gene encoding the chemoattractant CCL12 (TABLE 3).

The previous experiment was conducted using LVS organisms that had been cultured in our standard growth medium, MH II broth. A study by Hazlett *et al.* (14)

showed that the protein expression profile of *F. tularensis* grown in BHI medium closely resembles that of *F. tularensis* grown in macrophages and is different from that of the bacterium grown in MH II broth. To test whether this growth medium might affect the response of hepatocytes to *F. tularensis*, primary mouse hepatocytes were infected as above with the LVS grown in BHI. It was observed that hepatocytes up-regulated the expression of fewer genes in response to BHI-grown LVS compared to MH II-grown bacteria. Additionally, no hepatocytic genes were down-regulated in response to infection with the BHI-grown organisms. However, as for cells infected with bacteria grown in MH II broth, increased transcription was observed for the genes encoding CXCL5, CCL20, and CSF3. Also increased in response to the BHI-grown bacteria was the transcription of the gene for vascular endothelial growth factor A (VEGF-A) (TABLE 3).

Studies from our group have determined that live, but not killed, *F. tularensis* suppresses the proinflammatory response of endothelial cells (66). It was therefore investigated whether the response of hepatocytes to killed LVS would differ from that to viable LVS. For these experiments, LVS organisms were grown in MH II broth and then killed by heating. The killed bacteria were then incubated with primary mouse hepatocytes for 8 h. The genes for four chemoattractants, CXCL5, CCL20, CXCL1, and CCL2, were up-regulated by hepatocytes that were exposed to heat-killed LVS. Also up-regulated were the genes encoding CSF3 and IL-1β, a potent inflammatory mediator. Unlike hepatocytes infected with living MH II-grown bacteria, no genes were down-regulated by the killed bacteria. Interestingly, the up-regulation of *IL1b* was unique to hepatocytes challenged with the killed LVS (TABLE 3).

IX. Secretion of cytokines by primary hepatocytes infected with *F. tularensis*

In the previous study, it was observed that primary mouse hepatocytes are capable of regulating the expression of genes that encode inflammatory cytokines in response to *F. tularensis*. This led to the question of whether these cytokines are also secreted by the hepatocytes. To address this issue, conditioned medium was collected from hepatocytes that were infected with the LVS for 24 or 48 h. Note that in these studies, the hepatocytes were exposed to both intracellular and extracellular bacteria for the duration of the assay. ELISAs were used to measure the secretion of CXCL5, CXCL1, CCL2, and CCL20. CXCL5 was not secreted by unstimulated cells, but when hepatocytes were infected with the LVS secretion of this cytokine increased by more than 50-fold at 24 h and by more than 60-fold at 48 h (FIGURE 14A). Hepatocytes secreted some CXCL1 constitutively. However, infected hepatocytes secreted about 2-fold more CXCL1 compared to the controls (FIGURE 14B). CCL20 was also secreted constitutively, but its production was not augmented by the LVS (FIGURE 14C). Uninfected hepatocytes secreted a high level of CCL2 that was not increased in response to *F. tularensis* (FIGURE 14D).

TABLE 2. The LVS and Schu S4 strain are taken up by and persist in primary mouse hepatocytes. Primary mouse hepatocytes were infected with the LVS or Schu S4 strain at an MOI of 150 for 3 h. The infected hepatocytes then were treated with gentamicin to kill all extracellular bacteria. Cells were lysed at 4 h, 24 h, and 48 h post-infection, and the CFU were enumerated. These data are a summary of seven independent experiments with the LVS and a single experiment with the Schu S4 strain. The numbers are means of 3 to 6 replicate samples per experiment. *, $P < 0.05$ and ***, $P < 0.001$ compared to the numbers of intracellular bacteria at the previous time point.

EXPERIMENT	STRAIN	CFU (x 10^3)		
		4 h	**24 h**	**48 h**
1	LVS	16 ± 3.7	29 ± 2.1	41 ± 11.8
2	LVS	90 ± 18.1	117 ± 28.9	
3	LVS	313 ± 107	127 ± 11.5	
4	LVS	68 ± 6.5	140 ± 34.6	35 ± 39.5 *
5	LVS	42 ± 2.6	12 ± 3.5 ***	
6	LVS	64 ± 8.1	12 ± 4.5 ***	
7	LVS	350 ± 58.5	67 ± 20.1 ***	
8	Schu S4	1 ± 0.1	15 ± 4.4	73 ± 29.4 *

TABLE 3. Primary mouse hepatocytes increase the expression of genes encoding inflammatory cytokines in response to infection with the LVS. Primary mouse hepatocytes were infected at an MOI of 150 with the LVS grown in MH II or BHI broth. Other cultures were incubated with a preparation of the LVS that had been grown in MH II broth and then killed by heating. Total RNA was isolated from hepatocytes that were incubated with the bacteria for 8 h. The total hepatocyte RNA then was analyzed by RT^2 Profiler Arrays. The table is a summary of fold-change in hepatocyte gene expression for three independent experiments for live bacteria and two independent experiments for heat-killed bacteria. The data are shown as the mean ± SD for the live LVS and as an average for the killed LVS, with the values of each experiment given in parentheses. The genes listed are those with a 4-fold or greater change in expression compared to hepatocytes that were incubated in medium alone in every experiment.

GENE	FUNCTION	FOLD-CHANGE		
		MH II	BHI	HEAT-KILLED
Cxcl5	Neutrophil chemoattractant	70 ± 43.6	23 ± 19.7	191 (93,290)
Csf3	Granulocyte colony-stimulating factor	24 ± 13.4	13 ± 11.7	31 (35,27)
Ccl20	Neutrophil and lymphocyte chemoattractant	21 ± 6.1	17 ± 13.5	7 (6,8)
Cxcl1	Neutrophil chemoattractant	6 ± 0.6		5 (5,4)
Ccl2	Monocyte, DC, and T cell chemoattractant	5 ± 1.5		4 (5,8)
Vegfa	Vascular endothelial growth factor		6 ± 1.6	
IL1b	Inflammatory mediator			13 (6,19)
Ccl12	Eosinophil, monocyte, and lymphocyte chemoattractant	0.13 ± 0.2		

FIGURE 4. AML-12 and HH4 hepatocytes support replication of *F. tularensis*. Human HH4 hepatocytes (A) were infected at an MOI of 5000 and murine AML-12 hepatocytes (B) were infected at an MOI of 3000 with either ssp. *novicida* U112 or the LVS. Following 3 h of incubation to allow uptake, the cells were treated with gentamicin to kill all extracellular bacteria. The cells then were lysed at 4 h or 24 h post-infection, and CFU were enumerated. Panels A and B are representative of seven and 12 independent experiments, respectively. Bars represent the means ± SD from 3 replicate samples. *, $P < 0.05$ and ***, $P < 0.001$ compared to 4-h uptake.

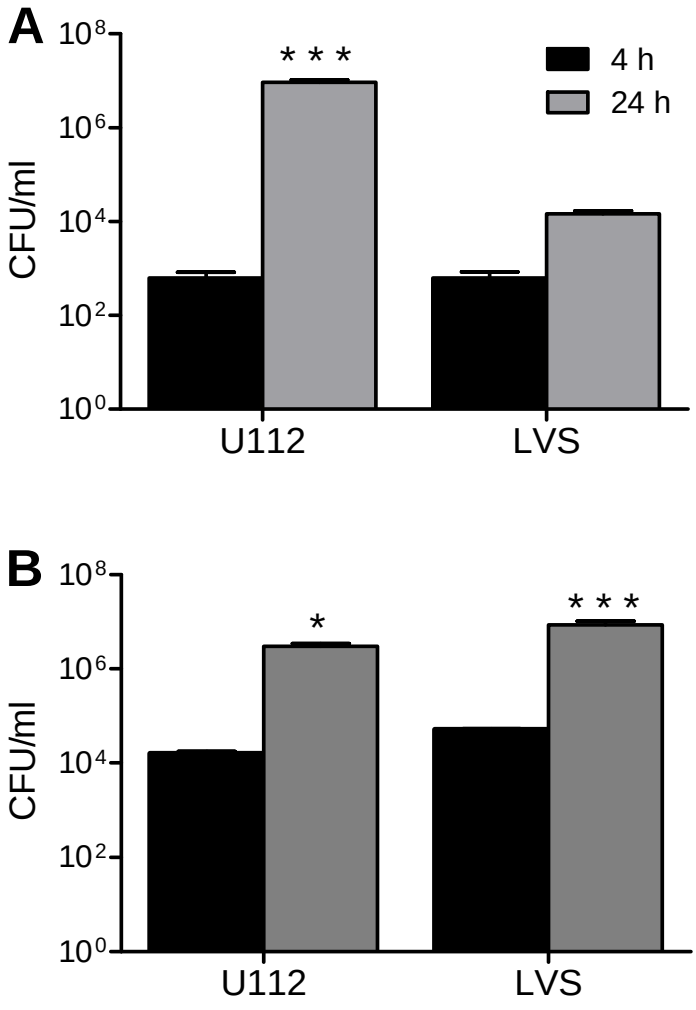
A
B
CFU/ml
4 h
24 h
* * *
*
U112
LVS

FIGURE 5. Hepatocytes have a limited capacity to take up *F. tularensis*.

HH4 hepatocytes were infected for 3 h with the LVS at MOIs ranging from 150 to 3530. The infected cells then were treated with gentamicin to remove all extracellular bacteria prior to lysis. The internalized bacteria were enumerated by CFU assay. Bars are means ± SD of four or six replicate samples per experiment, and data are combined from three separate experiments.

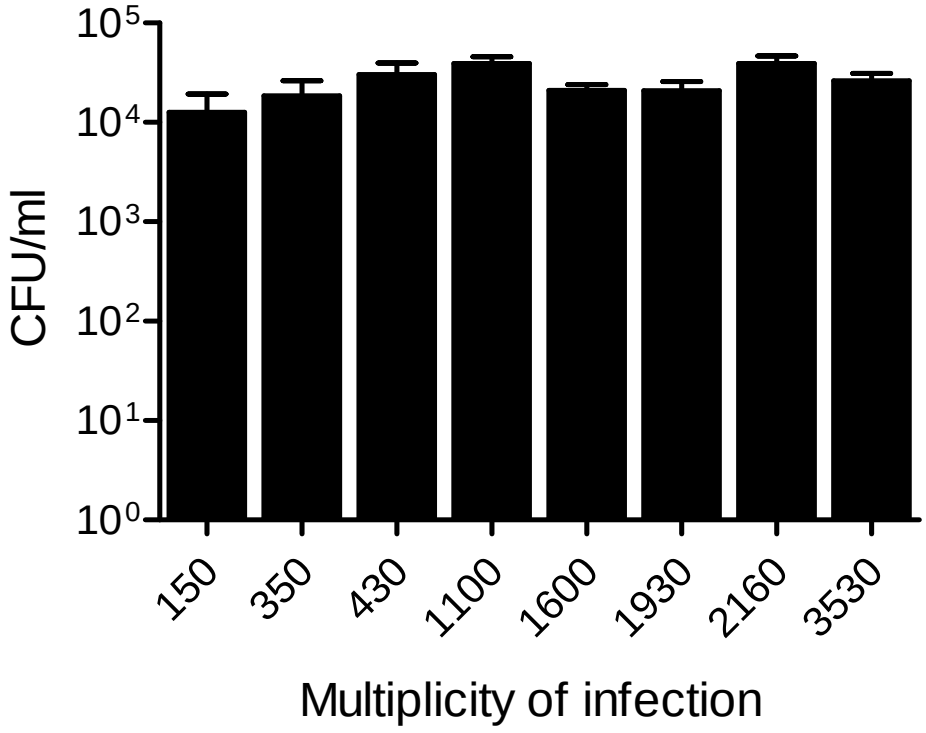
10^5
10^4
10^3
10^2
10^1
10^0
CFU/ml
150
350
430
1100
1600
1930
2160
3530
Multiplicity of infection

FIGURE 6. Hepatocytes can be cultured from the livers of mice. Primary mouse hepatocytes were isolated by collagenase digestion and then cultured on collagen-coated plates. A phase-contrast image of a typical culture at 40X magnification is shown in Panel A. The presence of leukocytes and endothelial cells in the hepatocyte cultures was analyzed by immunofluorescence microscopy. Panel B shows a positive control, where mouse leukocytes were labeled with an antibody against CD45. In Panel C, a section of mouse liver was labeled with an antibody against CD31 to identify endothelial cells, again as a positive control. In Panels B and C the leukocytes and endothelial cells appear red, while the cell nuclei are labeled with DAPI and appear blue. Three separate cultures of hepatocytes showed no staining for either CD45 or CD31.

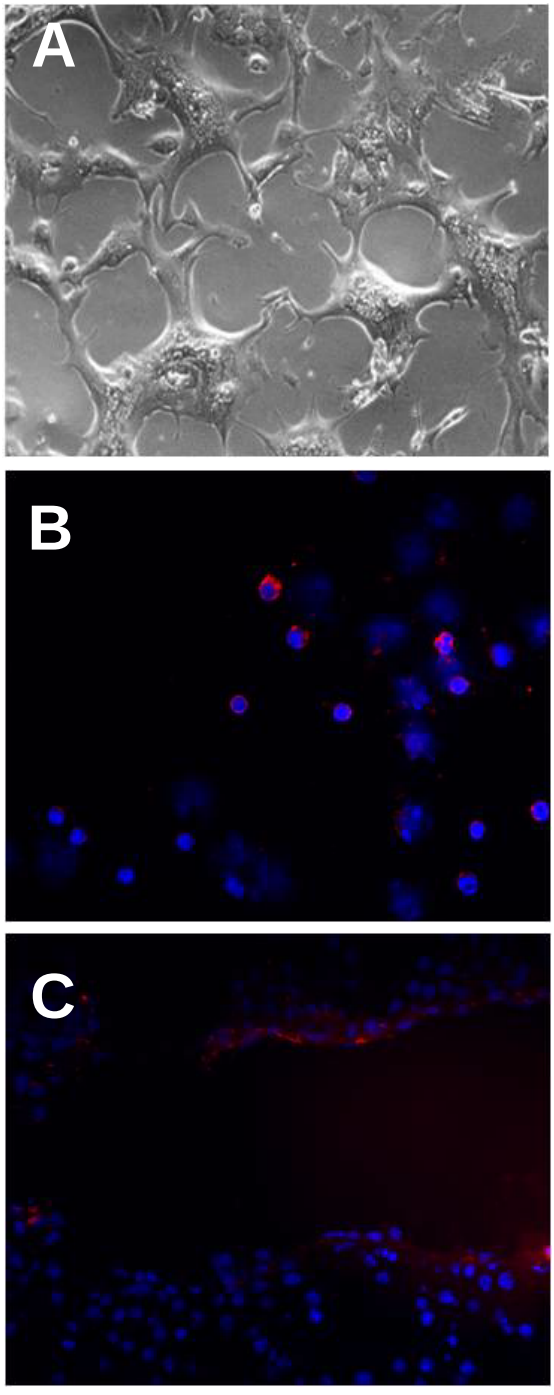
A
B
C

FIGURE 7. Polymerization of hepatocyte actin is required for the entry of *F. tularensis*. AML-12 hepatocytes were incubated with medium alone (A), with medium containing DMSO (0.2%) (B), or with medium containing cytochalasin D (3.9 μM in 0.2% DMSO) (C), beginning 2 h prior to infection. AML-12 cells were incubated with the LVS at an MOI of 1000 for 2 h to allow uptake. The cells were then treated with gentamicin for 1 hr to remove extracellular bacteria. Following an additional 21 hrs of incubation, bacteria were labeled by indirect immunofluorescent staining (green) and visualized by microscopy. The uptake and replication of the LVS following treatment with DMSO or cytochalasin D (CD) were also quantified by CFU assay in AML-12 hepatocytes (D) and primary mouse hepatocytes (E). The cells were lysed using saponin at 24 h post-infection for enumeration of colonies. These data are representative of two independent experiments. Bars represent the means ± SD from 3 replicate samples. *, $P < 0.05$, **, $P < 0.01$ and ***, $P < 0.001$ compared to uptake and replication under all other conditions.

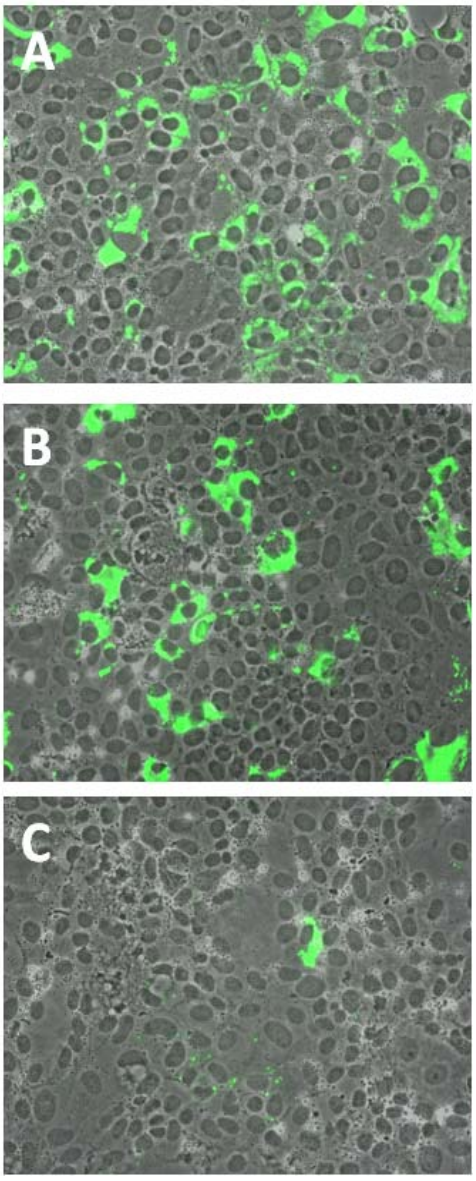
A
B
C

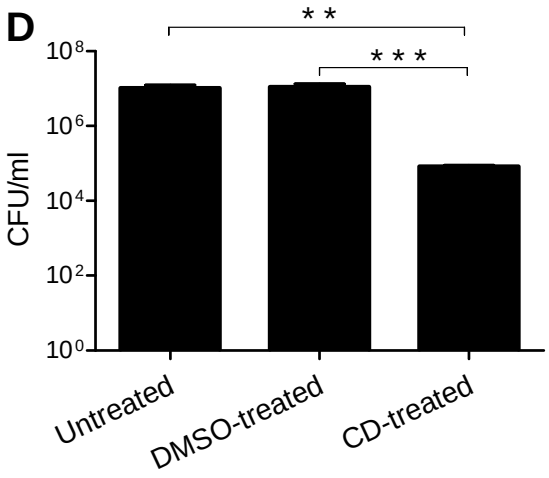
D
* *
* * *
10^8
10^6
10^4
10^2
10^0
CFU/ml
Untreated
DMSO-treated
CD-treated

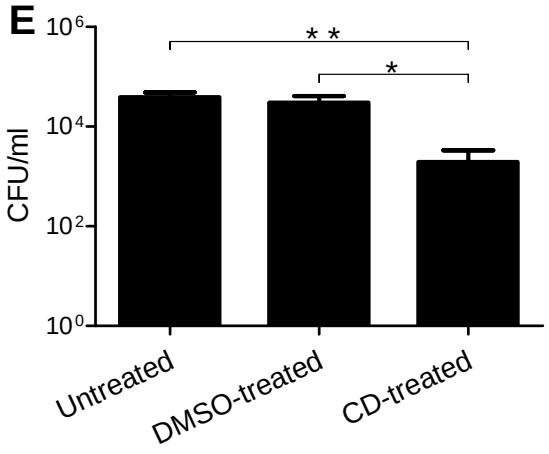
E
10^6
* *
*
10^4
10^2
10^0
CFU/ml
Untreated
DMSO-treated
CD-treated

FIGURE 8. Invasion of hepatocytes is a passive process on the part of *F. tularensis*. An MOI of 5000 was used to infect AML-12 cells (A-E) and an MOI of 150 was employed to infect primary mouse hepatocytes (F-J) with the LVS. The cells were incubated for 3 h with untreated (A and F), chloramphenicol-treated (2 μg/ml) (B and G), heat-killed (56^{o}C for 1 h) (C and H), or formalin-fixed (4% paraformaldehyde) (D and I) LVS organisms. The location of the bacteria was then determined by differential immunofluorescent labeling. The extracellular bacteria are double-labeled and appear orange, while intracellular bacteria are labeled only with FITC and appear green. Panels A-D show merged immunofluorescence and phase-contrast images, and in Panels F-I, the hepatocyte nuclei are stained with DAPI (blue) to visualize cells. Quantitation of bacteria internalized by AML-12 cells (E) or primary mouse hepatocytes (J) was achieved by counting the number of green bacteria per field at 40X magnification. The bars are means ± SD of three independent fields. The data are representative of three separate experiments using AML-12 cells and one experiment with primary mouse hepatocytes.

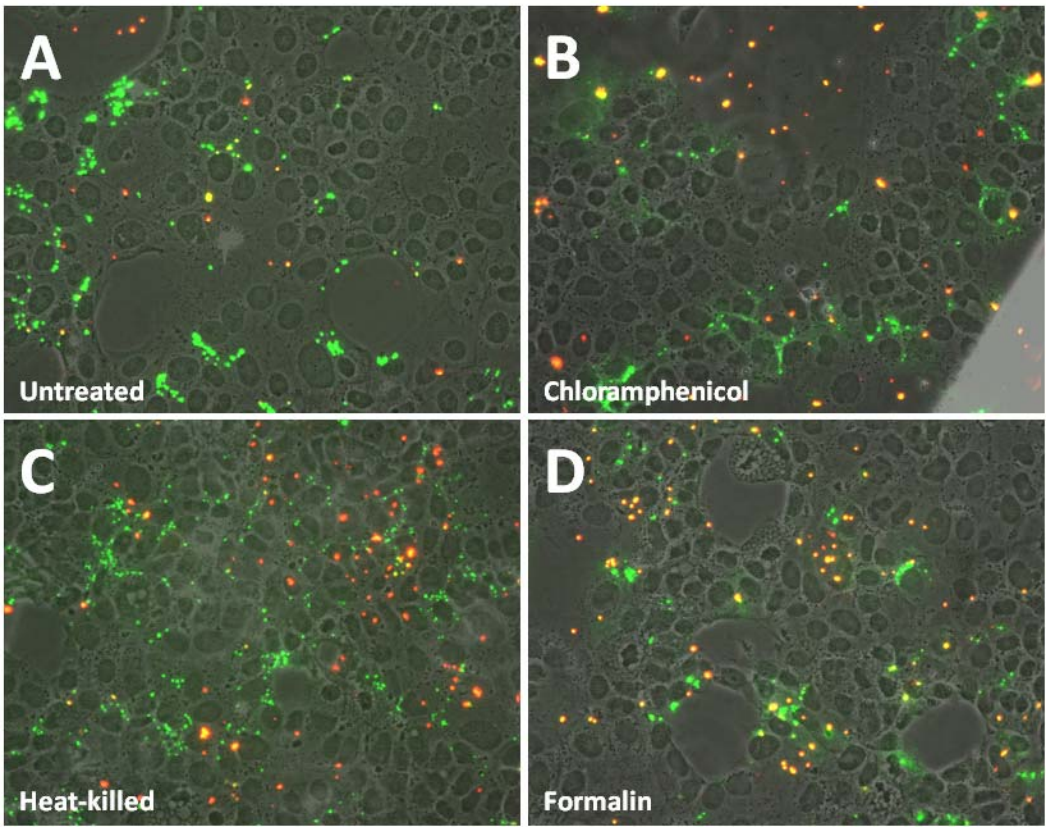
A
Untreated
B
Chloramphenicol
C
Heat-killed
D
Formalin

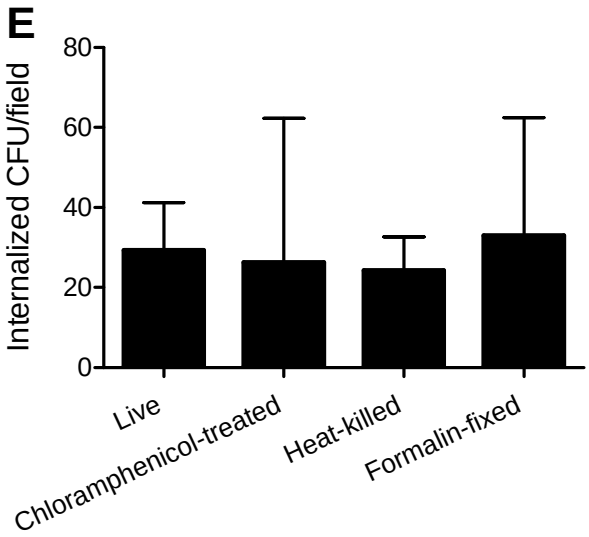
E
Internalized CFU/field
80
60
40
20
0
Live
Chloramphenicol-treated
Heat-killed
Formalin-fixed

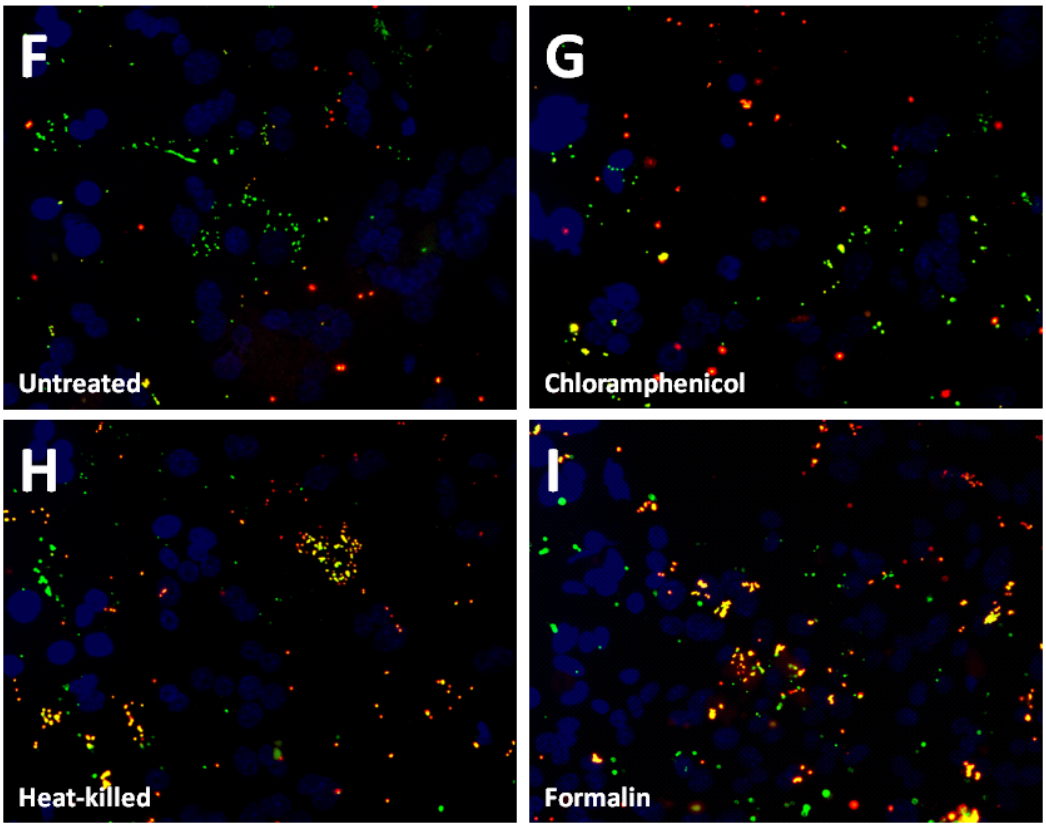
F
Untreated
G
Chloramphenicol
H
Heat-killed
I
Formalin

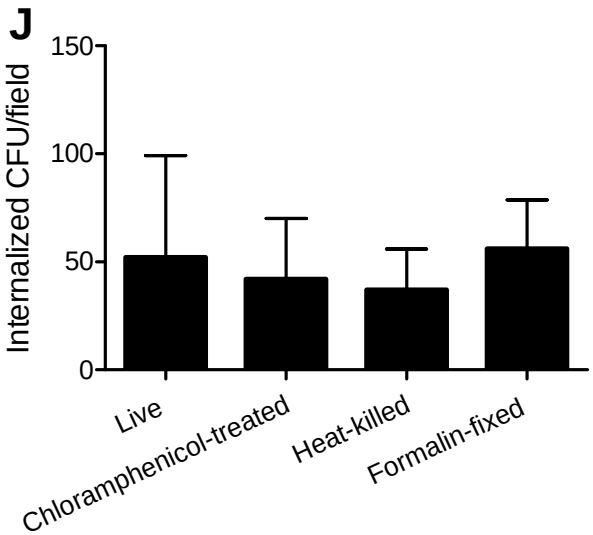
J
Internalized CFU/field
150
100
50
0
Live
Chloramphenicol-treated
Heat-killed
Formalin-fixed

FIGURE 9. Type IV pili are not required for entry of *F. tularensis* into hepatocytes. AML-12 hepatocytes (A) and primary mouse hepatocytes (B) were infected for 3 h with the LVS or with Δ*pilT*, Δ*pilF,* or Δ*pilE4* mutant strains. AML-12 cells and primary mouse hepatocytes were infected at MOIs of 5000 and 150, respectively. Uptake of bacteria by either cell type was measured by CFU assay. The infected cells were treated with gentamicin for 1 h to remove all extracellular bacteria and then lysed, and the recovered colonies were enumerated. The data in Panel A are representative of four separate experiments. Bars are means ± SD of three replicate samples per experiment. Panel B shows combined data from three separate experiments with the LVS and Δ*pilT* mutant and one experiment with the Δ*pilF* and Δ*pilE4* mutants. Triplicate samples were assessed in each experiment.

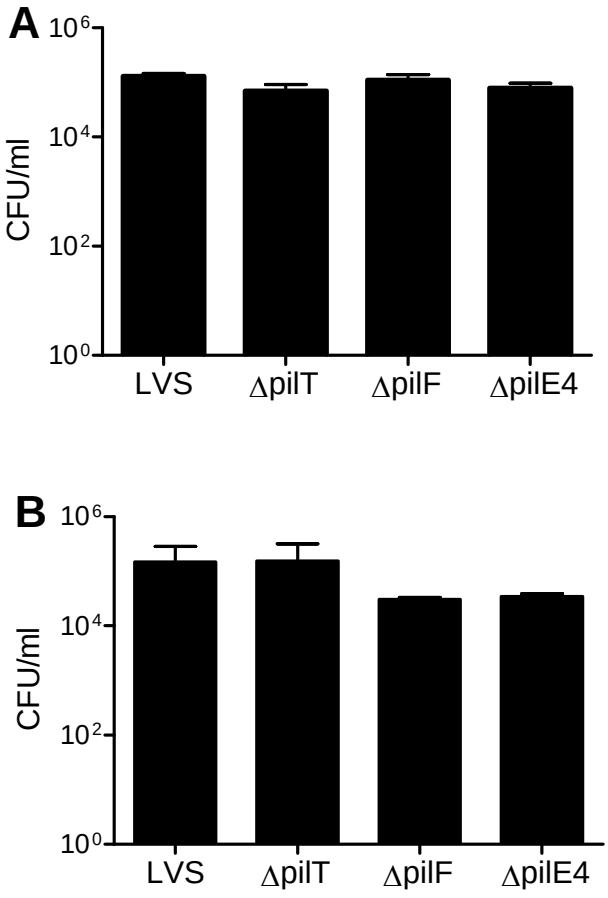
A
10^6
10^4
10^2
10^0
CFU/ml
LVS
ΔpilT
ΔpilF
ΔpilE4
B
10^6
10^4
10^2
10^0
CFU/ml
LVS
ΔpilT
ΔpilF
ΔpilE4

FIGURE 10. The *F. tularensis* type I secretion system does not mediate uptake of the bacteria by hepatocytes. AML-12 hepatocytes (A) and primary mouse hepatocytes (B) were infected for 3 h with the LVS or with Δ*tolC* or Δ*ftlC* mutant strains. AML-12 cells and primary mouse hepatocytes were infected at MOIs of 5000 and 150, respectively. Uptake of bacteria by either cell type was measured by CFU assay. The infected cells were treated with gentamicin for 1 h to remove all extracellular bacteria and lysed, and the recovered colonies were enumerated. The data in Panel A are representative of three separate experiments. Bars are means ± SD of three replicate samples per experiment. Panel B shows combined data from two separate experiments with the LVS and Δ*tolC* mutant and one experiment with the Δ*ftlC* mutant. Triplicate samples were assessed in each experiment.

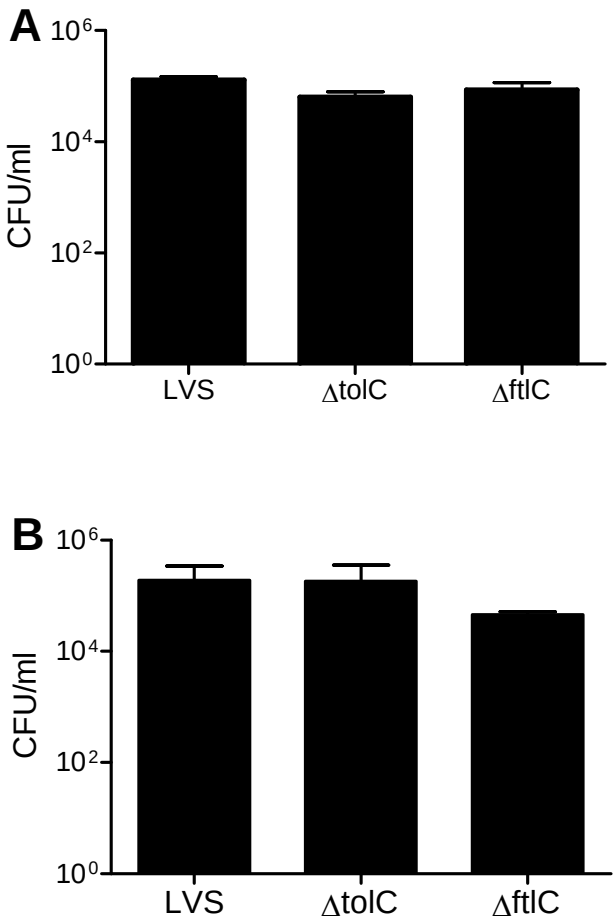
A
10^6
10^4
10^2
10^0
CFU/ml
LVS
ΔtolC
ΔftlC
B
10^6
10^4
10^2
10^0
CFU/ml
LVS
ΔtolC
ΔftlC

FIGURE 11. *F. tularensis* ssp. *novicida* possesses outer-membrane proteins that influence uptake by hepatocytes. Immunofluorescence microscopy (A) and CFU assays (B and C) were used to determine the ability of wild-type U112 and mutant strains (FTN::0119 and FTN::0714) to be taken up by or replicate in AML-12 hepatocytes. Hepatocytes were infected for 3 h at an MOI of 5000 with each bacterial strain. Following infection, some cells were immediately fixed to analyze uptake, while others were treated with gentamicin for an additional 21 h and then fixed to analyze replication. Cultures were differentially labeled for immunofluorescence microscopy. The extracellular bacteria appear orange, while the intracellular bacteria appear green (A). For quantification by CFU assay, the cells were lysed 4 h or 24 h post-infection, and the colonies were enumerated (B). Bars represent the means ± SD from 3 replicate samples. *, $P < 0.05$ compared to uptake of the wild-type U112 strain. Replication was measured as the fold difference between CFU measured at 4 h and 24 h (C). The immunofluorescence and CFU data are representative of two and four independent experiments, respectively.

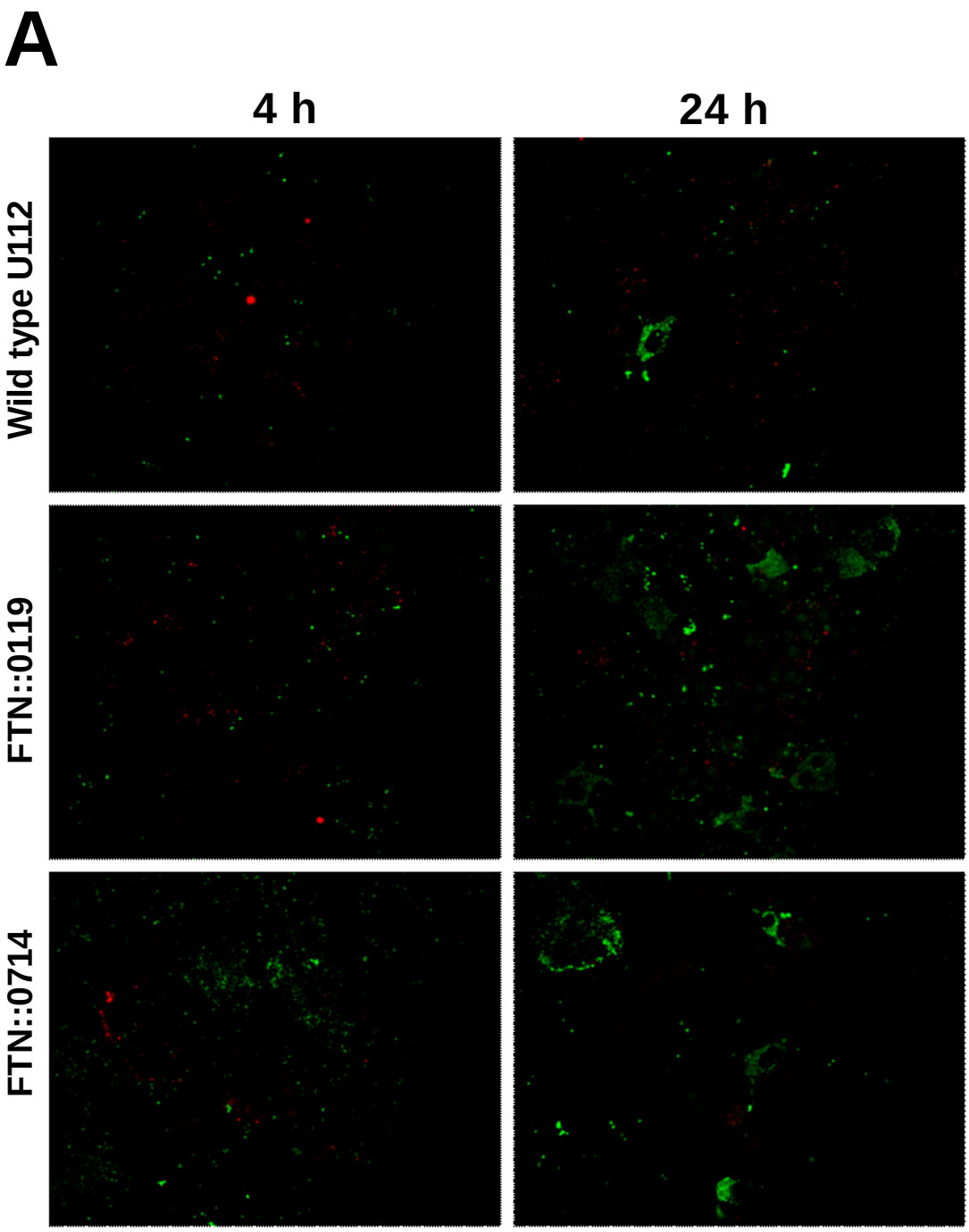
A
4 h
24 h
Wild type U112
FTN::0119
FTN::0714

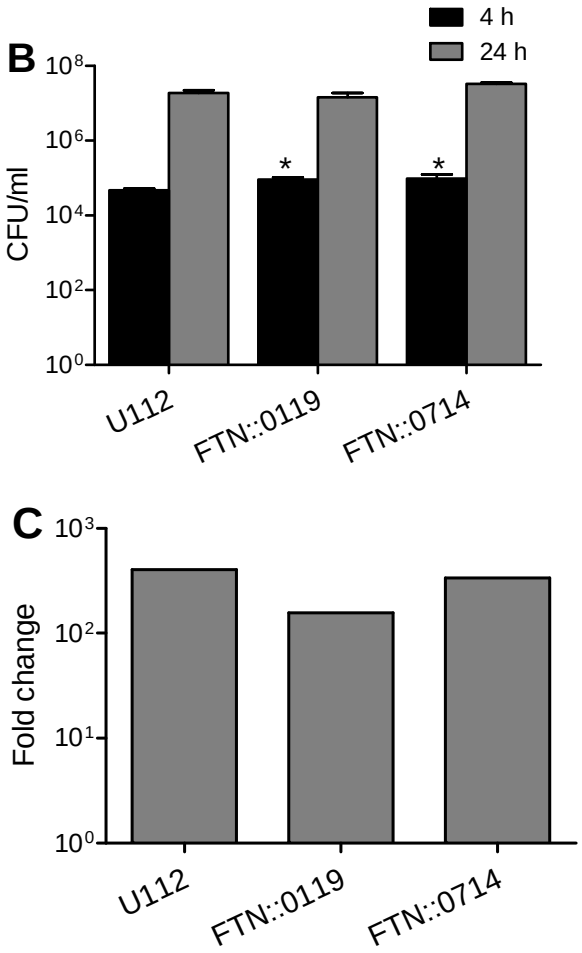
B
4 h
24 h
CFU/ml
10^8
10^6
10^4
10^2
10^0
*
*
U112
FTN::0119
FTN::0714
C
Fold change
10^3
10^2
10^1
10^0
U112
FTN::0119
FTN::0714

FIGURE 12. The phenotype of LVS mutants is different from that of the corresponding ssp. *novicida* mutants. HH4 hepatocytes were infected for 3 h at an MOI of 3000 with the wild-type LVS or the Δ0009, Δ0687 or Δ1371/1372 strains. The infected cells were treated with gentamicin to remove all extracellular bacteria prior to lysing the cells at 4 h and 24 h and enumerating the CFU (A). Bars are means ± SD of three replicate samples in a single experiment. Replication was measured as a fold change in CFU between 4 h and 24 h (B); again, a single experiment is depicted. Three independent experiments were performed with the LVSΔ0009 mutant, six with the LVSΔ0687 strain, and four with the LVSΔ1371/1372 mutant. The outcomes of the various experiments are discussed in the Results. ***, $P < 0.001$ compared to uptake of the wild-type LVS strain.

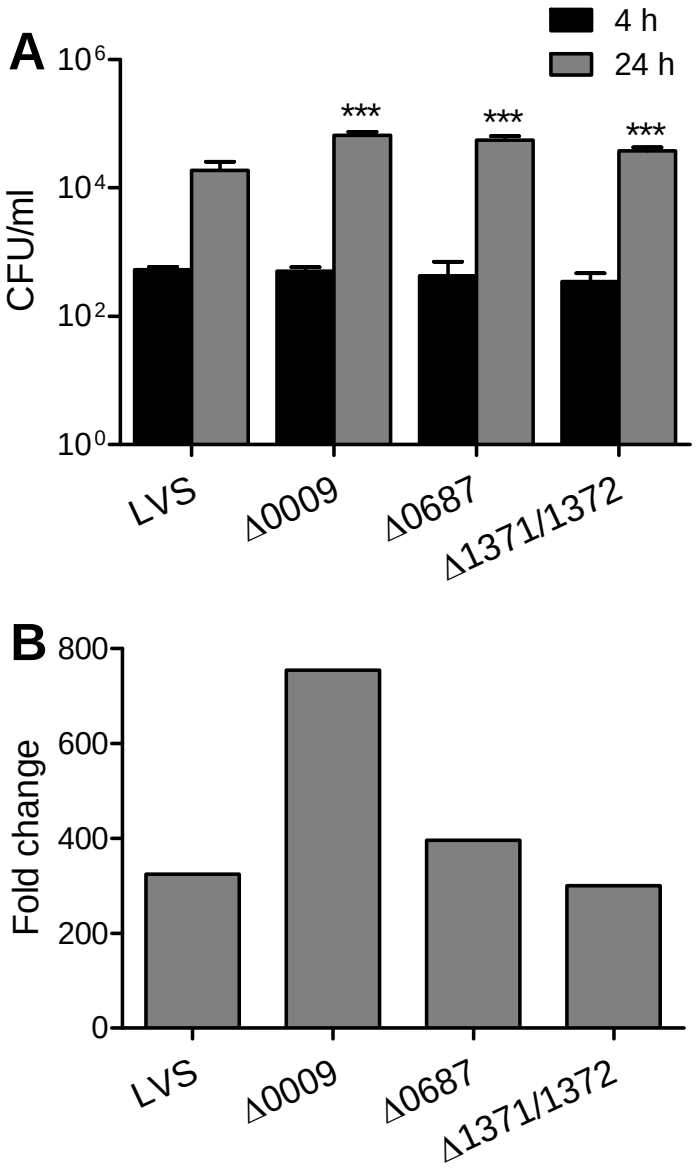
A
4 h
24 h
CFU/ml
10^6
10^4
10^2
10^0
***
***
***
LVS
Δ0009
Δ0687
Δ1371/1372
B
Fold change
800
600
400
200
0
LVS
Δ0009
Δ0687
Δ1371/1372

FIGURE 13. *F. tularensis* LVS possesses proteins that contribute to replication in hepatocytes. An LVS transposon collection was screened semi-quantitatively for mutants with altered uptake by or replication in AML-12 hepatocytes. The screen identified two mutants (LVS::9a1E and LVS::9a5B) with diminished uptake and replication. The agar plates show the LVS or various transposon mutants spotted in triplicate after harvesting from the AML-12 cells at 4 h (A) or 24 h (B) after infection. The uptake and replication of LVS::9a1E and LVS::9a5B were quantified by CFU assay (C). AML-12 hepatocytes were infected for 3 h at an MOI of 150. The cells then were treated with gentamicin to remove extracellular bacteria. Cells were lysed at 4 and 24 h, and the intracellular bacteria were enumerated. Bars are means ± SD of three replicate samples. ND, not detected. These data are representative of three independent experiments.

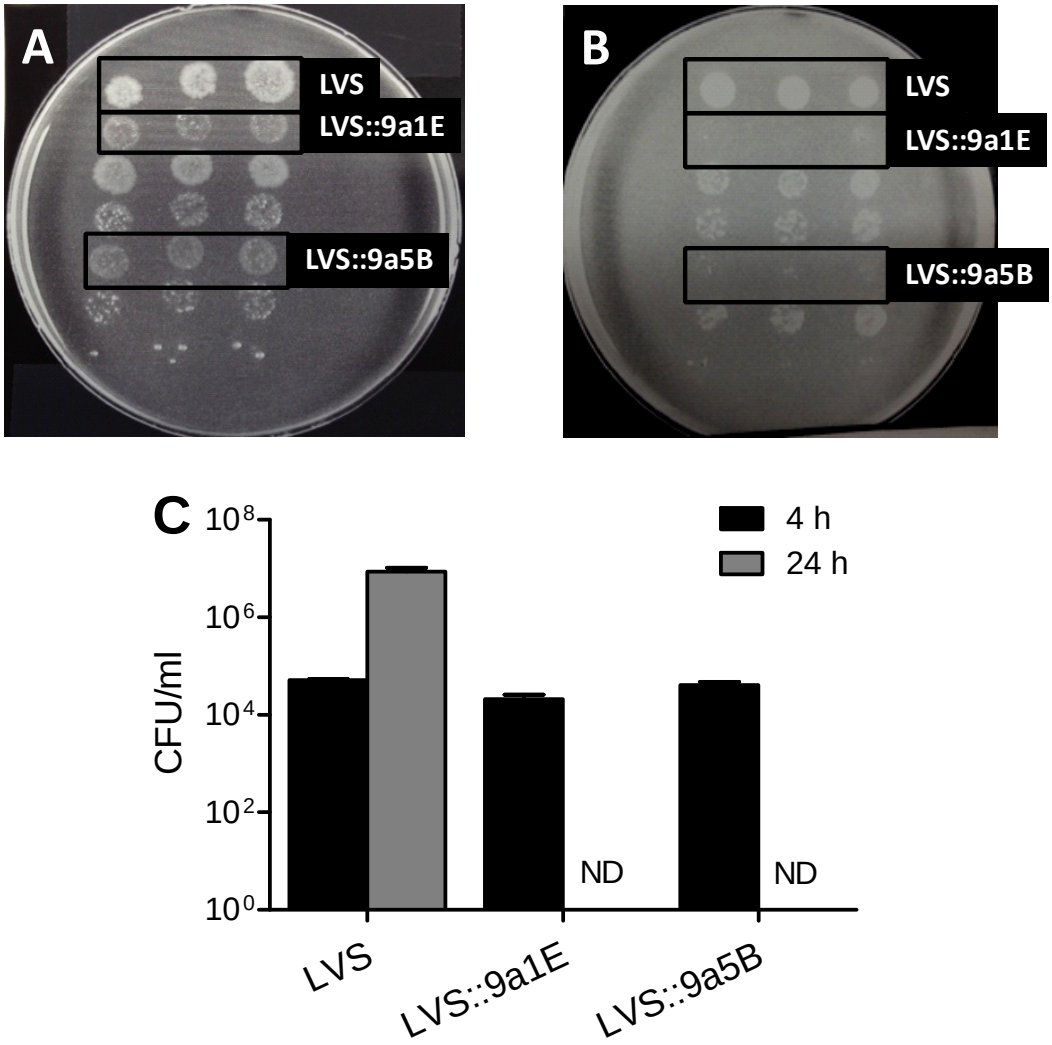
A
LVS
LVS::9a1E
LVS::9a5B
B
LVS
LVS::9a1E
LVS::9a5B
C
4 h
24 h
CFU/ml
10^8
10^6
10^4
10^2
10^0
ND
ND
LVS
LVS::9a1E
LVS::9a5B

FIGURE 14. Primary mouse hepatocytes secrete pro-inflammatory cytokines in response to *F. tularensis* LVS. Primary mouse hepatocytes were infected at an MOI of 150 with viable LVS organisms that had been grown in MH II broth. The cells and bacteria were co-incubated for 24 h or 48 h to assess the response of the hepatocytes to both intra- and extracellular bacteria. Conditioned media were collected at each time point, and the amount of CXCL5 (A), CXCL1 (B), CCL20 (C), and CCL2 (D) was measured by ELISA. Bars represent the means ± SD of 6 replicate samples combined from two independent experiments at 24 h and 3 replicate samples from one experiment at 48 h. ***, $P < 0.001$ compared to secretion under all other conditions.

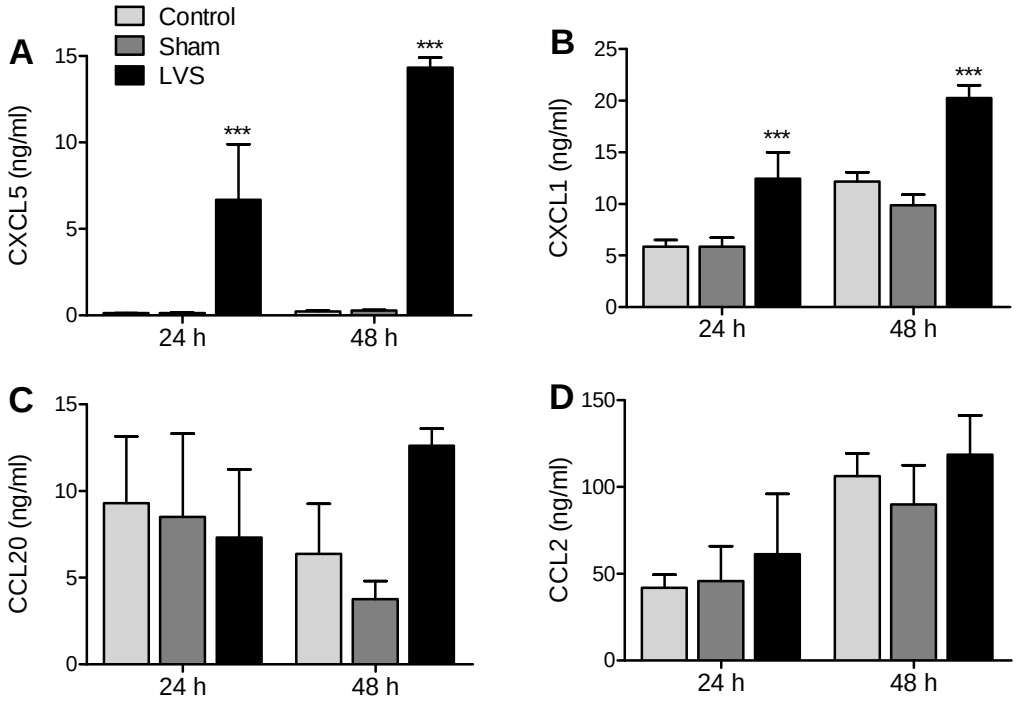
A
Control
Sham
LVS
CXCL5 (ng/ml)
15
10
5
0
***
***
24 h
48 h
B
CXCL1 (ng/ml)
25
20
15
10
5
0
***
***
24 h
48 h
C
CCL20 (ng/ml)
15
10
5
0
24 h
48 h
D
CCL2 (ng/ml)
150
100
50
0
24 h
48 h

DISCUSSION

The studies presented in this chapter demonstrate that *F. tularensis* interacts with hepatocytes. Several hepatocytic cell lines ingest and support replication of *F. tularensis* (44,119,121). In agreement with these previous observations, our studies confirmed that both the human HH4 and murine AML-12 hepatocytic cell lines took up *F. tularensis* LVS and the U112 strain. The U112 strain also replicated extensively in the HH4 and AML-12 cell lines (FIGURE 4). Although the LVS bacterium persisted in HH4 cells, extensive replication was seen only in the AML-12 cells (FIGURE 4B). AML-12 cells are derived from mice transgenic for transforming growth factor-α (124). HH4 cells, on the other hand, are derived from a human liver and express the E6 and E7 proteins from human papillomavirus (136). The differences in replication that were observed in the cell lines may be a result of dissimilar intrinsic properties of those lines.

Primary mouse hepatocytes took up the LVS at a level similar to the cell lines. However, unlike in the AML-12 cell line, the LVS did not replicate in the primary cells. In some cases, lower numbers of the LVS were recovered after 24 h compared to 4 h, an indication that the organisms were likely being killed intracellularly. To measure intracellular bacterial content, infected hepatocytes were incubated for 21 h in culture medium containing gentamicin. Hepatocytes are similar to epithelial cells, which actively take up extracellular material by macropinocytosis (46). Similarly, cultured hepatocytes are capable of ingesting by endocytosis more than 20% of their volume per hour (137). Therefore, the killing of the LVS in primary mouse hepatocytes may be due to the exposure of intracellular organisms to gentamicin that was taken up by the hepatocytes from the extracellular environment. Furthermore, intracellular pathogens rely on nutrients

from the host cytoplasm. Interactions between the intracellular pathogen and the host promote modification of the metabolic activity of that host cell. This process in turn provides an ideal environment for the replication of the pathogen (138). As discussed previously, the AML-12 cells are a transformed cell line. It is therefore entirely possible that the infinite proliferative capacity of these cells also allows them the sustain the intracellular replication of bacteria more avidly than untransformed hepatocytes (139).

In contrast to the LVS, the Schu S4 strain replicated in the primary hepatocytes. Inoculation of mice via the aerosol route with the highly virulent ssp. *tularensis* KU49 strain results in increased bacterial burdens in key organs, including the liver, compared with LVS-infected mice (120). Similarly, the highly virulent ssp. *tularensis* and the virulent OR96-0246 strain derived from ssp. *holarctica* replicate more extensively than the LVS in primary rat hepatocytes in culture (130). These observations suggest that the ability of *F. tularensis* organisms to replicate in primary hepatocytes is linked to virulence. Furthermore, these findings support the hypothesis that mechanisms related to virulence of the Schu S4 strain allow these organisms to replicate in the primary hepatocytes.

It has been well documented that rearrangement of the host actin cytoskeleton is dependent on actin polymerization (133,135,140). The cytoskeleton and associated elements interact with the cell membrane and can influence the membrane morphology (141). Cytochalasins are a class of mycotoxins that inhibit polymerization of the actin filament by binding to the growing end and preventing addition of globular actin. In addition to preventing polymerization, these molecules cause de-polymerization of actin filaments (142). In these dissertation studies, cytochalasin D was used to examine the

requirement of actin polymerization for the uptake of the LVS by hepatocytes. Treatment of hepatocytes with cytochalasin D inhibited the ingestion and subsequent replication of the LVS by more than 95%. As expected, the inhibitory effect was observed for both AML-12 hepatocytic cells and primary mouse hepatocytes (FIGURE 7). The inhibition of uptake of the LVS by hepatocytes incapable of forming actin filaments is in agreement with a previous observation in epithelial cells. Incubation of TC-1 lung epithelial cells with cytochalasin D results in a 99% decrease in uptake of the LVS (45). The extent of inhibition caused by cytochalasin D indicates that the hepatocyte actin cytoskeleton is a major player in the process of ingestion of the LVS. This observation is not unique to hepatocytes and *F. tularensis*, since it has been shown previously that uptake of organisms such as *Shigella flexneri* and *Salmonella enteric*a is highly dependent on actin filaments and does not involve microtubules (143,144).

Intracellular pathogens have evolved a variety of sophisticated mechanisms for activating their uptake by host cells (145). In many cases, the host cell provides shelter to the organism from the host immune system, a constant supply of nutrients, and a replicative niche (8,146). Enteropathogenic *Yersinia* ssps. use multiple mechanisms to gain entry into host cells. One well-studied mechanism is invasin-promoted uptake to enter M cells, which are specialized intestinal epithelial cells. Invasin is expressed on the bacterial surface and interacts with β1 integrins on the surface of the M cells. This interaction leads to the recruitment of host mediators of endocytosis and the eventual uptake of the organism (147). The type III secretion system expressed by *S. flexneri* is used to inject effector proteins directly into the host cell cytoplasm. These effectors result in the formation of actin-rich ruffles on the host membrane and, ultimately, the uptake of

the pathogen (135). *S. typhimurium* expresses a type III secretion system that is encoded by the *inv* and *spa* loci. Two proteins secreted by this type III secretion apparatus, SipB and SipC, are required for entry of the bacterium into intestinal epithelial cells (148). With respect to *F. tularensis*, live and killed LVS organisms are taken up at similar frequencies by TC-1 epithelial cells (45). Studies reported in this dissertation showed that live LVS organisms, killed LVS organisms, or LVS organisms incapable of synthesizing new proteins were taken up in similar numbers by both AML-12 hepatocytic cells and primary mouse hepatocytes (FIGURE 8). Furthermore, the *F. tularensis* type IV pili (FIGURE 9) and type I secretion system (FIGURE 10) were also dispensable in the uptake process. Together, these studies suggest that uptake of *F. tularensis* is a passive process on the part of the bacteria and therefore does not require the synthesis of new proteins. Furthermore, uptake may be initiated by a pre-formed bacterial structure that is not affected by heat-killing or formalin fixation. The normal uptake of the pilus mutants was particularly interesting, since LVS mutants lacking *pilT* or *pilF* are defective for adherence to FL83B hepatocytes (24). One possible explanation is that in our infection model, the contact between the organism and hepatocytes is encouraged through centrifugation. Therefore, the ability of the bacteria to adhere to the hepatocytes may not be a major contributor to the actual number of bacteria that are taken up. The ability to adhere to hepatocytes may be more important in the *in vivo* situation, where the organism disseminates to the liver via the blood.

Interestingly, infection of HH4 hepatocytic cells with the LVS at increasing MOI did not correspondingly increase the number of bacteria (FIGURE 5). These data demonstrated that HH4 hepatocytic cells have a finite capacity to take up the LVS.

Hepatocytes take up a variety of molecules, including insulin, via receptor-mediated endocytosis (137). Furthermore, the LVS targets cholesterol-rich domains for invasion of hepatocytes (44). Therefore, it is possible that uptake of *F. tularensis* by hepatocytes is limited by the availability of hepatocytic receptors and/or membrane domains. These studies provide additional support for the postulation that uptake of *F. tularensis* by hepatocytes is mediated by a pre-formed surface structure.

The intracellular life cycle of *F. tularensis* is well understood in macrophages. In this host cell, the organism is initially contained in a phagosome that transiently co-localizes with EEA1, a marker for early endosomes, and LAMP-1, a marker for late endosomes and lysosomes (8). Co-localization of the bacteria with these markers is indicative of the trafficking of the organism along the endocytic pathway. A similar pattern of intracellular trafficking occurs when *F. tularensis* is taken up by TC-1 lung epithelial cells (45). In the BNL CL.2 hepatocytic cell line, the uptake of *F. tularensis* by hepatocytes occurs by clathrin-mediated endocytosis (44), although it remains to be verified whether the same holds true in primary hepatocytes. It is therefore highly probable that this organism traffics along the endocytic pathway once taken up by hepatocytes and, as shown previously, by epithelial cells (45). However, as in macrophages, the organism has devised means by which to escape intracellular killing and replicate in hepatocytes (FIGURE 4) (121). The *igl* operon is a part of the FPI and includes the genes *iglABC,* which are required for intracellular replication in macrophages. Studies using *iglC* and *mglA* mutants in the LVS and ssp. *novicida* found that expression of either of the genes is required for normal trafficking of the bacteria within macrophages. Specifically, loss of these genes results in bacteria that are unable to

escape the intra-macrophage phagosome (8,39,40). Another operon composed of *capABC* is required for the efficient infection of the lungs, liver, and spleen of mice inoculated via the respiratory route with the LVS. Deletion of *capB* alone is sufficient to diminish the replicative capacity of the LVS in macrophages. A similar but less severe phenotype is seen when those genes are deleted in the Schu S4 strain (149). Several genes have been identified in the Schu S4 strain as being required for replication in HepG2 hepatocytes. Many of these genes are involved in nucleotide biosynthesis and acquisition of specific nutrients (119). The requirement for specific bacterial genes for intracellular replication is not limited to macrophages. The *F. tularensis* transposon mutant screen performed as part of this dissertation identified a gene, *fumA*, which is required for replication of the LVS in hepatocytes (FIGURE 13). *fumA* encodes a fumarate hydratase, which is a metabolic enzyme that catalyzes the hydration of fumarate to malate in the citric acid cycle. A transposon mutant of this gene in ssp. *novicida* has reduced growth capacity in macrophages. Additionally, this mutant protects mice against subsequent challenge with the Schu S4 strain (150). Collectively, these studies show that while *F. tularensis* does not actively promote its uptake by hepatocytes, the organism possesses genes that regulate its intracellular replication.

The liver is a major target for infection during tularemia. Infection of the organ with *F. tularensis* results in the recruitment of macrophages and neutrophils and the formation of granulomatous lesions (77,78,120). The predominant phenotype of the immune cell population within hepatic granulomas during tularemia is Mac-1^+. By 5 days post-infection, the population of Mac-1^+ Gr-1^+ cells increases significantly. The Mac-1^+ Gr-1^+ phenotype most likely represents immature myeloid cells recruited from the

vasculature, which are capable of differentiating into mature macrophages or granulocytes (77). Populations of immature myeloid cells also accumulate in the spleens of tularemic mice, where they appear to suppress the expansion of T cells and contribute to host protection (151).

A liver infected with *F. tularensis* contains a number of cells that are capable of producing an immune response to the organism. In tularemic livers, natural killer cells, T cells, and natural killer T cells are the main producers of IFN-γ, with natural killer cells constituting the dominant fraction (78). IFN-γ, which is a cytokine known to play a role in the protective response to *F. tularensis*, is essential for the formation of hepatic granulomas and for spatial restriction of the pathogen in the liver. The induction of cell death within tularemic livers is also dependent on the production of IFN-γ (78). In addition, activation of hepatic macrophages by IFN-γ is an important protective response to *F. tularensis*, which decreases the ability of this bacterium to survive intracellularly. IL-12 and IL-18 work synergistically to promote the production of IFN-γ by hepatic lymphocytes (152).

Immune cells that are recruited to tularemic livers at later times are undoubtedly a source of cytokines that perpetuate and amplify inflammation. However, an unanswered question is how inflammation in the livers of tularemic mice is initiated. Possible sources of cytokines that initiate inflammation in infected livers include resident macrophages, endothelial cells, and hepatocytes. The pro-inflammatory response of endothelial cells, as determined by the secretion of CCL2 and CXCL8, is suppressed by live but not killed *F. tularensis.* Furthermore, the live bacteria have the capacity to dampen the response of endothelial cells to killed organisms (66). Similar suppression of the immune response

occurs with macrophages (67,153). It is therefore possible that hepatocytes are an important source of cytokines that bring in the first wave of leukocytes in response to *F. tularensis*. In agreement with this hypothesis, primary hepatocytes challenged with the LVS increased transcription of genes encoding chemoattractants for neutrophils, monocytes, and lymphocytes, as well as a granulocyte colony-stimulating factor (TABLE 3). Additionally, two potent neutrophil chemoattractants, CXCL5 and CXCL1, were secreted at higher levels by the infected cells (FIGURE 14). Interestingly, *Cxcl1* and *Cxcl5* are linked genes located on chromosome 5 and chromosome 4 in mice and humans, respectively. Neutrophils are recruited to tularemic livers and result in lysis of infected hepatocytes (69). These data provide suggestive evidence that infected hepatocytes might be the source of chemokines required for the recruitment of neutrophils to the foci of infection in tularemic livers.

The protein expression profile of *F. tularensis* grown in BHI broth mimics that of the organisms grown in macrophages (13,14). Furthermore, *F. tularensis* grown in either BHI broth or macrophages has a reduced ability to stimulate the secretion of proinflammatory cytokines from naive macrophages. In contrast, organisms grown in MH II broth stimulate macrophages to secrete large amounts of TNF-α, CCL2, IL-6 and IL-12p40 (61). These observations have led to the conclusion that *F. tularensis* grown in BHI broth are less pro-inflammatory than organisms grown in MH II broth and more comparable to 'host-adapted' organisms. Expression of *Cxcl5*, *Csf3*, *Ccl20*, *Cxcl1,* and *Ccl2* was upregulated by more than 4-fold in hepatocytes infected with MH II broth-grown LVS. Similarly, in hepatocytes infected with BHI-grown LVS, *Cxcl5*, *Csf3,* and *Ccl20* were upregulated (TABLE 3). Although expression of *Cxcl5* by cells infected with

BHI-grown organisms was an average of 50% lower compared to cells infected with MH II-grown bacteria, the expression of *Ccl2* and *Csf3* was similar under both conditions. Furthermore, the BHI-grown, but not MH II-grown, bacteria stimulated increased expression of *Vegfa*. In general, then, these data do not support the notion that BHI-grown bacteria elicit a uniformly milder response compared to their MH II-grown counterparts. Furthermore, the observations of Hazlett *et al*. (14) may be specific to macrophages.

Previous studies from our laboratory showed that killed, but not live, *F. tularensis* stimulates the secretion of CCL2 by endothelial cells (65). Furthermore, live *F. tularensis* suppresses the ability of endothelial cells to secrete CCL2 in response to killed organisms (66). While both live and killed LVS bacteria stimulate the secretion of CXCL8 and CCL2 by human monocyte-derived macrophages, a more substantial response is elicited by the killed organisms (58). In the present studies, the response of hepatocytes to killed LVS organisms was investigated. A similar profile of gene upregulation, with the addition of *IL1b*, was seen in hepatocytes incubated with the killed LVS, compared to live organisms (TABLE 3). It is unknown whether IL-1β is secreted by hepatocytes incubated with the killed bacteria. However, this observation contrasts with an earlier report where the live, but not killed, LVS stimulated secretion of IL-1β by macrophages (58). The level of expression of *Cxcl5* by hepatocytes exposed to the killed LVS was more than twice that elicited by the live bacteria. However, levels of expression of *Csf3*, *Cxcl1,* and *Ccl2* were similar in cells incubated with the killed or live bacteria, and the level of *Ccl20* was much lower in the former condition. Overall, the expression of genes encoding immune mediators was not consistently higher in hepatocytes infected with the

killed bacteria compared to live organisms. These data imply that the hyper-stimulatory nature of the killed LVS may be specific with respect to both cell type and cytokine.

These dissertation studies provide suggestive evidence that hepatocytes could be major players in the pathogenesis of tularemia. Hepatocytes take up and may be capable of supporting intracellular replication of the organism, particularly virulent strains. Additionally, *F. tularensis* expresses molecules that modulate its replication in hepatocytes. Furthermore, in response to the presence of the organism, hepatocytes secrete pro-inflammatory mediators that have the potential to recruit leukocytes to the sites of infection within the liver. As a result, hepatocytes may be the instigators of the initial inflammatory response in tularemic livers. Definitive evidence of the function of hepatocytes in tularemia will require further investigation, particularly using in vivo approaches.

FUTURE DIRECTIONS

In these dissertation studies, the LVS did not appear to replicate in the primary mouse hepatocytes. This was not the same pattern that was observed for the hepatocytic cells lines. One possible reason could be endocytosis of gentamicin from the growth medium by primary cells. This possibility can be examined by reducing the time that the infected hepatocytes are exposed to gentamicin. Although it was established that *F. tularensis* is taken up by hepatocytes, their intracellular trafficking pathway has not been determined. Trafficking of the organism along the endocytic pathway can be examined by immunofluorescence microscopy using antibodies against EEA1 and LAMP-1. The goal of these experiments would be to assess co-localization of the bacteria with markers for early endosomes and lysosomes. Additionally, escape of the organism into the cytoplasm can be assessed by differentially labeling cytoplasmic bacteria and those contained within endosomes (37). It would also be interesting to determine how the trafficking of killed bacteria within hepatocytes compares to that of their living counterparts.

The *fumA* gene was identified as being required for the replication of the LVS in hepatocytes. A *fumA* transposon mutant in ssp. *novicida* is attenuated for virulence in mice (150), but it is unknown if the same holds true for the LVS::*fumA* mutant. It would be informative to determine the virulence of a mutant that lacks this gene in mice, as well as to continue the screen of the LVS transposon library to identify additional genes that are involved in the uptake and intracellular growth of this organism. An important outstanding question is whether there is a relationship between *F. tularensis* virulence, ability to be taken up by or replicate within primary hepatocytes, and ability to induce

death of hepatocytes. These studies can be carried out using *F. tularensis* strains of varying virulence, such as the attenuated LVS, the virulent ssp. *holarctica* strains OSU18 and FSC200, and the highly virulent Schu S4 strain. Analysis of uptake and replication of these organisms can be conducted in primary hepatocytes as performed for the LVS herein, while the ability of the strains to cause cell death can be assessed by the release of alanine aminotransferase from infected hepatocytes. This enzyme is found in the cytoplasm of several cell types, including hepatocytes. Its presence in the extracellular medium is indicative of a loss of cellular integrity.

The studies presented in this dissertation establish that the LVS replicates in hepatocytes, and that these cells are capable of responding to infection. ELISAs could be used to measure secretion of all the cytokines upregulated in response to LVS grown in MH II broth or BHI broth, or to the killed LVS. It would be extremely important to further analyze the replication of the highly virulent Schu S4 strain in primary hepatocytes. Furthermore, the response of primary hepatocytes to the Schu S4 strain would be informative. These studies can be performed using RT^2 Profiler Arrays for proinflammatory cytokines and receptors, as was done with the LVS. It is expected that these cells would also mount an immune response to the Schu S4 strain. However, it would be interesting to determine if the response of the hepatocytes to the highly virulent Schu S4 strain differs from their response to the attenuated LVS.

Additionally, it would be imperative to analyze whether hepatocytes secrete chemokines in tularemic mice. These studies can be performed using an in situ technique developed by Ramesh *et al*. (154). The livers of *F. tularensis* infected mice can be harvested and treated with brefeldin A to prevent secretion and allow intracellular

accumulation of cytokines. Liver sections can then be stained for cytokines of interest and markers, such as hepatocyte nuclear factor 4α, to differentiate between hepatocytes and other cell types.

Chapter 2: Acquisition of iron by *Francisella tularensis*

RESULTS

I. Growth of Δ*feoB* and Δ*fslC* mutants in iron-replete and iron-restrictive broth

Previous microarray studies from our laboratory determined that genes of the *fsl* operon are the most highly upregulated by *F. tularensis* grown in FL83B hepatocytes compared to MH II broth. Of these genes, *fslC* is the most highly expressed. In-frame deletion of the *fslC* gene in the LVS prevents production of siderophore, a phenotype that is reversed by complementation of the gene. Despite not being able to produce the siderophore, the Δ*fslC* mutant still grows comparably to the wild-type LVS in iron-rich MH II broth. This observation suggested the presence of an additional mechanism for the acquisition of iron by *F. tularensis*. The *feoB* gene, which encodes a putative ferrous iron transporter, was identified in the genome of the LVS. In-frame deletion of this gene results in slowed growth of the bacteria on chocolate agar, and supplementation of the agar with ferric phosphate restores the replication of the Δ*feoB* mutant to wild-type levels (121).

These observations suggested that FeoB is involved in assimilation of iron by *F. tularensis*, a hypothesis that I pursued in these dissertation studies. First, I examined the ability of the Δ*feoB* and Δ*fslC* mutants to replicate in iron-replete (7.2 μM) or iron-limiting (360 nM) liquid medium. Although ferrous iron was added to the medium, oxidation results in an equilibrium between the ferrous and ferric forms. The wild-type LVS, mutants, and their complemented strains all grew well in medium replete with iron (FIGURE 15A). In the presence of limiting amounts of iron, the Δ*fslC* mutant grew similarly to the wild-type organisms. In contrast, the Δ*feoB* strain displayed almost no

growth during the first 20 h of culture but, with time, reached a density comparable to that of wild-type bacteria. The delay in growth of the Δ*feoB* mutant was eliminated by complementation, demonstrating that the phenotype is specific to loss of *feoB* (FIGURE 13B).

II. Replication of the Δ*feoB* and Δ*fslC* strains in host cells

To address whether FslC and FeoB are important for the growth of *F. tularensis* in host cells, FL83B hepatocytes, human A549 lung epithelial cells, or human monocyte-derived macrophages were incubated with the wild-type LVS, Δ*fslC* mutant, Δ*feoB* mutant, or complemented strains. Uptake of all the strains by the hepatocytes, epithelial cells, or macrophages was similar (FIGURE 16). Whereas growth of the Δ*fslC* mutant in the hepatocytes (FIGURE 16A) and epithelial cells (FIGURE 16B) was comparable to that of the wild-type LVS, intracellular replication of the Δ*feoB* mutant in these cell types was negligible. In both cases, complementation rescued the ability of the Δ*feoB* mutant to replicate. In contrast, all strains grew equivalently in the macrophages (FIGURE 16C). These results show that FeoB is necessary for efficient replication of *F. tularensis* in some, but not all, host cells.

III. Virulence of the Δ*feoB* and Δ*fslC* mutants in mice

The contribution of the *fslC* and *feoB* genes to the virulence of *F. tularensis* was assessed by infecting C3H/HeN mice intradermally with a lethal amount of the LVS or comparable numbers of the mutant strains. The mice were then monitored for time of death. All mice that received either the wild-type LVS or Δ*feoB* mutant succumbed by day 7 post-infection, whereas 30% of mice inoculated with the Δ*fslC* strain survived

until the experiment was ended at day 20 post-infection. However, complementation did not restore the virulence of the Δ*fslC* strain (FIGURE 17).

IV. Colonization of organs following infection of mice with the Δ*feoB* and Δ*fslC* mutants

To investigate whether the mutants have a detectable phenotype when administered at a lower dose, bacterial burdens were measured in target organs after mice were inoculated intradermally with a sublethal amount of the mutants, their complemented counterparts, or the wild-type LVS. Three days after infection, livers (FIGURE 18A) and spleens (FIGURE 18C) contained comparable numbers of the Δ*fslC* mutant and wild-type organisms. In the lung, there was a modest decrease in Δ*fslC* organisms compared to wild-type bacteria, but there was no significant difference between the Δ*fslC* mutant and its complemented strain (FIGURE 18B). In striking contrast, the Δ*feoB* mutant showed substantially reduced burdens in all three organs, a defect that was reversed by complementation (FIGURE 18). These results indicate that the loss of FeoB results in a markedly diminished ability to establish systemic infection after intradermal inoculation of a sublethal dose.

FIGURE 15. Δ*feoB* mutant shows impaired growth in medium containing low levels of iron. Growth of the wild-type LVS, the Δ*feoB* and Δ*fslC* mutants, and their corresponding complemented strains (c. Δ*feoB* and c. Δ*fslC*) was assessed in Che-CDM containing 7.2 μM $FeSO_4$ (A), or Che-CDM containing 360 nM $FeSO_4$ (B). Growth of the bacterial strains was quantified by measuring the OD_{600} at various times. All experiments were repeated two more times with similar results.

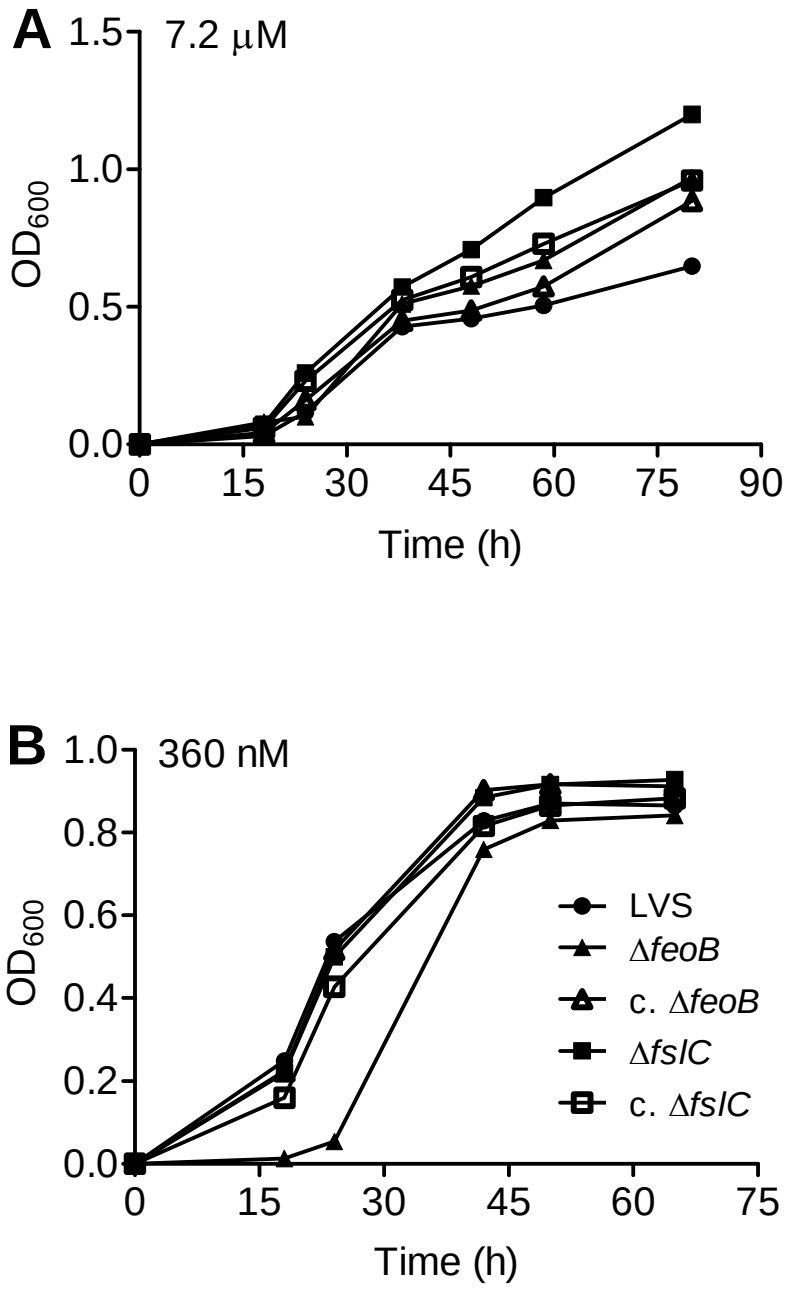
A
7.2 μM
1.5
1.0
0.5
0.0
OD600
0
15
30
45
60
75
90
Time (h)
B
360 nM
1.0
0.8
0.6
0.4
0.2
0.0
OD600
0
15
30
45
60
75
Time (h)
LVS
ΔfeoB
c. ΔfeoB
ΔfslC
c. ΔfslC

FIGURE 16. Δ*feoB* mutant shows impaired replication in hepatocytes and epithelial cells but not in macrophages. Murine FL83B hepatocytes (A), human A549 lung epithelial cells (B), or human monocyte-derived macrophages (C) were infected with the wild-type LVS, Δ*feoB* and Δ*fslC* mutants, or their corresponding complemented strains (c. Δ*fslC* and c. Δ*feoB*). The MOIs and times of infection were optimized for each cell type as follows: FL83B cells, MOI of 1000 for 2 h; A549 cells, MOI of 250 for 3 h; and macrophages, MOI of 50 for 2 h. The cultures were then treated with gentamicin for 1 h to kill extracellular bacteria. Some samples were lysed immediately after treatment with antibiotic to measure uptake using a CFU assay. Other samples were further incubated for a total of 24 h (A and B) or 16 h (C) to permit replication. Bars represent the means ± SD from 3 replicate samples. ***, $P < 0.001$ compared to replication of all other strains. For each type of host cell, there was no significant difference in uptake of the various bacterial strains. The experiments shown in Panels A and B were repeated one or two more times, respectively, yielding similar results. Similar growth of the wild-type LVS and Δ*feoB* mutant in human macrophages, as shown in Panel C, was confirmed in three additional experiments.

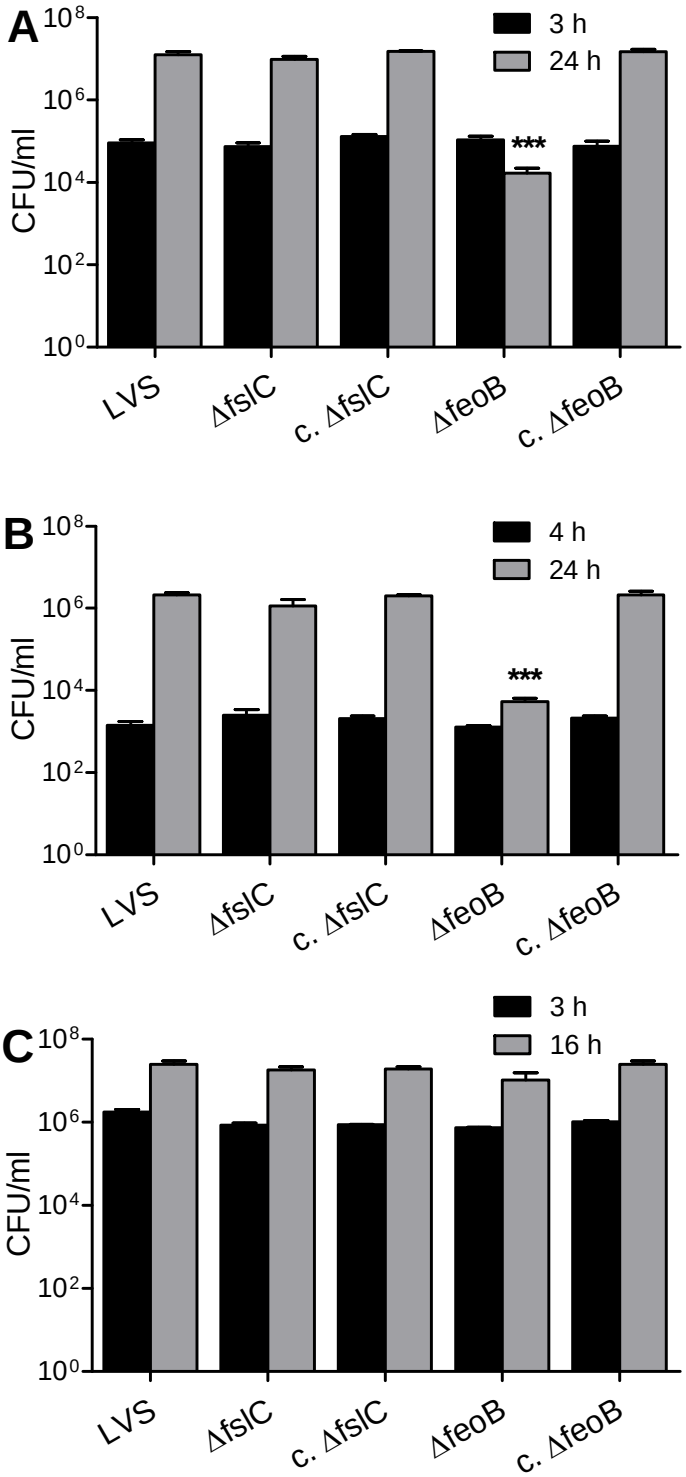
A
B
C
CFU/ml
3 h
24 h
4 h
16 h
***
LVS
ΔfslC
c. ΔfslC
ΔfeoB
c. ΔfeoB

FIGURE 17. Loss of FeoB does not prevent *F. tularensis* LVS from causing lethal disease in mice. C3H/HeN mice were infected intradermally with 2.0 x 10^7 bacteria of the wild-type LVS, the Δ*feoB* or Δ*fslC* strain, or the complemented Δ*fslC* strain (c. Δ*fslC*). Mice were monitored for 20 days, and the time of death was recorded. Data are combined from two experiments, each of which included 5 mice per group. The wild-type LVS and the Δ*fslC* and Δ*feoB* mutants were tested in the first experiment; the second experiment studied the wild-type LVS, the Δ*fslC* strain, and the complemented Δ*fslC* strain. Pairwise comparison revealed a significant difference only between the wild-type LVS and Δ*fslC* groups ($P = 0.0009$).

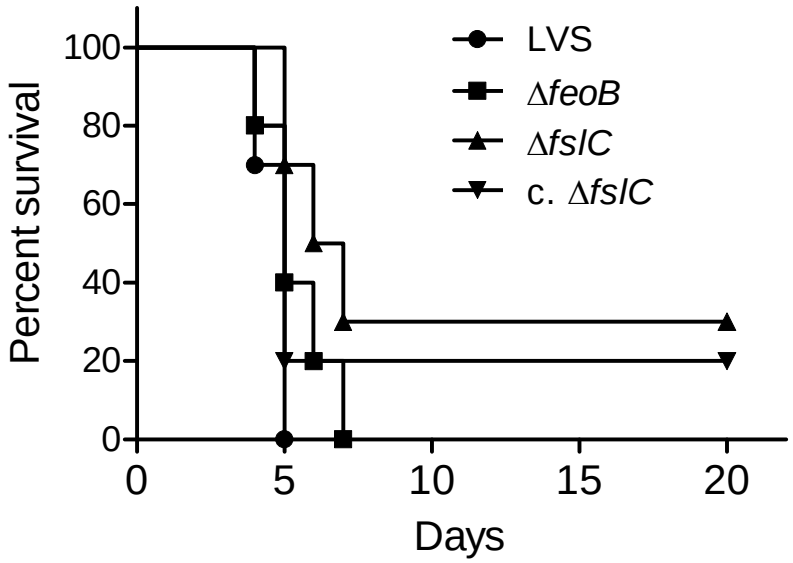
Percent survival
100
80
60
40
20
0
0
5
10
15
20
Days
LVS
ΔfeoB
ΔfslC
c. ΔfslC

FIGURE 18. Δ*feoB* mutant is defective for colonization of the liver, lungs, and spleen of infected mice. C3H/HeN mice were inoculated intradermally with a sublethal dose (3 x 10^5 CFU) of the wild-type LVS, the Δ*feoB* or Δ*fslC* mutant, or their complemented strains (c. Δ*fslC* and c. Δ*feoB*). Organs were harvested 3 days after infection, and the CFU/g of liver (A), lungs (B), and spleen (C) were determined. The data are combined from three independent experiments. A total of 8 mice per group in two experiments was used in studies of the Δ*feoB* and c. Δ*feoB* strains; samples from nine organs were lost to contamination. A total of 5 mice per group was used in one experiment with the Δ*fslC* and c. Δ*fslC* strains. The bars denote medians ± SD. *, $P < 0.05$; **, $P < 0.01$; ***, $P < 0.001$.

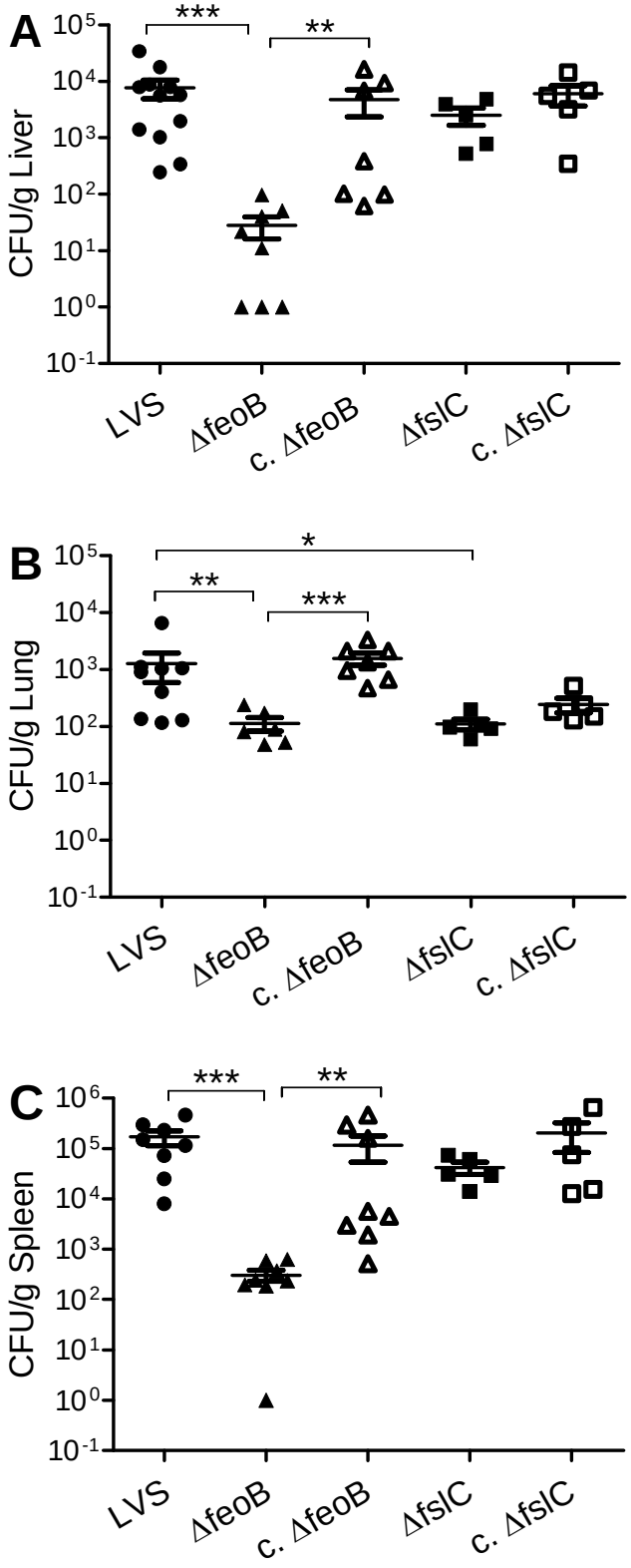
A
CFU/g Liver
***
**
LVS
ΔfeoB
c. ΔfeoB
ΔfslC
c. ΔfslC
B
CFU/g Lung
*
**
***
C
CFU/g Spleen

DISCUSSION

The studies presented in this chapter demonstrate that the FeoB protein is important for the acquisition of iron by *F. tularensis*. The *Francisella* siderophore locus has been well described. These genes of this operon are required for production of a siderophore and the acquisition of ferric iron by the bacterium (104,106,108). Many bacteria possess a Feo transport system that is used for acquisition of ferrous iron. Of the 250 completely sequenced bacterial genomes, 46% possess genes of the Feo system (110). Mutation of the *feo* genes in *E. coli* results in defective import of ferrous iron, lower levels of intracellular iron, and impaired ability to colonize the mouse intestine (114,155). Genes encoding FeoA and FeoB were identified in the LVS (104,116), but their biological functions had not been determined.

An in-frame deletion of *feoB* and the corresponding complemented strain were constructed in our laboratory to explore the role of this gene in acquisition of iron. The studies presented in this dissertation show that there was a 20-h delay in the growth of the Δ*feoB* mutant in medium containing restrictive levels of iron. However, the density of cultures of this mutant eventually reached that of the wild-type LVS (FIGURE 15B). Huaixin Zheng of our group conducted experiments to measure the replication of the Δ*feoB* mutant and the secretion of siderophores simultaneously. The siderophore activity was quantified by colorimetric chrome azurol sulfonate assays. These studies determined that the eventual burst of growth of the Δ*feoB* mutant under these conditions correlates with the accumulation of siderophore in the medium (121). The intracellular iron content of Δ*feoB* organisms was also determined over a period of 23 h of culture using a colorimetric ferrozine assay. Iron accumulated in both the wild-type LVS and the Δ*fslC*

strain, but not in the Δ*feoB* organisms (121). Collectively, these data establish a role for FeoB in acquisition of iron by *F. tularensis*. Despite repeated attempts, our laboratory could not delete *fslC* and *feoB* simultaneously. This failure suggests that the siderophore and FeoB are the major mechanisms by which *F. tularensis* takes up iron.

It has been well documented that *F. tularensis* invades hepatocytes *in vivo*. Inoculation of mice with the LVS by the intravenous or intradermal route results in infection of the liver, where the bacteria grow in both Kuppfer cells and hepatocytes (69,77). In the absence of IFN-γ, replication of the LVS in hepatocytes *in vivo* is extensive (78), and a highly virulent type A strain shows enhanced growth in hepatocytes compared to the LVS *in vitro* and *in vivo* (130,156). In the studies presented in Chapter 1 of this dissertation, the replication of the LVS in cultured hepatocytic lines confirms that this cell type provides a hospitable niche for *F. tularensis*. Furthermore, data in this chapter and from other investigators indicate that the siderophore-ferric iron system is not essential for intracellular replication. Growth of an LVS Δ*fslA* mutant and a Schu S4 Δ*fslE* mutant in murine J774 macrophage-like cells is the same as that of the wild-type parental bacteria (105,107). Similarly, growth of the Δ*fslC* mutant in hepatocytes, epithelial cells, and macrophages was similar to that of the wild-type LVS (FIGURE 16). To avoid toxicity, levels of free iron in hosts are tightly regulated. Extracellular iron is bound to proteins in the ferric form. Free ferrous iron is needed for various physiological and pathological processes within host cells, but any excess is oxidized and either exported or stored bound to ferritin (102). These data suggest that intracellular *F. tularensis* can acquire this ferrous iron via FeoB, since replication of the Δ*feoB* mutant was greatly reduced in both hepatocytic and epithelial cells (FIGURE 16A and B).

Notably, replication of the Δ*feoB* mutant was similar to that of the wild-type LVS in human macrophages (FIGURE 16C). Macrophages recycle iron from dead and damaged erythrocytes and are the main source of the body's iron (100). Perhaps, then, the amount of available iron differs in various types of cells, and loss of FeoB impairs the ability of intracellular *F. tularensis* to acquire iron when amounts are limited.

The impact of deletion of *feoB* and *fslC* on the virulence of *F. tularensis* in mice was evaluated. The Δ*feoB* mutant and the wild-type LVS were equally capable of causing fatal disease, at least by the intradermal route and using the dose tested. Fewer mice died when infected with a comparable inoculum of the Δ*fslC* mutant, but complementation did not alter this outcome (FIGURE 17). Similarly, complementation did not reverse the diminished bacterial loads in the lungs of mice infected with a sublethal amount of the Δ*fslC* mutant (FIGURE 18B). Studies performed in our laboratory showed that the complemented Δ*fslC* strain secretes siderophore *in vitro* (121), but it is possible that complementation was not effective in the more stringent *in vivo* environment. Regardless, it is not possible to conclude with certainty that the diminished virulence of the Δ*fslC* strain was specific to loss of the gene. Notably, ablation of *fslA* was previously reported to have no effect on the ability of *F. tularensis* Schu S4 to kill mice infected intradermally (109). Although deletion of *feoB* produced no phenotype in the survival assay, loss of this gene resulted in significantly reduced bacterial burdens in the lungs, liver, and spleen of mice infected with a sublethal dose. Moreover, these reductions were reversed by complementation (FIGURE 18). The observations made in this study are in agreement with the previous finding that a *feoB*::Tn5 mutant of the LVS is defective for replication in the lungs of mice after intranasal inoculation (117). Collectively, these

results indicate that FeoB contributes to virulence of *F. tularensis* in mice, but the consequences of disrupting its function become less important when large numbers of bacteria are administered.

In other Gram-negative bacteria, FeoB is located in the inner membrane (110). This observation raises the question of how iron crosses the outer membrane and enters the periplasm of *F. tularensis* for subsequent transport via FeoB. In the Schu S4 strain, this function is carried out by FupA, an outer membrane protein that is required for high-affinity uptake of ferrous iron (107). The LVS does not have a distinct *fupA* gene but rather a *fupA/B* hybrid gene. Whether transport of ferrous iron across the outer membrane of the LVS is carried out by FupA/B or a different molecule remains to be determined. If *fupA* and *feoB* are members of a sequential pathway, then mutants in either gene should have the same phenotype. However, Schu S4 Δ*fupA* strains are attenuated in survival studies in mice (107,109), whereas the LVS Δ*feoB* mutant retained wild-type virulence in this assay (FIGURE 17). This seeming disparity may reflect differences in the ways by which the LVS and Schu S4 strain acquire iron, or it may show that FupA has functions in addition to uptake of iron. In support of the latter possibility, the FupA homologue of *F. novicida* has been implicated in both immune evasion and maintenance of integrity of the bacterial outer membrane (157).

F. tularensis likely requires more than one mechanism to obtain iron due to the many different environments in which it grows. *F. tularensis* has been isolated from water and moist soil. The bacterium also has a broad range of hosts; it infects over 250 animal species, including mammals, birds, fish, invertebrates, and amoeba (10,158). In mice, viable *F. tularensis* is found both intracellularly and extracellularly in the blood

throughout the course of infection (159). It was determined here that FslC and FeoB both contribute to the acquisition of iron, but their functions are not completely redundant. FslC is required for production of a siderophore, which likely provides the bulk of iron when the bacterium grows in niches where ferric iron predominates. FeoB appears more important for replication of the bacterium within cells, at least in the case of hepatocytes and epithelial cells. FeoB also contributes to growth of *F. tularensis* before sufficient siderophore accumulates. Thus, multiple mechanisms for acquisition of iron appear to benefit *F. tularensis* by allowing it to flourish in diverse environments.

FUTURE DIRECTIONS

Reduced numbers of the Δ*feoB* mutant were recovered from the lungs, liver, and spleen of mice infected for 3 days. The intradermal route of infection requires that the organism first disseminate throughout the animal and then colonize the tissues of the organs analyzed. Using this route it is not possible to conclude if the defect lies in the inability of the mutant to disseminate to key organs or replicate once it reaches them. These possibilities can be distinguished by directly infecting the animals via the tail vein, and then measuring organ burdens. This route negates the need for dissemination and would therefore specifically measure colonization of the organs. The studies presented in this chapter were performed with the LVS. It would therefore be valuable to examine whether FeoB is used by the clinically relevant Schu S4 strain for the acquisition of iron. These studies would require generation of a Δ*feoB* mutant and complemented strain in the Schu S4 background. Characterization of the mutant could then be performed as was done herein with the LVS.

Replication of the Δ*feoB* and Δ*fslC* mutants and their complemented strains was assessed in hepatocytic cell lines. It is not known whether the requirement for FeoB might differ when the organism is grown in primary hepatocytes. It would therefore be valuable to repeat these studies using primary mouse hepatocytes. Furthermore, since the Δ*feoB* mutant replicated normally in human monocyte-derived macrophages, it would be useful to repeat this study using mouse bone marrow-derived macrophages. Such a study would help to distinguish between cell-type and species-specific differences.

SUMMARY OF OBSERVATIONS

Live, killed, or metabolically inactive *Francisella tularensis* is ingested by hepatocytes in a process that requires polymerization of the host cell's actin cytoskeleton. Following uptake, *F. tularensis* replicates in the cytoplasm of the hepatocytes. In response to live or killed LVS organisms, primary mouse hepatocytes increase their expression of several genes encoding proinflammatory cytokines. It is unknown whether intracellular or extracellular bacteria (or both) stimulate this hepatocytic response. Primary cells exposed to the live bacteria also secrete CXCL1 and CXCL5, two chemoattractants that potentially recruit neutrophils to the infected liver. Replication of the LVS in hepatocytes requires expression of *fumA* and *feoB* genes by the bacteria. The *feoB* gene is also required for the replication of the LVS in iron-restrictive medium and facilitates the uptake of iron by the organism (FIGURE 19).

FIGURE 19. Summary of observations. See text for details.

REFERENCES

1. Petersen, J. M., and M. E. Schriefer. 2005. Tularemia: emergence/re-emergence. *Vet. Res.* 36: 455-467.

2. Oyston, P. C., and J. E. Quarry. 2005. Tularemia vaccine: past, present and future. *Antonie Van Leeuwenhoek.* 87: 277-281.

3. Elkins, K. L., S. C. Cowley, and C. M. Bosio. 2003. Innate and adaptive immune responses to an intracellular bacterium, *Francisella tularensis* live vaccine strain. *Microbes Infect.* 5: 135-142.

4. Gallagher, L. A., E. Ramage, M. A. Jacobs, R. Kaul, M. Brittnacher, and C. Manoil. 2007. A comprehensive transposon mutant library of *Francisella novicida*, a bioweapon surrogate. *Proc. Natl. Acad. Sci. U. S. A.* 104: 1009-1014.

5. Saslaw, S., H. T. Eigelsbach, H. E. Wilson, J. A. Prior, and S. Carhart. 1961. Tularemia vaccine study. I. Intracutaneous challenge. *Arch. Intern. Med.* 107: 689-701.

6. Saslaw, S., H. T. Eigelsbach, J. A. Prior, H. E. Wilson, and S. Carhart. 1961. Tularemia vaccine study. II. Respiratory challenge. *Arch. Intern. Med.* 107: 702-14.

7. Dennis, D. T., T. V. Inglesby, D. A. Henderson, J. G. Bartlett, M. S. Ascher, E. Eitzen, A. D. Fine, A. M. Friedlander, J. Hauer, M. Layton, S. R. Lillibridge, J. E. McDade, M. T. Osterholm, T. O'Toole, G. Parker, T. M. Perl, P. K. Russell, and K. Tonat. 2001. Tularemia as a biological weapon: medical and public health management. *JAMA* 285: 2763-2773.

8. Clemens, D. L., and M. A. Horwitz. 2007. Uptake and intracellular fate of *Francisella tularensis* in human macrophages. *Ann. N. Y. Acad. Sci.* 1105: 160-86.

9. McCoy G.W, and Chapin C.W. 1912. Further observations on a plague-like disease of rodents with a preliminary note on the causative agent, *bacterium tularense*. *The J. Infect. Dis.* 10: 61-72.

10. Sjostedt, A. 2007. Tularemia: history, epidemiology, pathogen physiology, and clinical manifestations. *Ann. N. Y. Acad. Sci.* 1105: 1-29.

11. Greenfield, R. A., and M. S. Bronze. 2003. Prevention and treatment of bacterial diseases caused by bacterial bioterrorism threat agents. *Drug Discov. Today* 8: 881-888.

12. Horzempa, J., P. E. Carlson, Jr., D. M. O'Dee, R. M. Shanks, and G. J. Nau. 2008. Global transcriptional response to mammalian temperature provides new insight

into *Francisella tularensis* pathogenesis. *BMC Microbiol.* 8: 172. doi: 10.1186/1471-2180-8-172.

13. Hazlett, K. R., and K. A. Cirillo. 2009. Environmental adaptation of *Francisella tularensis*. *Microbes Infect.* 11: 828-834.

14. Hazlett, K. R., S. D. Caldon, D. G. McArthur, K. A. Cirillo, G. S. Kirimanjeswara, M. L. Magguilli, M. Malik, A. Shah, S. Broderick, I. Golovliov, D. W. Metzger, K. Rajan, T. J. Sellati, and D. J. Loegering. 2008. Adaptation of *Francisella tularensis* to the mammalian environment is governed by cues which can be mimicked in vitro. *Infect. Immun.* 76: 4479-4488.

15. Hajjar, A. M., M. D. Harvey, S. A. Shaffer, D. R. Goodlett, A. Sjostedt, H. Edebro, M. Forsman, M. Bystrom, M. Pelletier, C. B. Wilson, S. I. Miller, S. J. Skerrett, and R. K. Ernst. 2006. Lack of in vitro and in vivo recognition of *Francisella tularensis* subspecies lipopolysaccharide by Toll-like receptors. *Infect. Immun.* 74: 6730-6738.

16. Rebeil, R., R. K. Ernst, B. B. Gowen, S. I. Miller, and B. J. Hinnebusch. 2004. Variation in lipid A structure in the pathogenic *Yersiniae*. *Mol. Microbiol.* 52: 1363-1373.

17. Shaffer, S. A., M. D. Harvey, D. R. Goodlett, and R. K. Ernst. 2007. Structural heterogeneity and environmentally regulated remodeling of *Francisella tularensis* subspecies *novicida* lipid A characterized by tandem mass spectrometry. *J. Am. Soc. Mass Spectrom.* 18: 1080-1092.

18. Thanassi, D. G., J. B. Bliska, and P. J. Christie. 2012. Surface organelles assembled by secretion systems of Gram-negative bacteria: diversity in structure and function. *FEMS Microbiol. Rev.* 36: 1046-1082.

19. Kostakioti, M., C. L. Newman, D. G. Thanassi, and C. Stathopoulos. 2005. Mechanisms of protein export across the bacterial outer membrane. *J. Bacteriol.* 187: 4306-4314.

20. Gil, H., G. J. Platz, C. A. Forestal, M. Monfett, C. S. Bakshi, T. J. Sellati, M. B. Furie, J. L. Benach, and D. G. Thanassi. 2006. Deletion of TolC orthologs in *Francisella tularensis* identifies roles in multidrug resistance and virulence. *Proc. Natl. Acad. Sci. U. S. A.* 103: 12897-12902.

21. Platz, G. J., D. C. Bublitz, P. Mena, J. L. Benach, M. B. Furie, and D. G. Thanassi. 2010. A *tolC* mutant of *Francisella tularensis* is hypercytotoxic compared to the wild type and elicits increased proinflammatory responses from host cells. *Infect. Immun.* 78: 1022-1031.

22. Barker, J. R., and K. E. Klose. 2007. Molecular and genetic basis of pathogenesis in *Francisella tularensis*. *Ann. N. Y. Acad. Sci.* 1105: 138-59.

23. Gil, H., J. L. Benach, and D. G. Thanassi. 2004. Presence of pili on the surface of *Francisella tularensis*. *Infect. Immun.* 72: 3042-3047.

24. Chakraborty, S., M. Monfett, T. M. Maier, J. L. Benach, D. W. Frank, and D. G. Thanassi. 2008. Type IV pili in *Francisella tularensis*: roles of *pilF* and *pilT* in fiber assembly, host cell adherence, and virulence. *Infect. Immun.* 76: 2852-2861.

25. Zogaj, X., S. Chakraborty, J. Liu, D. G. Thanassi, and K. E. Klose. 2008. Characterization of the *Francisella tularensis* subsp. *novicida* type IV pilus. *Micro.* 154: 2139-2150.

26. Ark, N. M., and B. J. Mann. 2011. Impact of *Francisella tularensis* pilin homologs on pilus formation and virulence. *Microb. Pathog.* 51: 110-120.

27. Pierini, L. M. 2006. Uptake of serum-opsonized *Francisella tularensis* by macrophages can be mediated by class A scavenger receptors. *Cell Microbiol.* 8: 1361-1370.

28. Schulert, G. S., and L. A. Allen. 2006. Differential infection of mononuclear phagocytes by *Francisella tularensis*: role of the macrophage mannose receptor. *J. Leukoc. Biol.* 80: 563-571.

29. Balagopal, A., A. S. MacFarlane, N. Mohapatra, S. Soni, J. S. Gunn, and L. S. Schlesinger. 2006. Characterization of the receptor-ligand pathways important for entry and survival of *Francisella tularensis* in human macrophages. *Infect. Immun.* 74: 5114-5125.

30. Clemens, D. L., B. Y. Lee, and M. A. Horwitz. 2005. *Francisella tularensis* enters macrophages via a novel process involving pseudopod loops. *Infect. Immun.* 73: 5892-5902.

31. Barel, M., A. G. Hovanessian, K. Meibom, J. P. Briand, M. Dupuis, and A. Charbit. 2008. A novel receptor - ligand pathway for entry of *Francisella tularensis* in monocyte-like THP-1 cells: interaction between surface nucleolin and bacterial elongation factor Tu. *BMC Microbiol.* 8: 145. doi: 10.1186/1471-2180-8-145.

32. Barel, M., K. Meibom, and A. Charbit. 2010. Nucleolin, a shuttle protein promoting infection of human monocytes by *Francisella tularensis*. *PLoS. One.* 5: e14193.

33. Tamilselvam, B., and S. Daefler. 2008. *Francisella* targets cholesterol-rich host cell membrane domains for entry into macrophages. *J. Immunol.* 180: 8262-8271.

34. Clemens, D. L., B. Y. Lee, and M. A. Horwitz. 2005. *Francisella tularensis* enters macrophages via a novel process involving pseudopod loops. *Infect. Immun.* 73: 5892-5902.

35. Clemens, D. L., B. Y. Lee, and M. A. Horwitz. 2009. *Francisella tularensis* phagosomal escape does not require acidification of the phagosome. ***Infect. Immun.*** 77: 1757-1773.

36. Clemens, D. L., B. Y. Lee, and M. A. Horwitz. 2004. Virulent and avirulent strains of *Francisella tularensis* prevent acidification and maturation of their phagosomes and escape into the cytoplasm in human macrophages. ***Infect. Immun.*** 72: 3204-3217.

37. Geier, H., and J. Celli. 2011. Phagocytic receptors dictate phagosomal escape and intracellular proliferation of *Francisella tularensis*. ***Infect. Immun.*** 79: 2204-2214.

38. Santic, M., M. Molmeret, K. E. Klose, S. Jones, and Y. A. Kwaik. 2005. The *Francisella tularensis* pathogenicity island protein IglC and its regulator MglA are essential for modulating phagosome biogenesis and subsequent bacterial escape into the cytoplasm. ***Cell Microbiol.*** 7: 969-979.

39. Lindgren, H., I. Golovliov, V. Baranov, R. K. Ernst, M. Telepnev, and A. Sjostedt. 2004. Factors affecting the escape of Francisella tularensis from the phagolysosome. J. Med. Microbiol. 53: 953-958.

40. Lai, X. H., I. Golovliov, and A. Sjostedt. 2004. Expression of *IglC* is necessary for intracellular growth and induction of apoptosis in murine macrophages by *Francisella tularensis*. ***Microb. Pathog.*** 37: 225-230.

41. Schmerk, C. L., B. N. Duplantis, P. L. Howard, and F. E. Nano. 2009. A *Francisella novicida pdpA* mutant exhibits limited intracellular replication and remains associated with the lysosomal marker LAMP-1. ***Microbiology.*** 155: 1498-1504.

42. Asare, R., and Y. A. Kwaik. 2010. Exploitation of host cell biology and evasion of immunity by *Francisella tularensis*. ***Front Microbiol.*** 1:145. doi:10.3389/fmicb.2010.00145.

43. Melillo, A., D. D. Sledjeski, S. Lipski, R. M. Wooten, V. Basrur, and E. R. Lafontaine. 2006. Identification of a *Francisella tularensis* LVS outer membrane protein that confers adherence to A549 human lung cells. ***FEMS Microbiol. Lett.*** 263: 102-108.

44. Law, H. T., A. E. Lin, Y. Kim, B. Quach, F. E. Nano, and J. A. Guttman. 2011. *Francisella tularensis* uses cholesterol and clathrin-based endocytic mechanisms to invade hepatocytes. ***Sci. Rep.*** 1: 192. doi: 10.1038/srep00192.

45. Craven, R. R., J. D. Hall, J. R. Fuller, S. Taft-Benz, and T. H. Kawula. 2008. *Francisella tularensis* invasion of lung epithelial cells. ***Infect. Immun.*** 76: 2833-2842.

46. Bradburne, C. E., A. B. Verhoeven, G. C. Manyam, S. A. Chaudhry, E. L. Chang, D. C. Thach, C. L. Bailey, and M. L. van Hoek. 2013. Temporal transcriptional response during infection of type II alveolar epithelial cells with *Francisella tularensis* live vaccine strain (LVS) supports a general host suppression and bacterial uptake by macropinocytosis. *J. Biol. Chem.* 288: 10780-10791.

47. Iwasaki, A., and R. Medzhitov. 2004. Toll-like receptor control of the adaptive immune responses. *Nat. Immunol.* 5: 987-995.

48. Broz, P., and D. M. Monack. 2011. Molecular mechanisms of inflammasome activation during microbial infections. *Immunol. Rev.* 243: 174-190.

49. Brown, G. D. 2006. Dectin-1: a signalling non-TLR pattern-recognition receptor. *Nat. Rev. Immunol.* 6: 33-43.

50. Cotran, R. S. 21999. Inflammation: Historical Perspectives. In *Inflammation: Basic principles and Clinical Correlates*, 3rd ed. J. I. Gallin and R. Snyderman, eds. Lippincott Williams and Wilkins, Philidelphia. 5-10.

51. Ley, K., C. Laudanna, M. I. Cybulsky, and S. Nourshargh. 2007. Getting to the site of inflammation: the leukocyte adhesion cascade updated. *Nat. Rev. Immunol.* 7: 678-689.

52. Kelly, M., J. M. Hwang, and P. Kubes. 2007. Modulating leukocyte recruitment in inflammation. *J. Allergy Clin. Immunol.* 120: 3-10.

53. Petri, B., and M. G. Bixel. 2006. Molecular events during leukocyte diapedesis. *FEBS J.* 273: 4399-4407.

54. Tacke, F., T. Luedde, and C. Trautwein. 2009. Inflammatory pathways in liver homeostasis and liver injury. *Clin. Rev. Allergy Immunol.* 36: 4-12.

55. Blanchet, X., M. Langer, C. Weber, R. R. Koenen, and H. P. von. 2012. Touch of chemokines. *Front Immunol.* 3: 175. doi: 10.3389/fimmu.2012.00175.

56. Fu, H., J. Karlsson, J. Bylund, C. Movitz, A. Karlsson, and C. Dahlgren. 2006. Ligand recognition and activation of formyl peptide receptors in neutrophils. *J. Leukoc. Biol.* 79: 247-256.

57. Muller, W. A. 2011. Mechanisms of leukocyte transendothelial migration. *Annu. Rev. Pathol.* 6: 323-44. doi: 10.1146/annurev-pathol-011110-130224.

58. Bolger, C. E., C. A. Forestal, J. K. Italo, J. L. Benach, and M. B. Furie. 2005. The live vaccine strain of *Francisella* tularensis replicates in human and murine macrophages but induces only the human cells to secrete proinflammatory cytokines. *J. Leukoc. Biol.* 77: 893-897.

59. Noah, C. E., M. Malik, D. C. Bublitz, D. Camenares, T. J. Sellati, J. L. Benach, and M. B. Furie. 2010. GroEL and lipopolysaccharide from *Francisella tularensis* live vaccine strain synergistically activate human macrophages. ***Infect. Immun.*** 78: 1797-1806.

60. Forestal, C. A., H. Gil, M. Monfett, C. E. Noah, G. J. Platz, D. G. Thanassi, J. L. Benach, and M. B. Furie. 2008. A conserved and immunodominant lipoprotein of *Francisella tularensis* is proinflammatory but not essential for virulence. ***Microb. Pathog.*** 44: 512-523.

61. Loegering, D. J., J. R. Drake, J. A. Banas, T. L. McNealy, D. G. Mc Arthur, L. M. Webster, and M. R. Lennartz. 2006. *Francisella tularensis* LVS grown in macrophages has reduced ability to stimulate the secretion of inflammatory cytokines by macrophages in vitro. ***Microb. Pathog.*** 41: 218-225.

62. Bosio, C. M., H. Bielefeldt-Ohmann, and J. T. Belisle. 2007. Active suppression of the pulmonary immune response by *Francisella tularensis* Schu4. ***J. Immunol.*** 178: 4538-4547.

63. Bosio, C. M., and S. W. Dow. 2005. *Francisella tularensis* induces aberrant activation of pulmonary dendritic cells. ***J. Immunol.*** 175: 6792-6801.

64. Bauler, T. J., J. C. Chase, and C. M. Bosio. 2011. IFN-beta mediates suppression of IL-12p40 in human dendritic cells following infection with virulent *Francisella tularensis*. ***J. Immunol.*** 187: 1845-1855.

65. Forestal, C. A., J. L. Benach, C. Carbonara, J. K. Italo, T. J. Lisinski, and M. B. Furie. 2003. *Francisella tularensis* selectively induces proinflammatory changes in endothelial cells. ***J. Immunol.*** 171: 2563-2570.

66. Bublitz, D. C., C. E. Noah, J. L. Benach, and M. B. Furie. 2010. *Francisella tularensis* suppresses the proinflammatory response of endothelial cells via the endothelial protein C receptor. ***J. Immunol.*** 185: 1124-1131.

67. Telepnev, M., I. Golovliov, T. Grundstrom, A. Tarnvik, and A. Sjostedt. 2003. *Francisella tularensis* inhibits Toll-like receptor-mediated activation of intracellular signalling and secretion of TNF-alpha and IL-1 from murine macrophages. ***Cell Microbiol.*** 5: 41-51.

68. Gao, B., W. I. Jeong, and Z. Tian. 2008. Liver: An organ with predominant innate immunity. ***Hepatology.*** 47: 729-736.

69. Conlan, J. W., and R. J. North. 1992. Early pathogenesis of infection in the liver with the facultative intracellular bacteria *Listeria monocytogenes*, *Francisella tularensis*, and *Salmonella typhimurium* involves lysis of infected hepatocytes by leukocytes. ***Infect. Immun.*** 60: 5164-5171.

70. Conlan, J. W., and R. J. North. 1991. Neutrophil-mediated dissolution of infected host cells as a defense strategy against a facultative intracellular bacterium. *J. Exp. Med.* 174: 741-744.

71. Conlan, J. W., and R. J. North. 1992. Monoclonal antibody NIMP-R10 directed against the CD11b chain of the type 3 complement receptor can substitute for monoclonal antibody 5C6 to exacerbate listeriosis by preventing the focusing of myelomonocytic cells at infectious foci in the liver. *J. Leukoc. Biol.* 52: 130-132.

72. Sjostedt, A., J. W. Conlan, and R. J. North. 1994. Neutrophils are critical for host defense against primary infection with the facultative intracellular bacterium *Francisella tularensis* in mice and participate in defense against reinfection. *Infect. Immun.* 62: 2779-2783.

73. Sample, A. K., and C. J. Czuprynski. 1991. Priming and stimulation of bovine neutrophils by recombinant human interleukin-1 alpha and tumor necrosis factor alpha. *J. Leukoc. Biol.* 49: 107-115.

74. Jaeschke, H., and T. Hasegawa. 2006. Role of neutrophils in acute inflammatory liver injury. *Liver Int.* 26: 912-919.

75. Wong, J., B. Johnston, S. S. Lee, D. C. Bullard, C. W. Smith, A. L. Beaudet, and P. Kubes. 1997. A minimal role for selectins in the recruitment of leukocytes into the inflamed liver microvasculature. *J. Clin. Invest.* 99: 2782-2790.

76. Shi, C., P. Velazquez, T. M. Hohl, I. Leiner, M. L. Dustin, and E. G. Pamer. 2010. Monocyte trafficking to hepatic sites of bacterial infection is chemokine independent and directed by focal intercellular adhesion molecule-1 expression. *J. Immunol.* 184: 6266-6274.

77. Rasmussen, J. W., J. Cello, H. Gil, C. A. Forestal, M. B. Furie, D. G. Thanassi, and J. L. Benach. 2006. Mac-1+ cells are the predominant subset in the early hepatic lesions of mice infected with *Francisella tularensis*. *Infect. Immun.* 74: 6590-6598.

78. Bokhari, S. M., K. J. Kim, D. M. Pinson, J. Slusser, H. W. Yeh, and M. J. Parmely. 2008. NK cells and gamma interferon coordinate the formation and function of hepatic granulomas in mice infected with the *Francisella tularensis* live vaccine strain. *Infect. Immun.* 76: 1379-1389.

79. Delpino, M. V., P. Barrionuevo, R. Scian, C. A. Fossati, and P. C. Baldi. 2010. *Brucella*-infected hepatocytes mediate potentially tissue-damaging immune responses. *J. Hepatol.* 53: 145-154.

80. Au, A. Y., J. M. Hasenwinkel, and C. G. Frondoza. 2011. Silybin inhibits interleukin-1beta-induced production of pro-inflammatory mediators in canine hepatocyte cultures. *J. Vet. Pharmacol. Ther.* 34: 120-129.

81. Dragomir, A. C., J. D. Laskin, and D. L. Laskin. 2011. Macrophage activation by factors released from acetaminophen-injured hepatocytes: potential role of HMGB1. *Toxicol. Appl. Pharmacol.* 253: 170-177.

82. Hentze, M. W., M. U. Muckenthaler, and N. C. Andrews. 2004. Balancing acts: molecular control of mammalian iron metabolism. *Cell* 117: 285-297.

83. Pollycove, M., and R. Mortimer. 1961. The quantitative determination of iron kinetics and hemoglobin synthesis in human subjects. *J. Clin. Invest.* 40: 753-782.

84. Leong, W. I., and B. Lonnerdal. 2004. Hepcidin, the recently identified peptide that appears to regulate iron absorption. *J. Nutr.* 134: 1-4.

85. Fuqua, B. K., C. D. Vulpe, and G. J. Anderson. 2012. Intestinal iron absorption. *J. Trace Elem. Med. Biol.* 26: 115-119.

86. Riedel, H. D., A. J. Remus, B. A. Fitscher, and W. Stremmel. 1995. Characterization and partial purification of a ferrireductase from human duodenal microvillus membranes. *Biochem. J.* 309: 745-748.

87. McKie, A. T. 2008. The role of Dcytb in iron metabolism: an update. *Biochem. Soc. Trans.* 36: 1239-1241.

88. Courville, P., R. Chaloupka, and M. F. Cellier. 2006. Recent progress in structure-function analyses of Nramp proton-dependent metal-ion transporters. *Biochem. Cell Biol.* 84: 960-978.

89. Fleming, M. D., C. C. Trenor, III, M. A. Su, D. Foernzler, D. R. Beier, W. F. Dietrich, and N. C. Andrews. 1997. Microcytic anaemia mice have a mutation in Nramp2, a candidate iron transporter gene. *Nat. Genet.* 16: 383-386.

90. Gunshin, H., B. Mackenzie, U. V. Berger, Y. Gunshin, M. F. Romero, W. F. Boron, S. Nussberger, J. L. Gollan, and M. A. Hediger. 1997. Cloning and characterization of a mammalian proton-coupled metal-ion transporter. *Nature.* 388: 482-488.

91. Donovan, A., A. Brownlie, Y. Zhou, J. Shepard, S. J. Pratt, J. Moynihan, B. H. Paw, A. Drejer, B. Barut, A. Zapata, T. C. Law, C. Brugnara, S. E. Lux, G. S. Pinkus, J. L. Pinkus, P. D. Kingsley, J. Palis, M. D. Fleming, N. C. Andrews, and L. I. Zon. 2000. Positional cloning of zebrafish *ferroportin1* identifies a conserved vertebrate iron exporter. *Nature.* 403: 776-781.

92. Donovan, A., C. A. Lima, J. L. Pinkus, G. S. Pinkus, L. I. Zon, S. Robine, and N. C. Andrews. 2005. The iron exporter ferroportin/Slc40a1 is essential for iron homeostasis. *Cell Metab.* 1: 191-200.

93. Abboud, S., and D. J. Haile. 2000. A novel mammalian iron-regulated protein involved in intracellular iron metabolism. *J. Biol. Chem.* 275: 19906-19912.

94. Vulpe, C. D., Y. M. Kuo, T. L. Murphy, L. Cowley, C. Askwith, N. Libina, J. Gitschier, and G. J. Anderson. 1999. Hephaestin, a ceruloplasmin homologue implicated in intestinal iron transport, is defective in the sla mouse. *Nat. Genet.* 21: 195-199.

95. Syed, B. A., N. J. Beaumont, A. Patel, C. E. Naylor, H. K. Bayele, C. L. Joannou, P. S. Rowe, R. W. Evans, and S. K. Srai. 2002. Analysis of the human hephaestin gene and protein: comparative modelling of the N-terminus ecto-domain based upon ceruloplasmin. *Protein Eng.* 15: 205-214.

96. De, D., I, D. M. Ward, M. C. di Patti, S. Y. Jeong, S. David, G. Musci, and J. Kaplan. 2007. Ferroxidase activity is required for the stability of cell surface ferroportin in cells expressing GPI-ceruloplasmin. *EMBO J.* 26: 2823-2831.

97. Sheftel, A. D., A. B. Mason, and P. Ponka. 2012. The long history of iron in the Universe and in health and disease. *Biochim. Biophys. Acta.* 1820: 161-187.

98. Nemeth, E., and T. Ganz. 2009. The role of hepcidin in iron metabolism. *Acta Haematol.* 122: 78-86.

99. Kurz, T., J. W. Eaton, and U. T. Brunk. 2011. The role of lysosomes in iron metabolism and recycling. *Int. J. Biochem. Cell Biol.* 43: 1686-1697.

100. Andrews, N. C. 2000. Iron metabolism: iron deficiency and iron overload. *Annu. Rev. Genomics Hum. Genet.* 1: 75-98.

101. Andrews, S. C., A. K. Robinson, and F. Rodriguez-Quinones. 2003. Bacterial iron homeostasis. *FEMS Microbiol. Rev.* 27: 215-237.

102. Doherty, C. P. 2007. Host-pathogen interactions: the role of iron. *J. Nutr.* 137: 1341-1344.

103. Ratledge, C., and L. G. Dover. 2000. Iron metabolism in pathogenic bacteria. *Annu. Rev. Microbiol.* 54: 881-941.

104. Sullivan, J. T., E. F. Jeffery, J. D. Shannon, and G. Ramakrishnan. 2006. Characterization of the siderophore of *Francisella tularensis* and role of *fslA* in siderophore production. *J. Bacteriol.* 188: 3785-3795.

105. Deng, K., R. J. Blick, W. Liu, and E. J. Hansen. 2006. Identification of *Francisella tularensis* genes affected by iron limitation. *Infect. Immun.* 74: 4224-4236.

106. Ramakrishnan, G., A. Meeker, and B. Dragulev. 2008. *fslE* is necessary for siderophore-mediated iron acquisition in *Francisella tularensis* Schu S4. *J. Bacteriol.* 190: 5353-5361.

107. Ramakrishnan, G., B. Sen, and R. Johnson. 2012. Paralogous outer membrane proteins mediate uptake of different forms of iron and synergistically govern virulence in *Francisella tularensis tularensis*. *J. Biol. Chem.* 287: 25191-25202.

108. Sen, B., A. Meeker, and G. Ramakrishnan. 2010. The *fslE* homolog, FTL_0439 (*fupA/B*), mediates siderophore-dependent iron uptake in *Francisella tularensis* LVS. *Infect. Immun.* 78: 4276-4285.

109. Lindgren, H., M. Honn, I. Golovlev, K. Kadzhaev, W. Conlan, and A. Sjostedt. 2009. The 58-kilodalton major virulence factor of *Francisella tularensis* is required for efficient utilization of iron. *Infect. Immun.* 77: 4429-4436.

110. Cartron, M. L., S. Maddocks, P. Gillingham, C. J. Craven, and S. C. Andrews. 2006. Feo--transport of ferrous iron into bacteria. *Biometals.* 19: 143-157.

111. Hantke, K. 2003. Is the bacterial ferrous iron transporter FeoB a living fossil? *Trends Microbiol.* 11: 192-195.

112. Velayudhan, J., N. J. Hughes, A. A. McColm, J. Bagshaw, C. L. Clayton, S. C. Andrews, and D. J. Kelly. 2000. Iron acquisition and virulence in *Helicobacter pylori*: a major role for FeoB, a high-affinity ferrous iron transporter. *Mol. Microbiol.* 37: 274-286.

113. Naikare, H., K. Palyada, R. Panciera, D. Marlow, and A. Stintzi. 2006. Major role for FeoB in *Campylobacter jejuni* ferrous iron acquisition, gut colonization, and intracellular survival. *Infect. Immun.* 74: 5433-5444.

114. Kammler, M., C. Schon, and K. Hantke. 1993. Characterization of the ferrous iron uptake system of *Escherichia coli*. *J. Bacteriol.* 175: 6212-6219.

115. Perry, R. D., I. Mier, Jr., and J. D. Fetherston. 2007. Roles of the Yfe and Feo transporters of *Yersinia pestis* in iron uptake and intracellular growth. *Biometals.* 20: 699-703.

116. Lindgren, H., M. Honn, E. Salomonsson, K. Kuoppa, A. Forsberg, and A. Sjostedt. 2011. Iron content differs between *Francisella tularensis* subspecies tularensis and subspecies holarctica strains and correlates to their susceptibility to H(2)O(2)-induced killing. *Infect. Immun.* 79: 1218-1224.

117. Su, J., J. Yang, D. Zhao, T. H. Kawula, J. A. Banas, and J. R. Zhang. 2007. Genome-wide identification of *Francisella tularensis* virulence determinants. *Infect. Immun.* 75: 3089-3101.

118. Oyston, P. C., A. Sjostedt, and R. W. Titball. 2004. Tularaemia: bioterrorism defence renews interest in *Francisella tularensis*. *Nat. Rev. Microbiol.* 2: 967-978.

119. Qin, A., and B. J. Mann. 2006. Identification of transposon insertion mutants of *Francisella tularensis tularensis* strain Schu S4 deficient in intracellular replication in the hepatic cell line HepG2. ***BMC. Microbiol.*** 6: 69.

120. Conlan, J. W., W. Chen, H. Shen, A. Webb, and R. KuoLee. 2003. Experimental tularemia in mice challenged by aerosol or intradermally with virulent strains of *Francisella tularensis*: bacteriologic and histopathologic studies. ***Microb. Pathog.*** 34: 239-248.

121. Thomas-Charles, C. A., H. Zheng, L. E. Palmer, P. Mena, D. G. Thanassi, and M. B. Furie. 2013. FeoB-mediated uptake of iron by *Francisella tularensis*. ***Infect. Immun.*** 81: 2828-2837.

122. LoVullo, E. D., L. A. Sherrill, L. L. Perez, and M. S. Pavelka, Jr. 2006. Genetic tools for highly pathogenic *Francisella tularensis* subsp. tularensis. ***Microbiology.*** 152: 3425-3435.

123. LoVullo, E. D., C. R. Molins-Schneekloth, H. P. Schweizer, and M. S. Pavelka, Jr. 2009. Single-copy chromosomal integration systems for *Francisella tularensis*. ***Microbiol.*** 155: 1152-1163.

124. Wu, J. C., G. Merlino, and N. Fausto. 1994. Establishment and characterization of differentiated, nontransformed hepatocyte cell lines derived from mice transgenic for transforming growth factor alpha. ***Proc. Natl. Acad. Sci. U. S. A.*** 91: 674-678.

125. Breslow, J. L., H. R. Sloan, V. J. Ferrans, J. L. Anderson, and R. I. Levy. 1973. Characterization of the mouse liver cell line FL83B. ***Exp. Cell Res.*** 78: 441-453.

126. Block, G. D., J. Locker, W. C. Bowen, B. E. Petersen, S. Katyal, S. C. Strom, T. Riley, T. A. Howard, and G. K. Michalopoulos. 1996. Population expansion, clonal growth, and specific differentiation patterns in primary cultures of hepatocytes induced by HGF/SF, EGF and TGF alpha in a chemically defined (HGM) medium. ***J. Cell Biol.*** 132: 1133-1149.

127. Petersen, B., C. J. Yee, W. Bowen, R. Zarnegar, and G. K. Michalopoulos. 1994. Distinct morphological and mito-inhibitory effects induced by TGF-beta 1, HGF and EGF on mouse, rat and human hepatocytes. ***Cell Biol. Toxicol.*** 10: 219-230.

128. LoVullo, E. D., L. A. Sherrill, and M. S. Pavelka, Jr. 2009. Improved shuttle vectors for *Francisella tularensis* genetics. ***FEMS Microbiol. Lett.*** 291: 95-102.

129. Lo, K. Y., M. D. Chua, S. Abdulla, H. T. Law, and J. A. Guttman. 2013. Examination of in vitro epithelial cell lines as models for *Francisella tularensis* non-phagocytic infections. ***J. Microbiol. Methods.*** 93: 153-160.

130. Ray, H. J., P. Chu, T. H. Wu, C. R. Lyons, A. K. Murthy, M. N. Guentzel, K. E. Klose, and B. P. Arulanandam. 2010. The Fischer 344 rat reflects human

susceptibility to *Francisella* pulmonary challenge and provides a new platform for virulence and protection studies. *PLoS. One.* 5: e9952.

131. Spaniol, V., N. Heiniger, R. Troller, and C. Aebi. 2008. Outer membrane protein UspA1 and lipooligosaccharide are involved in invasion of human epithelial cells by *Moraxella catarrhalis*. *Microbes. Infect.* 10: 3-11.

132. Wang, H., F. X. Liang, and X. P. Kong. 2008. Characteristics of the phagocytic cup induced by uropathogenic *Escherichia coli*. *J. Histochem. Cytochem.* 56: 597-604.

133. Guiney, D. G., and M. Lesnick. 2005. Targeting of the actin cytoskeleton during infection by *Salmonella* strains. *Clin. Immunol.* 114: 248-255.

134. Lambotin, M., I. Hoffmann, M. P. Laran-Chich, X. Nassif, P. O. Couraud, and S. Bourdoulous. 2005. Invasion of endothelial cells by *Neisseria meningitidis* requires cortactin recruitment by a phosphoinositide-3-kinase/Rac1 signalling pathway triggered by the lipo-oligosaccharide. *J. Cell Sci.* 118: 3805-3816.

135. Haglund, C. M., and M. D. Welch. 2011. Pathogens and polymers: microbe-host interactions illuminate the cytoskeleton. *J. Cell Biol.* 195: 7-17.

136. Tang, W., C. A. Lazaro, J. S. Campbell, W. T. Parks, M. G. Katze, and N. Fausto. 2007. Responses of nontransformed human hepatocytes to conditional expression of full-length hepatitis C virus open reading frame. *Am. J. Pathol.* 171: 1831-1846.

137. Scharschmidt, B. F., J. R. Lake, E. L. Renner, V. Licko, and R. W. Van Dyke. 1986. Fluid phase endocytosis by cultured rat hepatocytes and perfused rat liver: implications for plasma membrane turnover and vesicular trafficking of fluid phase markers. *Proc. Natl. Acad. Sci. U. S. A.* 83: 9488-9492.

138. Eisenreich, W., J. Heesemann, T. Rudel, and W. Goebel. 2013. Metabolic host responses to infection by intracellular bacterial pathogens. *Front Cell Infect. Microbiol.* 3: 24. doi: 10.3389/fcimb.2013.00024.

139. Smith, J. R., Y. Ning, and O. M. Pereira-Smith. 1992. Why are transformed cells immortal? Is the process reversible? *Am. J. Clin. Nutr.* 55: 1215S-1221S.

140. Gruenheid, S., and B. B. Finlay. 2003. Microbial pathogenesis and cytoskeletal function. *Nature.* 422: 775-781.

141. Doherty, G. J., and H. T. McMahon. 2008. Mediation, modulation, and consequences of membrane-cytoskeleton interactions. *Annu. Rev. Biophys.* 37:65-95. doi: 10.1146/annurev.biophys.37.032807.125912.

142. Flanagan, M. D., and S. Lin. 1980. Cytochalasins block actin filament elongation by binding to high affinity sites associated with F-actin. *J. Biol. Chem.* 255: 835-838.

143. Patel, J. C., and J. E. Galan. 2005. Manipulation of the host actin cytoskeleton by *Salmonella*-all in the name of entry. *Curr. Opin. Microbiol.* 8: 10-15.

144. Dramsi, S., and P. Cossart. 1998. Intracellular pathogens and the actin cytoskeleton. *Annu. Rev. Cell Dev. Biol.* 14: 137-166.

145. Moulder, J. W. 1985. Comparative biology of intracellular parasitism. *Microbiol. Rev.* 49: 298-337.

146. Oyston, P. C. 2008. *Francisella tularensis*: unravelling the secrets of an intracellular pathogen. *J. Med. Microbiol.* 57: 921-930.

147. Isberg, R. R., Z. Hamburger, and P. Dersch. 2000. Signaling and invasin-promoted uptake via integrin receptors. *Microbes. Infect.* 2: 793-801.

148. Kaniga, K., S. Tucker, D. Trollinger, and J. E. Galan. 1995. Homologs of the *Shigella* IpaB and IpaC invasins are required for *Salmonella typhimurium* entry into cultured epithelial cells. *J. Bacteriol.* 177: 3965-3971.

149. Su, J., R. Asare, J. Yang, M. K. Nair, J. E. Mazurkiewicz, Y. Abu-Kwaik, and J. R. Zhang. 2011. The *capBCA* Locus is Required for Intracellular Growth of *Francisella tularensis* LVS. *Front Microbiol.* 2: 83. doi: 10.3389/fmicb.2011.00083.

150. Tempel, R., X. H. Lai, L. Crosa, B. Kozlowicz, and F. Heffron. 2006. Attenuated *Francisella novicida* transposon mutants protect mice against wild-type challenge. *Infect. Immun.* 74: 5095-5105.

151. Rasmussen, J. W., J. W. Tam, N. A. Okan, P. Mena, M. B. Furie, D. G. Thanassi, J. L. Benach, and A. W. van der Velden. 2012. Phenotypic, morphological, and functional heterogeneity of splenic immature myeloid cells in the host response to tularemia. *Infect. Immun.* 80: 2371-2381.

152. Wickstrum, J. R., K. J. Hong, S. Bokhari, N. Reed, N. McWilliams, R. T. Horvat, and M. J. Parmely. 2007. Coactivating signals for the hepatic lymphocyte gamma interferon response to *Francisella tularensis*. *Infect. Immun.* 75: 1335-1342.

153. Telepnev, M., I. Golovliov, and A. Sjostedt. 2005. *Francisella tularensis* LVS initially activates but subsequently down-regulates intracellular signaling and cytokine secretion in mouse monocytic and human peripheral blood mononuclear cells. *Microb. Pathog.* 38: 239-247.

154. Ramesh, G., X. Alvarez, J. T. Borda, P. P. Aye, A. A. Lackner, and K. Sestak. 2005. Visualizing cytokine-secreting cells in situ in the rhesus macaque model of chronic gut inflammation. *Clin. Diagn. Lab Immunol.* 12: 192-197.

155. Stojiljkovic, I., M. Cobeljic, and K. Hantke. 1993. *Escherichia coli* K-12 ferrous iron uptake mutants are impaired in their ability to colonize the mouse intestine. *FEMS Microbiol. Lett.* 108: 111-115.

156. Wickstrum, J. R., S. M. Bokhari, J. L. Fischer, D. M. Pinson, H. W. Yeh, R. T. Horvat, and M. J. Parmely. 2009. *Francisella tularensis* induces extensive caspase-3 activation and apoptotic cell death in the tissues of infected mice. *Infect. Immun.* 77: 4827-4836.

157. Nallaparaju, K. C., J. J. Yu, S. A. Rodriguez, X. Zogaj, S. Manam, M. N. Guentzel, J. Seshu, A. K. Murthy, J. P. Chambers, K. E. Klose, and B. P. Arulanandam. 2011. Evasion of IFN-gamma signaling by *Francisella novicida* is dependent upon *Francisella* outer membrane protein C. *PLoS. One.* 6: e18201.

158. Foley, J. E., and N. C. Nieto. 2010. Tularemia. *Vet. Microbiol.* 140: 332-338.

159. Forestal, C. A., M. Malik, S. V. Catlett, A. G. Savitt, J. L. Benach, T. J. Sellati, and M. B. Furie. 2007. *Francisella tularensis* has a significant extracellular phase in infected mice. *J. Infect. Dis.* 196: 134-137.